HAL
open science

Simple models for complex physics

Norbert Kern

To cite this version:

Norbert Kern. Simple models for complex physics. Soft Condensed Matter [cond-mat.soft]. Université Montpellier 2, 2015. tel-01930091

HAL Id: tel-01930091

https://hal.science/tel-01930091

Submitted on 21 Nov 2018

HAL is a multi-disciplinary open access archive for the deposit and dissemination of scientific research documents, whether they are published or not. The documents may come from teaching and research institutions in France or abroad, or from public or private research centers.

L'archive ouverte pluridisciplinaire **HAL**, est destinée au dépôt et à la diffusion de documents scientifiques de niveau recherche, publiés ou non, émanant des établissements d'enseignement et de recherche français ou étrangers, des laboratoires publics ou privés.

Simple models for complex physics

Habilitation a diriger des recherches

Spécialité Physique

Université Montpellier II
École doctorale I2S
(Information, Structures, Systèmes)

Soutenue par

Norbert Kern

le 17 juin 2015. devant le jury composé de :

I. Cantat	
E. Carlon	
V. Lorman	(Président)
I. Pagonabarraga	(Rapporteur)
M.-C. Romano	(Rapporteur)
C. Vanderzande	(Rapporteur)

Contents

1 Synopsis **7**
1.1 Grenoble (pre-doc) . . . 8
1.2 Amsterdam (post-doc) . . . 9
1.3 Dublin (Marie Curie fellow) . . . 11
1.4 Montpellier ('Maître de Conférences') . . . 12

Appendix 1.A Curriculum Vitæ . . . 16

2 Simple fluids mimicking globular proteins **23**
2.1 Tour d'horizon . . . 23
2.2 Selected publications . . . 27
2.2.1 Gelation vs. fluid-fluid coexistence . . . 27
2.2.2 Fluid-fluid coexistence of 'patchy' particles . . . 31
2.3 Follow-up . . . 34

3 Foams: structure **37**
3.1 Tour d'horizon . . . 37
3.2 Selected publications . . . 46
3.2.1 Foam structure: 'loaded' foams . . . 46
3.2.2 Foam structure: the dry limit . . . 49
3.3 Follow-up . . . 53

4 Foams: dynamics and flow **55**
4.1 Tour d'horizon . . . 55
4.2 Selected publications . . . 57
4.2.1 Dissipation in 2d foams . . . 58
4.2.2 The viscous froth model for a 2d foam . . . 60
4.3 Follow-up . . . 65

5 Active transport on quasi-1d structures **67**
5.1 Tour d'horizon . . . 67
5.2 Selected publications . . . 77
5.2.1 TASEP on structures of branched filaments . . . 77
5.2.2 TASEP transport on a network . . . 82
5.2.3 Active transport vs. diffusion . . . 86
5.2.4 Towards cytoskeletal transport: TASEP networks and beyond . . . 90
5.3 Follow-up . . . 95

6 Present work and outlook **99**

Bibliography **104**

Acknowledgements

Many elements enter the preparation of a 'habilitation', some very rigid (like the administrative procedure), others surprisingly open (like how to organise the manuscript and the 'soutenance' so it would reflect so many years of work in only a few pages and less than an hour). Many colleagues, collaborators, friends and family members have been incredibly helpful throughout the process, one way or another, and I would like to sincerely thank all of them for their support.

First of all, my sincere thanks go to the referees and members of jury for accepting the task of evaluating my work: I am glad that Isabelle Cantat, Mamen Romano, Enrico Carlon, Carlo Vanderzande, Ignacio Pagonabarraga and Vladimir Lormann have all taken upon them to judge the present manuscript, to participate in the viva (involving considerable travel for many) and, for several of you, also to provide an extensive report on the present manuscript. I certainly appreciate your investment in terms of time and effort, which I know is significant.

Lucyna Firlej has kindly offered efficient and benevolent guidance through the habilitation procedure within the School of Physics and Engineering, in the fast changing environment of merging Universities, for which I am particularly grateful.

The synthes which I have chosen to present in my manuscript and in my presentation is based on selected contributions, all part of my research work, which has touched upon a variety of fields, methods, problems and techniques. Throughout the years this has given me the opportunity to meet and interact with many scientists, and these collaborations, discussions and exchanges of ideas have been precious for me. It will be impossible to address all of them, but following a (roughly) chronological order should allow me to at least mention some of the things which I am grateful for.

As I was straying abroad, geographically and scientifically, Bertrand Fourcade has taken me on first for a Master project in Grenoble, and has later also accepted to supervise my doctorate: thank you for the excellent training I have received during those years. Amongst many other elements this includes conveying the importance of an open mind, for example towards biologically inspired physics: the summer schools you have made it possible for me to attend have been important building blocks. Your kind advice and guidance, both in hard science itself as well as its impact on the boundary conditions of real life, have been precious throughout my PhD project and beyond. Many further exchanges dating from this period have been both particularly pleasant and fruitful, such as those with Thierry Charitat (who made me realise that good humour leads to even better science), Francois Graner (who so enthousiastically introduced me to the fascinating world of foams), as well as many others: Isabelle Cantat, Pierre-Francois Lenne, Alois Würger, etc. etc.

Daan Frenkel has offered me the possibility to further broaden my horizon and discover new Physics: thank you for giving me this opportunity, and for providing such a stimulating environment. I have learned many, many things in Amsterdam. I treasure quasi-romantic memories of the time in the 'Frenkel Villa' (which also involve espresso and darts), and of interactions with many other scientists: Massimo Noro (who guided me through my first exploration of phase diagrams), Sander Pronk (who made me discover the Python programming language), Jürgen Horbach, Chinmay Das, Stefan Auer and many, many others. This period also comprises extensive interactions with Bela Mulder, on yet another orthogonal topic: thank you for letting me participate in your infallibly enthousiastic exploration of Science, as well as for your ongoing advice and support over many years.

Denis Weaire and Stefan Hutzler have accepted to host me for a Marie Curie project: thank you for your incredibly kind reception, for the prolonged exchanges on many topics, and for giving me a glance at how Physics can be both rigourous and creative. Again, this is another element which it is precious to have been exposed to: it will always remind me that doing Physics, despite being hard labour, is also a lot of fun. There are many further interactions which I am grateful for, such as those with Simon Cox (for sharing your experience in foam physics, as well as helping to carry moving boxes), Wiebke Drenckhan (for letting me participate, during your confinement to the basement, in making soap bubbles do things they never dreamed of), Isabelle Cantat and Renaud Delannay (for your support, as well as for letting me get my hands wet in Rennes), Frank Morgan and John Sullivan (for letting me get a glimpse of the mathematical side of foam physics), Charles Patterson, etc. etc.

In Montpellier, I wish to particularly thank my fellow group members for making me feel so welcome at my arrival, for the pleasant working environment in general, and for many fruitful discussions, interactions and collaborations, as well as numerous exchanges in the context of teaching Physics: Daniele Coslovich (for sharing a lot of interesting physics, as well as an office), Walter Kob, Ludovic Berthier, Simona Ispas, Estelle Pittard, Maxime Clusel, etc. Among the other members of the laboratory I would especially like to thank Andrea Parmeggiani (for introducing me to TASEP, as well as for a steady and fruitful collaboration), Vladimir Lorman (for ongoing advice and encouragement, and in particular for applying friendly but steady pressure towards undertaking this habilitation ...) and Luca Ciandrini (for many interesting exchanges, of which there will hopefully be many more).

My thanks also go to the students and postdocs I have had the pleasure to work with closely: Izaak Neri, Ben Embley (as well as his 'real' supervisor, Paul Grassia, for entrusting him to me for several months), Adélaïde Raguin, Pascal Nadal, Étienne Loiseaux, Mirko Mikosalec.

A big thank you also goes to my parents in law (for their hospitality in Bercimuel, where the first half of this manuscript was written), with special thanks to Juan and Carmen (for kindly letting me tap into their wireless network).

Finally, I would especially like to thank my family: Esmeralda (for painstakingly underlining typographic errors - as well as asking science questions! - in this manuscript, but more generally for your continuous support and encouragement, far beyond this particular exercise), as well as Lucas, Sebastián and Sarah (for your patience during many busy weeks of writing). Thanks to all of you for making it all worthwhile!

Chapter 1

Synopsis

According to my initial thoughts this document should have started by pointing out the coherent red line, the guiding principle, the meaning of it all. Provide a careful argumentation of why I have planned my scientific career in this particular way, and why this was the optimal way to procede. However, after searching very hard, I decided to face the facts: there is no such master plan, not even in retrospect. There never was one. Coming to think about it, it seems to me that such a Newtonian vision of a research career no longer applies to junior scientists as they make their way into science, and in my case I have no regrets about this. At the end of the day, a part of it is simply random. Indeed, it would appear useless to deny all the numerous elements of randomness involved, such as personal encounters, availability of funding, colleagues one happens to overlap with, personal constraints etc. etc. etc.

Thus, as the opposite caricatural representation, the idea would spring to mind that my research trajectory should really be envisaged as a random walk. On the other hand, even acknowledging the significant number of unforeseeable influences, I would certainly like to believe that we are at least looking at a *biased* random walk. Which in turn raises the question as to the nature of the bias (a question which is more easily answered with hindsight). It certainly involves curiosity, the desire to complete my understanding of Physics from complementary points of view, as well as a taste for statistical mechanics, simple models, for numerical simulation and for Biology-inspired problems. I feel that a common theme in my research work translates my personal viewing angle of Physics, as a way of understanding the world (within and beyond Physics): reducing complexity to an (overly) *simplified* representation, in order to extract the most generic features, which can then be contrasted to reality. Any outcome of this comparison then helps me to better understand the world: either a fundamental mechanism has been revealed, or we then know that other ingredients are missing in the description. In some sense this way of seeing things has influenced many of the choices I have made. Problems more or less directly inspired from Biology are probably a perfect example for this: text-book explanations for a complex biological process based on boxes and arrows have always left me wondering about what they actually mean, and in which way they might be 'real'. Understanding how, in many cases, it is ultimately statistical physics or non-linear physics which make those explanations work has been a huge source of satisfaction for me.

Another element seems important, which I think is clearly reflected in my career to date: I like things to be simple and, somewhat non-scientifically, there is an element of esthetics to this. I am most pleased with a piece of research work when it leads to a simple model, the assumptions of which can be stated clearly. The phenomenology will more often than not be

complicated, and the mathematics or the simulation methods to establish conclusions may be technically involved. But at the end of the day what I look for on top of the potentially complex results as such is a hand-waving argument, which makes one feel that the result is indeed qualitatively expected, or at least why it is reasonable. This is when I feel that a problem has been properly solved, and I certainly hope this transpires in the publications I have been involved in.

This report thus is a guided tour of selected topics along the path of my research trajectory. To start, a brief chronological sketch appears useful in order to outline my activities in various domains of soft matter physics, often with inspiration from biological problems, mostly exploiting the tool of computer modelling. The intention is to give an overview, before developing some of the topics in greater detail in the following chapters, but also to convey some of my motivations. Overlapping and bifurcating projects make it difficult to present all ramifications of my activities in an exhaustive yet coherent manner. The following outline is therefore rather pragmatically labeled in terms of geographical locations, corresponding to the successive positions I have held. This also reflects the spirit of a journey both through Europe and through Physics, in the fashion of a not-quite-random walk, and consequently includes personal reflections on this apprenticeship at the end of each step of this trajectory.

1.1 Grenoble (pre-doc)

Although not entirely within the scope of this document, it seems appropriate to define a starting point by briefly recalling the topic of my 'doctorate', with B. Fourcade at the Université Joseph Fourier in Grenoble. This is not only because it constitutes my first incursion into research, but also since it has been a great motivation for me to engage in a scientific career, and since I still consider useful and important many of the things I have learned at this stage.

At that point I worked on models for phospholipidic vesicles. The phospholipidic bilayers constituting their membranes imply elastic properties which are, in most situations, governed by a resistance to bending this membrane. The water-filled vesicle can be modeled as a topologically closed shape of given volume and area, but subject to a bending energy, such as the one defined by Helfrich [92]. The typical vesicle shapes are then obtained by minimisation of this energy subject to the constraints that both their volume and total membrane area are fixed. This defines the equilibrium shape of a vesicle, around which thermal fluctuations occur. Vesicles are commonly studied as model systems in soft matter experiments, and one aspect of the interest they receive is that their bilayer structure is also present in the (infinitely more complex) lipid membranes of biological cells [2]. My contribution was twofold.

One aspect was to explore the effects one could produce by using ferro-fluids [168, 169], i.e. stabilised suspensions of nanometric magnetic particles, in the presence of a magnetic field, as had been done experimentally by Bacri and co-workers [8]. Using the response to the applied field in order to deduce the membrane elastic parameters is one potential application. The simplest scenario is the one where the magnetic grains stick to the membrane, in which case an approximate description can be made in terms of an additional magnetic surface energy. An applied magnetic field can then be used to provoke shape changes, leading to elongated ('prolate') shapes in the presence of a static uniform field and a flattened ('oblate') shape if a (rapidly) rotating field is applied. The magnetic field furthermore reduces the amplitude of thermal shape fluctuations, an effect which can be described in terms of a magnetic contribution to the tension in the membrane [109]. Similar systems have been revisited in recent experiments [124–126].

The other aspect of my work was concerned with shape changes due to hydrodynamic effects as vesicles are dragged through the surrounding aqueous solution, as would for example be the case for ferro-vesicles in a field gradient. The approach, following Kraus et al. [119], was to discretise the 3d shape of a vesicle, modelling its elastic properties by finite element-like methods. The relevant low-Reynolds hydrodynamics were then treated, based on the same discretisation, via boundary integral methods exploiting the Oseen tensor approach for hydrodynamic interactions [119,129,153]. It turns out [110] that both prolate and oblate shapes are stationary when pulled, but undergo deformations due to the flow. Rather more surprisingly, we have shown that a vesicle sedimenting under the effect of gravity should take a pear-like shape, somewhat counter-intuitively exposing its broad side towards the flow direction. The approach has recently been re-visited by Leonetti and Boedec [22, 23], with similar results but with a much finer resolution, due to the gain in computational performance. The pear shape, amongst others, has recently been observed in experiments [96].

Personal upshot This entry point into research in Physics has been a fantastic opportunity to discover a whole variety of domains and techniques. Elasticity theory and finite element methods, which had not been part of my academic curriculum to any great extent, are such topics which I have been able to discover and put to use. Variational calculus has been another such element. The low Reynolds hydrodynamics, and in particular the boundary layer techniques, have given me useful insight into the micrometric world, which I still benefit from today. Exploiting Stokes hydrodynamics, coupled with the problem of membrane elasticity as well as volume and area constraints has been a challenge, and developing taylor-made codes, in this case using the C++ programming language, has been one of the key ingredients. This has since remained a constant in most of my work.

On a more general level my PhD work has helped me to lay the foundations of my physical intuition, as well as to develop the necessary working methodology for research. The opportunity to attend summer schools, on soft matter physics as well as on the interface between Physics and Biology, has also been an important factor for opening my eyes towards the vaster fields in Physics, and ultimately for making me wish to pursue a career in research.

I have also been fortunate enough to have been offered a complementary teaching contract (known as 'monitorat' at the time), which has given me a first teaching experience in an undergraduate level academic context. Getting a first glimpse of what the activity of an 'enseignant-chercheur' represents has also been an important element for my subsequent career choice.

1.2 Amsterdam (post-doc)

After having completed a PhD using models based on a continuous, macroscopic description, it was my wish to also acquire intuition on microscopic processes. This aim took me to a post-doctorat in Daan Frenkel's group at Amolf in Amsterdam. There I have worked on the phase behaviour of simple models for complex fluids, in particular with respect to the fluid phase. One inspiration for this project was the problem of protein crystallisation, an important practical step in the study of structural features of these biologically omnipresent macro-molecules. Indeed, it has been shown that certain aspects of their phase behaviour are well described by rather simple 'effective' parameters (the second virial coefficient, as it happens). This suggests that rather simple, generic models, in the spirit of what is usually known as 'simple fluids', may

be useful for understanding the overall phase behaviour of protein solutions.

One result of this work has been to point out the importance of the range of the potential with respect to gelation: although the virial coefficient characterises the overall attractivity resulting from an interaction, one must be aware that short-ranged contributions in particular affect the occurrence of gelation [143]. This implies that the fluid-fluid critical point may become pre-empted by a metastable but long-lived gel state. Since the fluid-fluid critical point has been shown to play a role in the nucleation of the crystal [189], this supplies an argument why proteins may crystallise in conditions where artificial colloids do not [143].

Another aspect of my work was to devise a model for highly directional interactions. This is also directly inspired by proteins, for which interactions are often specific to certain zones on their surface. But the description is also relevant to artificial colloidal systems, which it has since become possible to synthesise with great control (see for example [52, 121, 204]). The model I have worked on combines a hard-sphere excluded volume with an additional short-ranged attractive potential which requires attractive 'patches' on the particle surface to face each other. In particular I have studied the effect of patchiness on the fluid-fluid coexistence, using (amongst others) Gibbs-ensemble Monte Carlo simulations. It turns out that for patchy attractions the virial coefficient is no longer the only parameter characterising the fluid-fluid critical point [111]. The model we have introduced in this context has since then been used in many further studies [80, 131, 166, 176] and remains of interest today [72].

During this time I have also had the opportunity to interact with Bela Mulder on the topic of diffusive transport in tip growth. This is a particular growth mode typical for funghi, in which vesicles appear to be produced in one very localised region, usually associated with a physiological feature known as *Spitzenkörper*. The formulation established by Bartnicki and Garcia [15, 78] assimilates this process to a so-called *vesicle supply center*, where vesicles are liberated and then travel in a diffusive manner to deliver the membrane material necessary for the cell wall expansion. The problem is to solve for a stationary growth mode, observed in living funghi, in which the supplied material is incorporated in a way which maintains the shape of the tip. An initial model was formulated in 2d [15], a 3d model was given later [78], but both of them remained unsatisfactory to a physicist in that they used a ballistic, rather than diffusive, delivery process. I started with Bela Mulder to develop a formulation which would be suitable for including the actual diffusion process, and this work has later been continued by Simon Tindemans [191]. The main result is that corrections to the stationary tip shapes can now be calculated, for various growth modes and properly accounting for the diffusive transport process.

Personal upshot Entirely on purpose, this postdoc position has exposed me to the microscopic vision of matter, and of soft matter in particular. I have thus had the opportunity to discover the methods of stochastic simulations (in particular Monte Carlo methods), as well as a certain number of the subtleties and pitfalls that come with it. In terms of physics, this was my first real-world contact with thermodynamic calculations and simulations in general, and with analysing phase behaviour in particular.

I have had the opportunity to implement rather complex simulations (such as Gibbs ensemble simulations) and also to get a glimpse into the world of parallel computing (when implementing the parallel tempering procedure required to achieve equilibration). Acquiring skills in scripting languages, and in particular in the Python language, has been another bonus, which I still exploit regularly, both for research and for teaching activities.

Again, I have found the contact points with biological questions very stimulating. This wa the case for the idea of using colloidal models as a way of understanding the collective behaviour of biologically relevant proteins. The project on tip growth in fungal cells, which I have collaborated on with Bela Mulder, has constituted another element in this sense: it has allowed me for the first time to think about a specific biological situation, on the scale of a cell, to which modelling could be applied, and has indeed permitted to clarify the effect of certain (heretofore unphysical) assumptions.

1.3 Dublin (Marie Curie fellow)

The opportunity of obtaining a Marie Curie scholarship has made it possible for me to join the group of Denis Weaire at Trinity College in Dublin to work on various aspects of foam physics, a topic I had become interested in since my PhD work. At the first level of description the cellular structure of foams can be represented as an ensemble of bubbles separated by films, the features of which are ultimately all determined by surface tension effects. This conceptually simple description of the structure, both in 2d or 3d, provides a seducing starting point, making foams interesting to both theory and experiments, but also for pure and applied mathematics [199]. More complex aspects of foam physics may then be understood by building on and refining this description, such as physico-chemical effects, which become particularly relevant for phenomena of foam flow and/or rheology. The projects I have worked on have concerned both the structure and the dynamics of foams.

Concerning the static structure, I have mainly explored the question how the description of foams, in terms of films delimiting bubbles and subject to surface tension, might need to be complexified in certain situations. One such case is the scenario of 'loaded' foams, where the weight of the fluid present in the liquid-filled channels known as 'Plateau borders' is taken into account. It turns out that this gravitational energy contribution can be shown to modify the equilibrium rules known as Plateau's laws [199] which dictate, amonst others, the angles at which the Plateau borders meet in a vertex. Another case concerns the closer inspection of what one means by the currently used 'dry foam approximation', which is the case where there is only negligible fluid content in the foam, and for which our analysis has provided new insight. In particular we have characterised the asymptotic behaviour of very dry foams, and provided the relevant scaling as a function of the liquid fraction, for example for rheological situations [112]. The argument is that the liquid content leads to an energy term which may be interpreted as a negative line tension, and which can lead to an instability in numerical work. The presence of such a term has indeed been verified experimentally shortly after [87], and has been exploited very recently [57] for an experimental characterisation of the elastic properties of a Plateau border.

A major result concerning the dynamical behaviour of foams, including dissipation effects, has been obtained for so-called 2d foams (bubbles squeezed between two parallel plates): for this case we have formulated the *viscous froth model*, which includes dissipation effects due to the displacement of Plateau borders over the glass plates. The model maintains the description of (2d) bubbles, but includes a linear drag force on the Plateau borders as they move. A numerical strategy to solve this simple model for 2d foam dynamics has been provided and implemented [108]. It has even been possible, in collaboration with R. Delannay and I. Cantat, to experimentally elucidate the dissipation relation to be expected in real systems [31].

Personal upshot Working on the physics of foams has been a great opportunity for me to explore this system, about which I had become very curious over the preceding years: a curiosity nurtured by many discussions with F. Graner, who so rightly highlighted the richness of the physics underlying such cellular fluids. The context of the renowned Trinity College group has been a perfect environment, encouraging me to work on many different aspects, ranging from theory on the static structure to numerical simulations on the flow of foams, to direct contact with rather original experiments on bubbles flowing through narrow channels, and which have ultimately lead to the notion of 'discrete microfluidics' [51].

My collaboration with I. Cantat and R. Delannay in Rennes has even allowed me to take part in actual experiments (getting my hands wet for real!): this too has been a very interesting experience, which I would be ready to renew if the right opportunity were to present itself. It has certainly given me yet more appreciation for the experimental work which Physics ultimately relies on.

There has not been an opportunity within my activity on foams to work on biologically inspired problems. On the other hand, models inspired from cellular fluids have been exploited for a long time to model cellular tissues (see, e.g., [79, 82–84]), and recent developments have lead to much refined approaches inspired by methods and descriptions which have proven useful in foams (see [25, 101] for two recent publications). It is one of the topics I would be curious about returning to in a biology-inspired setting such as biological tissues.

In this context the question of specificity springs to mind: if one intends to use a cellular-liquid based description for actual biological tissues, one must clearly be aware of the potential limitations, due to the fact that many interactions between cells are in fact quite complex, and in many cases specific. In addition, dealing with a living tissue, interactions can be regulated by the tissue itself. The real challenge therefore is to evaluate to which extent it will be possible to isolate generic feature, which it would be useful to address based on physics-based arguments.

In this respect, foam physics nicely illustrates that, even within the realm of Physics, certain questions become subject to the influence of physico-chemistry. This is highlighted rather strikingly by the debate [53, 115, 201] whether the drainage of liquid through a foam is limited by flow through the Plateau borders or through the junctions. The ultimate conclusion has been that it depends ... on whether one uses *Fairy* or *Dawn* washing up liquid (or, more precisely, on the surface viscosity of the surfactant). To me this has come as a reminder, not without irony: Yes, it is possible to obtain useful insight by simplifying away the specificity of a microscopic system (like the biological protein interactions in the previous topic). But it is just as well possible to discover that unsuspected specificities play an important role in a supposedly simple, well characterised system, as it is required for a description by macroscopic physics. This example will always serve me as a reminder to be careful before drawing conclusions from simple models for any specific system, a precaution which applies even more so to biologically inspired questions.

1.4 Montpellier ('Maître de Conférences')

My work in Montpellier, in the context of the group of Statistical Physics (formerly Theory and Simulation) has seen me, and is still seeing me, work on various topics, involving Molecular Dynamics and Monte Carlo simulations on systems both in and out of thermal equilibrium.

Scientific context Arriving at the University of Montpellier, I joined what was at the time the 'Laboratoire des Verres', with a strong tradition on glasses, out-of-equilibrium dynamics and glassy dynamics in particular. I thus became involved in the study of a simple model for a particle gel, a study which has also allowed me to gain experience in Molecular Dynamics simulations. In this model we have considered particles with a propensity to forming a particle gel, stabilised by suitable energy barriers in the pair interactions. We have explored [184] the dynamics with which a gel-like fractal assembly of particles ages, or finally desintegrates, depending on the applied conditions (and the temperature in particular). The simulations have furthermore given access to the microscopic processes corresponding to the structural rearrangements which lead to aging over time. In particular, a subdiffusive dynamics arises after long waiting times. The scaling of the mean-squared displacement with time has been linked to the collective dynamics of particle *chains* in the gel.

I am thus presently part of a renowned group with experts in statistical physics in general and out-of-equilibrium dynamics and glassy systems in particular, but also in computer techniques of molecular simulation. But I was also fortunate enough to find myself in an open environment, favourable to interdisciplinary work. My own research has evolved towards stochastically driven out-of-equilibrium transport, as it would model the biological situation of molecular motors (such as myosin, kinesin or dynein) driving transport along bio-filaments (actin fibers or microtubules). In its simplest variant the corresponding model is called the TASEP (Totally Asymmetric Simple Exclusion Process [130]), in which particles stochastically hop along a regularly spaced lattice, subject only to an excluded volume interaction. This model is also a paradigm in fundamental physics, since it is arguably the simplest model for stochastically driven out-of-equilibrium transport. Much of my recent research effort has been spent, in collaboration with Andrea Parmeggiani, on understanding the physics of this type of process in the presence of branched structures on a network. In the interdisciplinary context this amounts to an attempt to develop minimal models for understanding some of the mechanisms at work in cytoskeletal transport.

The results include a straightforward procedure allowing to model, with many simplifying assumptions, the flow of molecular motors on a complex network. We have presented the method in [140]. It builds upon our earlier approach [61] with a different angle, by decomposing the network structure in a mean-field spirit, exploiting the fact that the transport properties of a single segment are known. Indeed, we have shown that one can construct the entire flow pattern by decomposing the global network into segments, which couple at the junction points only. This mean-field analysis works remarkably well. Thanks to this approach we have been able to devise a numerical algorithm which allows to handle TASEP transport on large networks very efficiently. With this tool it has become possible to investigate the role of the network topology: *regular* networks (having an equal number of incoming and outgoing segments at all of their nodes) behave differently from *irregular* ones, and in particular they are prone to showing 'traffic-jam'-like density discontinuities. The approach furthermore generalises to more complex variants of the model. Most importantly this is the case for the process including the attachment and detachment of motors, as they occur in a biological setting, thus coupling the transport on the network to a (homogeneous) bulk concentration [142]. Beyond the particular models considered, a convenient representation has been identified which may be used to characterise the transport state of the entire network by mapping it onto that of a single segment. Remarkably, this simple view captures many important features of the resulting physics, and it can furthermore be expected to be applicable to many future generalisations of the transport model [141]. Finally, we have taken a further step towards modelling actual biological transport processes, by highlighting how local rules at the junctions affect the flow [160].

An ongoing PhD project (P. Nadal) on modelling the effect of conformational changes on the collective behaviour of protein-like particles is closer to my postdoc work on simple fluids, but still biologically inspired. It also has points in common with my research activity on motor protein based transport (see the final chapter).

Teaching and tuition of research students Holding a teaching position since my arrival in Montpellier, there is of course another side to my activities. Having arrived in 2003 I have had the opportunity to discover the program preceding the major reform of 2004, as well as the system following that reform, and the reformed version of that (if there is a stationary state it appears to be characterised by a high rate of reforms...). I have thus contributed to a whole variety of classes, from teaching introductory physics to students in geological sciences, through computer modelling for undergraduate Physics students, to simulation techniques for students taking a combined Master in Physics and Computer Sciences. In many cases I have also been able to set up these modules and define their content, as well as the pedagogical approach. Most of these have been a real pleasure to teach, and interacting with students has been an important part of the process, requiring continually to revise one's approach, just like one has to do in research.

I have furthermore been fortunate enough to contribute my share towards mentoring graduate students and PhD students. This activity is of course more closely related to my research work, and the work of several of these students has found its way directly or indirectly into the resulting publications. I would specifically like to mention the Master students whose projects I have contributed to supervising: Étienne Loiseaux (M1), Mirko Mikosalec (M1), Adélaïde Raguin (M2), Pascal Nadal (M2), and a joint project by F. Honno, M. A. Kamoun et J.-F. Zaragoci (M1).

Some of these projects have evolved into PhD projects, and I thus have co-supervised the PhD project of Adélaïde Raguin (with Andrea Parmeggiani). Others have come as an 'extra', like a stay of several months by Ben Embley, sent by his Phd supervisor (Paul Grassia) to explore an orthogonal topic to his PhD work, in the context of a European PhD scholarship. Currently I am involved in the PhD project of P. Nadal mentioned above (with Daniele Coslovich and Vladimir Lorman).

Although not considered student tuition, I would also especially like to mention Izaak Neri, whose postdoc activity I have contributed to supervising: this, too, has been a very fruitful and rewarding experience.

Responsibilities within the local scientific community In terms of administrative and community activities, beyond the regular share of paperwork that comes with both teaching and research, two contributions come to mind. One has been playing the role of group leader for what was then called the group of 'Theory and Simulation'. This has given me the opportunity to discover the inner workings of a research laboratory and, to a lesser extent, a University. The other activity has consisted in being part of an interdisciplinary committee of three colleagues taking on the responsibility to implement the certification of computer literacy (C2i), at the level of the University Montpellier 2. I have contributed to developing the underlying courses and the associated evaluation process over a number of years.

Finally, I have also had the opportunity to be a member of recruiting commissions for openings at the 'Maître de Conférences' (lecturer) level.

Personal upshot My research activity here in Montpellier has been tremendously motivating for me. The topic of active quasi-1d transport has allowed me to learn new Physics, as well as work on models which clearly have their place at the interface with molecular cell biology, and which have proven to appeal to a number of experimentalists working on molecular motors.

The collaboration with Andrea Parmeggiani has provided the context for such a topic to prosper. One interesting point was to see in full size how problems at an interface with other sciences can lead to a 'cross-fertilisation': here, the physics-based approach attempts to provide insight into molecular mechanisms which may be relevant, for living systems or at least for *in vitro* experiments. But at the same time, the biological context also raises new questions, which may be challenging to Physics. Here, a simple stochastic transport process has provided a useful concept, but ultimately requires refinements (for particle attachment/detachment, bulk diffusion, internal degrees of freedom in the stepping process, etc.), which all raise further interesting questions within out-of-equilibrium physics.

In terms of mentoring PhD and Master students, I have taken great pleasure in this part of my work. Taking on the responsibility for a project at this level of a student's curriculum is always a challenge, but it is also very satisfying from a personal point of view: helping PhD students on their way into Physics research has proven to be another rewarding aspect of the life of an 'enseignant-chercheur'. In terms of the scientific implications, without much surprise, I can definitely confirm that the additional questioning and discussing with young scientists systematically leads to deeper understanding. I am grateful for the contribution of all the students and postdocs I have worked with.

1.A Curriculum Vitæ

Personal Details

Born 10 may 1969, German nationality.
Married, three children (born in 2001, 2003, 2007).
National service accomplished (1988/89).

Contact details :
Laboratoire Charles Coulomb UMR 5221 CNRS-UM2
Université Montpellier
Place Eugène Bataillon - CC069
F-34095 Montpellier Cedex 5 - France
Tél : +33 (0)4 67 14 93.06
Fax : +33 (0)4 67 14 34 98

Education and Career

2003-... : **Maître de Conférences**
Université Montpellier 2

2001-03 : **European 'Marie Curie' scholarship**
c/o *D. Weaire*, Trinity College, Dublin (Ireland)
topic: structure and dynamics of foams

1998-01 : **Post-doctorat**
c/o *D. Frenkel*, Amolf/Fom, Amsterdam (Netherlands)
topic: proteins vs. colloids

1995-98 : **Doctorat in Physics**;
Université Joseph Fourier, Grenoble (France)
topic: "Ferro-vésicules et hydrodynamique de vésicules",
Advisor : *B. Fourcade*
"très honorable avec félicitations" (oct. 1998)

1989-96 : **Diploma in Physics**
Universität Karlsruhe (Germany)
"sehr gut" (top grade)
As part of these studies: stays at the University of Edinburgh (Scotland, 92/93) and at the Université Joseph Fourier in Grenoble (DEA 94/95, "Diplomarbeit" 95/96), with a mobility scholarship attributed by the Collège Franco-Allemand

1988-89 : National service

1988 : "**Abitur**" (baccalauréat); Karolinen-Gymnasium Frankenthal (Allemagne)

Distinctions

- ANR "ModelN" (responsible for partner 2, University Montpellier 2) (2010-13)
- Funding (3500 euros) for interdiscplinary research projects (with A. Parmeggiani) from the *Conseil Scientifique* of University Montpellier 2 (2007)
- Sabbatical (6 months) for interdisciplinary research, University Montpellier 2 (2005-06)
- European scholarship "Marie Curie" for postdoc at Trinity College, Dublin (2001-03)
- 'Monitorat' (additional contract as teaching assistant) during doctorate (1995-98)
- Scholarship of the "Collège Franco-Allemand" for studying at the Université J. Fourier, Grenoble (1994-95)

Tuition of Postgraduate and PhD students

PhD students

- P. Nadal (2013-. . .), joint tuition (33 %) with D. Coslovich and V. Lorman
- A. Raguin (2010-2013), joint tuition (50 %) with A. Parmeggiani
  CNRS interdisciplinary scholarship (physics-biology)

Master students

- P. Nadal: *M1, Master Physique-Informatique* (2013), co-tuition with D. Coslovich
- M. Mikolasek: *M1, Master Physique-Recherche* (2012)
- A. Raguin: *M2, Master Physique-Recherche* (2010), co-tuition with A. Parmeggiani
- E. Loiseaux: *M1, Master Recherche* (2006), co-tuition with A. Parmeggiani
- F. Honno, M. A. Kamoun and J.-F. Zaragoci: *M1, Master Physique-Informatique* (2005), co-tuition with I. Mougenot and A. Parmeggiani
- A. Martin: *Master, Trinity College Dublin* (2002-3), under the responsibility of D. Weaire

Participation in PhD committees and examinations

- F. Turci (2012), c/o E. Pitard, Montpellier
- T. Green (2008), c/o P. Grassia and L. Lue, Manchester

Participation in PhD 'steering' committees

- O. Dauloudet (2013/14 - ...), c/o A. Parmeggiani, Montpellier
- F. Turci (2009/10 - 2011/12), c/o E. Pitard, Montpellier
- R. Garces (2009/10 - 2013/14.), c/o V. Lorman, Montpellier

Implication in the local scientific community

- Group leader 'Théorie et Simulation' (2009-2011)
- Member of recruiting commissions
  - Member of the "Commission de Spécialistes", UM2 (Section 28), juin 2007 (full member)
  - Member of "Pool d'Experts" for the recruiting commissions, UM2, 2013
  - Member of the "Commission de Spécialistes", UM2 (Sections 29-30), mars 2008 (additional member)
- Creation (with M. Rolland et T. Libourel) of the certificate of computer literacy 'c2i' at the Faculté des Sciences, UM2 (2007-2010)
- In charge of the 'delocalised' library, LCVN (2005-2012)

Refereeing for Scientific Journals

Refereeing activity for Physical Review Letters, Physical Review E, Journal of Chemical Physics, Philosophical Magazine Letters

Publications

Scientific Journals

- *"Modelling Collective Cytoskeletal Transport and Intracellular Traffic"*
  A. Parmeggiani, I. Neri, N. Kern
  chapter in: The Impact of Applications on Mathematics: Proceedings of the Forum of Mathematics for Industry Vol. 1, Springer (2014)

- *"The crucial role of junctions for TASEP transport on networks"*
  A. Raguin, A. Parmeggiani, N. Kern
  Phys. Rev. E 88, 042104 (2013)

- *"Exclusion processes on networks as models for cytoskeletal transport"*
  I. Neri, N. Kern, and A. Parmeggiani
  New Journal of Physics 15, 085005 (2013)

- *"Modelling cytoskeletal traffic: an interplay between passive diffusion and active transport"*
  I. Neri, N. Kern, and A. Parmeggiani
  Phys. Rev. Lett. 110 (9), 098102 (2013)

- *"Totally Asymmetric Simple Exclusion Process on Networks"*
  I. Neri, N. Kern, and A. Parmeggiani
  Phys. Rev. Lett., 107 (6), 068702 (2011)

- *"Understanding totally asymmetric simple-exclusion-process transport on networks: generic analysis via effective rates and explicit vertices"*
  B. Embley, A. Parmeggiani, N. Kern
  Phys. Rev. E 80, 041128 (2009)

- *"Aging dynamics of a fractal model gel"*
  M. A. Suarez, N. Kern, E. Pitard, W. Kob
  J. Chemical Physics, 130, 194904 (2009)

- *"Hex-Tasep: Dynamics of Pinned Domains for Tasep transport on a Periodic Lattice of Hexagonal Topology"*
  B. Embley, A. Parmeggiani, N. Kern
  Phys. Cond. Matt, 20, 295213 (2008)

- *"The diffusive vesicle supply center model for tip growth in fungal hyphae"*
  S.H. Tindemans, N. Kern, B. Mulder
  Journal of Theoretical Biology, 238 (4), 937-948 (2006)

- *"Rheology of ordered foams - on the way to discrete microfluidics"*
  W. Drenckhan, S.J. Cox, G. Delaney, H. Holste, D. Weaire, N. Kern
  Colloids and Surfaces A: Physicochemical and Engineering Aspects, 263 (1-3), 52-64 (2005)

- *"The two-dimensional viscous froth model for foam dynamics"*
  N. Kern, D. Weaire, A. Martin, S. Hutzler, S.J. Cox
  Phys. Rev. E, 70, 041411 (2004)

- *Loaded foam structures"*
  D. Weaire, N. Kern, G. Verbist
  Phil. Mag. Lett., 84, 117-125 (2004)

- *"Dissipation in foam flowing through narrow channels"*
  I. Cantat, N. Kern & R. Delannay
  Europhys. Lett., 65 (5), 726-732 (2004)

- *"Pressures in periodic foams"*
  D. Weaire, N. Kern, S.J. Cox, J.M. Sullivan, F. Morgan
  Proc. Royal Soc. Math. Phys. Eng. Sci. 460, 569-579 (2004)

- *"Approaching the dry limit in foam"*
  N. Kern & D. Weaire
  Phil. Mag. 83(26), 2973-2987 (2003)

- *"The fluid dynamics of foam"*
  D. Weaire, S. Hutzler, S.J. Cox, N. Kern, M.D. Alonso & W. Drenckhan
  J. Phys. : Cond. Matter 14, S 65-73 (2003)

- *"Phase behaviour of colloidal particles with short-ranged, strongly directional attraction"*
  N. Kern & D. Frenkel

J. Chem. Phys. 118, 9882-9889 (2003)

- *"The role of long-ranged forces in the phase behaviour of colloids and proteins"*
  M. Noro, N. Kern & D. Frenkel
  Europhys. Lett. 48(3), pp. 332-338 (1999)

- *"Vesicles in linearly forced motion"*
  N. Kern & B. Fourcade
  Europhys. Lett. 46(2), pp. 262-267 (1999)

- *"Vesicles decorated with magnetic particles"*
  N. Kern & B. Fourcade
  Europhys. Lett. 38(5), pp. 395-400 (1997)

General articles written about our results

- *"Transport sur réseau irrégulier"*, by M. Mashaal,
  `http://www.pourlascience.fr/ewb_pages/a/actu-transport-sur-reseau-irregulier-27804.php`

- *"Les grandes artères ne profitent pas au trafic !"*
  Actus Labo, Sciences & Vie, Octobre (2011), 28

- *"Random Roads Less Travelled"*, by M. Schirber,
  Phys. Rev. Focus 28, 6 (2011)

Recent presentation of results at conferences, etc.

- DPG meeting, 2014 (Berlin), "Exclusion processes on networks" (talk), I. Neri, N. Kern, A. Parmeggiani

- GDR Phénix, "Complex Network Dynamics", 2013 (Montpellier), "Characterising stationary states in exclusion processes on networks" (invited talk), N. Kern, I. Neri, A. Raguin, A. Parmeggiani

- Conference, 2013 (Coventry, England), "Understanding quasi-1d active transport on networks" (talk), N. Kern, I. Neri, A. Raguin, A. Parmeggiani

- International Summer School Fundamental Problems in Statistical Physics XIII, 2013 (Leuven), "Exclusion processes on networks" (talk), I. Neri, N. Kern, A. Parmeggiani

- 4ième École Interdisciplinaire sur les Syst'emes Complexes, 2012 (Rennes), "Transport stochastique sur réseau" (invited talk), N. Kern, I. Neri, A. Raguin, A. Parmeggiani

- Conference Mechanisms driving the organization of intra-cellular organelles 2012 (Zaragoza, Spain), "Towards modelling motor protein driven cytoskeletal transport" (talk), N. Kern, A. Parmeggiani, A. Raguin , I. Neri

- Journées de Physique Statistique, 2012 (Paris), "Totally asymmetric simple exclusion process on networks" (talk), I. Neri, N. Kern, A. Parmeggiani

- European conference on complex systems, 2012 (Brussels), "Modelling active transport and spatial-temporal organisation of motor proteins along the cytoskeleton" (talk), I. Neri, N. Kern, A. Parmeggiani

- Journées de la Physique Statistique, ESPCI, 2012 (Paris), "Transport sur réseaux complexes d'inspiration biologique : topologie et dynamique aux jonctions" (communication), A. Raguin, N. Kern, A. Parmeggiani
- Journées de la Matière Condensée (JMC13), 2012 (Montpellier), "Statistical physics for modelling cytoskeletal intracellular transport" (communication), A. Raguin, N. Kern, A. Parmeggiani
- DPG Physics School on Forces and Flow in Biological Systems, 2012 (Bad-Honnef) "Modelling active transport and spatial-temporal organization of motor proteins along the cytoskeleton" (poster), I. Neri, N. Kern, A. Parmeggiani
- 13èmes Journées de la Matière Condensée, 2012 (Montpellier), "Modelling active transport and spatial-temporal organisation of motor proteins along the cytoskeleton" (poster), I. Neri, N. Kern, A. Parmeggiani
- GDR 2588 "Microscopie fonctionnelle du vivant", 2012 (Toulouse), "Cytoskeletal Transport: Stochastic Model and Simple Topological Elements" (poster), A. Raguin, N. Kern, A. Parmeggiani
- Journées du GDR 3070 "Physique de la cellule au tissu", 2012 (Autrans), "Cytoskeletal Transport: Stochastic Model and Simple Topological Elements" (poster), A. Raguin, N. Kern, A. Parmeggiani
- Journées plénières, Physique de la cellule au tissue, 2011 (Lille), "Transport on networks" (short talk), I. Neri, N. Kern, A. Parmeggiani
- Workshop on Systems Biology, 2011 (Lübeck), "Transport on networks" (poster), I. Neri, N. Kern, A. Parmeggiani
- GDR 3070 "Physique de la cellule au tissu", 2011 (Lille) , "Cytoskeletal Transport: Stochastic Model and Simple Topological Elements" (poster), A. Raguin, N. Kern, A. Parmeggiani
- EMBO Conference "Physics of the Cell: From the Edge to the Heart", 2009 (Primosten, Croatie), "Non-equilibrium Collective Transport on and off Molecular Highways" (poster), B. Embley, N. Kern, A. Parmeggiani
- Journées plenières du GDR 3070 "CellTiss", 2009 (Dourdan), "Non-equilibrium Collective Transport on and off Molecular Highways" (poster), B. Embley, N. Kern, A. Parmeggiani

Chapter 2

Simple fluids mimicking globular proteins

2.1 Tour d'horizon

The phase behaviour of simple, or not quite so simple, fluids is obviously a huge topic, and research over the last century has progressively made it possible to link the macroscopic behaviour of fluids to the microscopic features of the interactions between its constituents ('particles' in the following) [13,90]. This is an important conceptual progress from the point of view of fundamental physics, but also has many direct applications. In particular, this holds for the problem of protein crystallisation, which is an important issue in structural biology. Accordingly, the questions addressed in this section are motivated by experimental situations, but may also be viewed as fundamental considerations.

Indeed, initially the notion of fluids is often understood in molecular terms, its constituents ('particles') taken to be atoms or simple molecules. The interactions then are the direct physical interactions (electrostatic forces, Van der Waals forces etc.) if one is interested in making predictions on any particular sample or material. However, one important achievement, and a rather beautiful one, due to research on 'simple' fluids is the fact that it is possible to largely simplify the interaction potential, for example in the spirit of a Lennard Jones fluid, and still preserve its essential features. In this frame of mind one sacrifices the ability to quantitatively predict material properties (such as the melting point, the heat capacity etc.) for a specific substance. On the other hand, the approach allows to establish a deeper understanding of what the *generic* features are due to. In the above example, the Lennard Jones potential, which combines a hard core-like repulsion with an attraction, produces a gas phase, a liquid phase and a solid phase. It thus allows one to study all corresponding transitions, in a rather generic way, but which remains useful for many materials once the interaction parameters are adjusted accordingly.

It is both convenient and intriguing that even simpler models allow to further analyse the generic phase behaviour of liquids, and in fact obtain further insight. Indeed, one may be surprised at how much one can learn from almost caricatural potentials like hard sphere repulsion or square well attraction, or slightly more sophisticated variations thereof (hard ellipsoids, sticky hard spheres, etc.). Historically this push for further simplifications was of course due to constraints of analytical tractability, but it is also this approach which has made it possible to address many issues based on computer simulations from a very early stage on. As an example, it is remarkable how the very first simulations of hard sphere liquids [3, 203] have allowed to make the point that hard spheres, despite being purely repulsive, undergo a freezing transi-

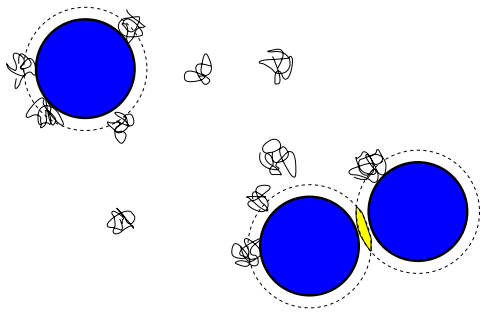

Figure 2.1: *Schematic illustration of a depletion interaction, here having in mind a suspension of colloids (large spheres) to which coiled polymers are added. Due to the steric interaction of the colloids and the polymer coils, spherical on average, the centre of gravity of the latter cannot access the 'depletion shell' around the colloidal particles. As two colloids approach their depletion shells overlap, thus reducing the overall depleted volume, which therefore effectively increases the available free volume. Attraction through depletion is thus seen to be an entropic effect.*

tion. This approach has provided decisive evidence for the presence of a real phase transition, driven by an entropic effect, rather than an artifact due to an approximation in the analytical treatment. The problems considered in the following may be viewed in the line of such considerations on simple (or not quite so simple) fluids. But they are also directly inspired by questions relevant for experimental systems.

Colloidal suspensions It turns out that the hard sphere liquid is also a very natural starting point for describing colloidal suspensions. Here the size of the interacting particles are not atomic but rather, for artificially produced colloids, micrometric. Their interactions can be complex (and typically they are), including electrical charges, counter-ions in the solution, Van der Waals forces, etc. In addition, special procedures are used in experiments as to modify the interactions in order to stabilise the colloids against aggregation (such as application of polymer brushes to the surface) and against sedimentation (density matching), but also to achieve better visibility in light scattering experiments (refractive index matching). Finally, more and more frequently selected molecules, and in particular bio-molecules, are grafted to the colloids in order to achieve specific interactions [52]. Despite this complexity, it is obvious that the steric exclusion between colloidal particles remains a major effect, and thus the hard-sphere repulsion may indeed serve as a first, albeit crude, description of the interaction between colloidal particles.

Depletion interactions One advantage in using colloidal systems, rather than atoms, to study collective effects and phase behaviour is that one can intervene and tune the interactions. One particularly convenient way to induce a well controlled attraction is by means of adding polymer molecules to the suspension. The idea here is that each polymer chain forms a coil of a certain (average) size corresponding to its radius of gyration, typically chosen smaller but not much smaller than the colloids. Therefore its centre of gravity cannot approach the colloids beyond the radius of gyration, which corresponds to a depletion zone around each colloidal particle (see Fig. 2.1 for a schematic illustration). As two colloidal particles approach, their respective depletion zones overlap, which in turn frees volume elsewhere for occupation by the polymer coils, which thus ultimately leads to an entropic attraction. The resulting so-called *depletion interaction* [7] is therefore a way to induce an attractive interaction between colloidal particles, the size of which is set by the radius of gyration of the polymer coils, and the intensity of which can be adjusted via the polymer concentration. These qualitative arguments have

been made explicit by Vrij [197] and its effect on applied to the phase behaviour of colloidal particles, explored both theoretically [74] and experimentally [128].

The upshot here is that the interactions between colloidal particles can be tuned, and that depletion forces may be used to provoke a short-ranged attraction on top of the hard-sphere excluded volume interaction.

Proteins and protein suspensions One particularly interesting case where a description in terms of colloidal suspensions proves useful concerns proteins, as they are omnipresent in biological cells.

Proteins are macromolecules, consisting of a chain of typically several hundreds of amino-acids in a sequence specific to each variant of protein, synthesised by living organisms according to their genetic code [2]. This sequence constitues the *primary structure* of a protein. But the interactions between the amino-acids also imply a certain local structure, which typically organises the polypeptide chain in terms of common motifs (alpha-helices, beta-strands or beta-sheets), which are stabilised by hydrogen bonds between the amino-acid groups; this is known as *secondary structure*. These local sub-structures in turn spatially organise in a specific way, which thus defines the protein's *tertiary structure*. Often (but not always) this results in rather compact structures, and in this case we speak of *globular* proteins.

The process how the protein chain curls into its final shape is known as *protein folding*, and is highly non-trivial: Molecular Dynamics simulations of the folding process are only just becoming possible, for proteins with a particularly fast folding process and with huge computational effort. Other approaches are typically based on highly simplified models for the interactions between the amino-acids, coarse-grained and not including explicit solvent molecules. A major difficulty is that, as it turns out, there is typically a large number of intermediate metastable states which the conformation gets trapped in. Indeed, studying artificial 'proteins' made of random sequences of amino-acids has highlighted this process, which is often assimilated to 'glassy' dynamics, thus exposing the difficulty in predicting the folding process [145]. As a result, predicting the stable structure of a protein based only on its sequence of amino-acids is a timely field of research, but such predictions remain extremely difficult.

This has furthermore direct implications for biologists, since the full 3d structure of a protein determines which functional groups are exposed at the surface of the globule, and this in turn gives valuable hints at the biological function which the protein carries out in an organism. To measure the difficulty, one may consider that even mutations of single amino-acids have been shown to modify the interaction between the proteins significantly [72].

Protein cristallisation as a colloidal problem In practice, the structure of proteins is thus essentially determined using X-ray crystallography. These experiments are not only difficult to analyse, but also require crystals, and good quality crystals for that matter, for the scattering methods to work. Unfortunately, the task of achieving protein crystallisation is a tremendously difficult task: there is no straightforward stategy which would allow to predict the appropriate conditions to provoke crystallisation within a particular sample of proteins in solution. Indeed, looking at some of the 'nucleating agents' tells a tale by itself: cellulose, dried seaweed and horse hair are among them [41]. Achieving protein crystallisation is thus often a matter of trial and error, using educated guesses based on what has worked for similar proteins, and thus often requires significant time to succeed (if succeed they do). Consequently the cristallisation step is often the main bottleneck in experimentally determining the structure

of a protein: it has been estimated that, even today, appropriate crystallisation conditions have been found not even for 30% out of those proteins which have been expressed and purified. As a result, all in all we know the structure of only about one percent of the 10 million distinct protein sequences known [71]. Any attempt at providing physical insight is thus bound to be acknowledged even for any partial success.

At this stage it is useful to realise that proteins in suspension may be viewed as colloidal particles. They differ from the artificial ones in that their size is in the namometre range (as opposed to micrometres for artifical colloids). But also, whereas the synthesis of colloids typically leads to a polydisperse size distribution (typically of the order of a few percent), the size distribution of proteins is essentially monodisperse by construction: since they have an identical sequence they fold to an identical structure (if we exclude a small portion of misfolded configurations and the existence of several competing folded states, a case we will return to in the following).

One may thus hope that a description in terms of colloidal fluids might be applicable to protein suspensions, or at least so for a majority of globular proteins. Experimental evidence that this is indeed the case has been provided [75,167], pointing to the fact that the crystallisation curves of a number of (globular) proteins can be understood in terms of hard spheres with a short-ranged (Yukawa) attraction [88]. They built on the observation that the interactions between colloidal particles can be characterised by an overall 'attractiveness', quantified by the (second) virial coefficient.

Virial coefficients Virial coefficients are most conveniently introduced through an expansion of the pressure-density relation in terms of the particle number density ρ:

$$\frac{p}{k_B T} = \rho + B_2\,\rho + B_3\,\rho^3 + \dots \; . \tag{2.1}$$

They thus characterise the non-idealness of particles, i.e. their interactions. It is furthermore interesting for our purpose that the first correction term, the second virial coefficient B_2, can be measured experimentally in light-scattering experiments [4].

A link with the microscopic vision of statistical physics can be made via the relation

$$B_2 = \frac{1}{2}\int_0^\infty \left(1 \,-\, e^{-u(r)/kT}\right)\; 4\pi\, r^2 dr \tag{2.2}$$

which links the second virial coefficient directly to the interaction potential $u(r)$ between *pairs* of particles (which, for this discussion, we have taken to be isotropic). It thus reflects the *overall* attractiveness ($B_2 < 0$) or repulsiveness ($B_2 > 0$) between particles, but carries no trace of their range.

The main point of Rosenbaum et al. [167] as well as George and Wilson [75] has been to show that the crystallisation conditions for many globular proteins can be associated with a particular window in the virial coefficient. An interpretation in terms of the physics of phase transitions can be made as follows.

Nucleation and gelation It is worth recalling that, depending on the interaction parameters, a fluid-fluid critical point may not be present in the equilibrium phase diagram. Typically, an attraction of sufficient range is required for a stable fluid-fluid phase [74]. However, even when the fluid-fluid phase is metastable and buried in the gas-solid coexistence region, the

location of the fluid-fluid critical point remains important with respect to crystallisation. Indeed, this has been illustrated by Ten Wolde and Frenkel [189], using computer simulations of a Lennard-Jones fluid. They have shown that in this case the nucleation rate for forming crystallite germs which are sufficiently large to initiate crystallisation is increased by orders of magnitude close to the fluid-fluid critical point. This effect, which can be attributed to the presence of critical fluctuations, therefore suggests a potentially interesting way to provoke crystallisation.

Modelling strategy In terms of a modelling strategy, the choice is necessarily simple. Representing each amino-acid by an atomistically realistic potential, or even and effective atomic potential, is not feasible in terms of the required computing power. One could thus envisage models regrouping parts of the protein chains into effective units, representing for example sections of alpha-helices or beta-sheets, as an attempt to devise effective interactions between these. This is indeed an approach which is useful for understanding details in the structure of proteins and the associated functions they perform, but it requires significant input in terms of the protein structure. For the question of protein crystallisation raised above, however, this is not an option, since the structure is unknown: the goal is to attempt to determine crystallisation conditions for experiments, precisely in order to determine this structure. The way to cut this gordian knot is to start from overly simplistic models, retaining only the essential features of the interactions, and to establish an overall understanding of the phase behaviour of protein solutions. This is quite in line with the above discussion on modelling colloidal interactions, the models of which will be borrowed. In practice it amounts to re-defining the goal as making predictions for typical proteins, or certain classes of proteins, acknowledging the fact that they may not hold for those proteins showing specific features in their structure or in their interactions.

2.2 Selected publications

The introduction has outlined a range of phenomena involved in the crystallisation process of proteins, and leaves many open questions. Amongst them are the following. Can the virial coefficient systematically be used to characterise the fluid-fluid critical point of protein suspensions? Can simulations help to elucidate the nature and dynamics of a gel of particles? Can one devise criteria to understand under which circumstances gelation is expected to interfere with crystallisation? The following discussion briefly summarises the research contributions I have been involved in concerning these questions.

2.2.1 Gelation vs. fluid-fluid coexistence

Reference to the original work:

> *"The role of long-range forces in the phase behavior of colloids and proteins"*
> *Massimo Noro, Norbert Kern and Daan Frenkel*
> *Europhys. Lett., p. 332 (1999)*

As argued in the introduction, it is a useful starting point to describe a protein suspension as a fluid of simple colloidal particles. Amongst others, this provides hints at what might be underlying the observation that the crystallisation conditions of many different proteins all fall into a narrow window characterised by the value of the second virial coefficient. In essence, the argument is that there is a metastable fluid-fluid critical point, which leads to critical fluctuations which, in turn, help the formation of a crystal by lowering the nucleation barrier [189].

However, the same mechanism does *not* appear to hold for the artificially produced colloids, thus contradicting the above analogy between protein solutions and colloidal suspensions. Indeed, rather than showing a fluid-fluid coexistence, colloidal solutions instead produce a disordered gel-like structure which turns out to be metastable but very long-lived, which can delay or suppress crystallisation [100, 181]. In this respect, one has to be aware that the equilibrium phase diagram does not contain all elements required as to the formation of a crystal. To that matter, it is entirely possible that a suspension which is expected to crystallise will instead evolve to a disordered metastable state, with a cluster spanning the whole sample and which can be very long-lived. This is known as *gelation*, and whenever such long-lived metastable structures form it becomes exceedingly difficult to obtain a crystal. In order to establish a comprehensive understanding of the differences between suspensions of colloids and proteins, it is thus important to elucidate this point.

The difference in scale (proteins are a thousand times smaller than colloids) should not matter as such, since the particle size only sets the reference scale on which the range of interactions are to be measured. The interactions between proteins on the other hand cannot be expected to be necessarily similar to those between colloids, which opens a very complex discussion. However, basing the arguments on simplified, schematic interactions opens a path for exploring the effect of such differences. For example, directionality may be expected to play a role (see below). The present study provides a qualitative argument showing that it may be the presence of long-range forces which accounts for the absence of gelation in protein solutions.

The argument may be made in three steps.

Fluid: Short-ranged vs. long-ranged attraction Here we wish to point out the respective roles of long-ranged and short-ranged contributions to the attraction. To make our point we oppose somewhat schematically two extreme contributions, one with an infinitely short range (in the spirit of Baxter's 'sticky spheres' [11, 16], see below) and the other one with an infinitely long-ranged (Van-der-Waals mean-field) attraction.

For the long-ranged attractions, we attribute them to *pairs* of particles, considering their range to be infinite. This leads to a pressure term proportional to the square of the particle density, but indifferent to the particle positions:

$$u_{vdW} = -\alpha\,\eta^2 \tag{2.3}$$

where α is a constant and we have used the packing fraction η

$$\eta = \frac{\pi}{6}\,\sigma^3\rho \sim \rho\ , \tag{2.4}$$

which is proportional to the number density ρ, for compatibility with the following expressions.

As concerns the short-ranged attractions, it is important to realise that the precise distance dependence is not crucial for *very* short ranges (compared to the particle size) [162, 163]. We can thus consider for example an attractive potential of the form

$$u_\epsilon(r) = -\epsilon\left(\frac{r}{\sigma}\right)^{-n} \tag{2.5}$$

for an exponent n, where σ is the particle diameter and ϵ is the coefficient setting the attraction strength of the short-ranged contribution. For numerical purposes we have used $n = 50$ in order to ensure a very short range, but analytically it is convenient to assimilate the potential

to the limiting case of *sticky hard spheres* introduced by Baxter [11, 16]. These are conceived as a somewhat subtle limiting case where the attraction is only present upon contact (zero range) but where the attraction is infinitely strong. These two limits are taken simultaneously, maintaining the virial coefficient constant, which therby characterises the 'sticky' limit.

Role of the virial coefficients The analytical arguments are helped by this scenario since every contribution to the interactions corresponds to a particular distance: hard sphere exclusion for $r < \sigma$, 'sticky' attraction for $r = \sigma$ and (constant) long-range attraction for $r > \sigma$. This simplifies determining the virial coefficient from the potential via Eq. (2.2), since every contribution to the potential leads to an additive term in the virial coefficient:

$$B_2 = B_2^{(HS)} + \Delta B_2^{(SS)} + \Delta B_2^{(VdW)} \quad , \tag{2.6}$$

where both attractions contribute negatively to the virial coefficient.

It will furthermore be convenient to characterise the respective attractiveness of each attractive contribution by a *stickiness coefficient* τ, anologous to the one introduced by Baxter for sticky hard spheres:

$$B_2 = B_2^{(HS)} \left(1 - \frac{1}{4\,\tau_{SS}} - \frac{1}{4\,\tau_{VdW}}\right) = B_2^{(HS)} \left(1 - \frac{1}{4\,\tau_{eff}}\right) \tag{2.7}$$

where the factor of four is pure convention.

Equilibrium phase diagram The equation of state can now easily be established from the three contributions. The starting point for the pressure-density relation in the fluid phase is the Carnahan Sterling equation of state for hard spheres [32]. We must then add a contribution accounting for the stickiness, established by Baxter, which depends on the density and the 'stickiness' parameter τ^{SS}. And finally a simple mean-field term represents the infinitely long-ranged attraction:

$$P_{fl} = p^{(HS)}(\eta, T) \;+\; p^{(SS)}(\eta, T; \tau_{SS}) \;+\; p^{(VdW)}(\eta, T; \tau_{VdW}) \;. \tag{2.8}$$

A similar argument can be made for the solid phase, using the inverse-power potential and applying a cell theory where all particles are assumed to rattle around their position in the crystal, as in [40].

Based on these constitutive equations the phase diagram can now be solved for numerically via the Maxwell construction. They are conveniently characterised in terms of the total attractiveness parameter τ_{eff}, which thus accounts for the *overall* attractiveness due to both long-ranged and short-ranged contributions. Three results are shown in Fig. 2.2, contrasting the case of short-ranged interactions only ($\alpha_0 = 0$) with two others having progressively more long-ranged contributions. At this stage we discuss the phase boundary of the solid phase (continuous line) and of the fluid-fluid phase (dashed line).

One thus sees that the location of the fluid-fluid critical point varies very little as the attraction is shifted from the short to the long range; this is coherent with the results by Vliegenthart et al. [195]. Furthermore, the fluid-fluid phase is metastable for the parameter range considered, and would become stable only if the long-range attractions became yet more important, in agreement with results by Ilett et al. [100]. This sets the scene for discussing gelation.

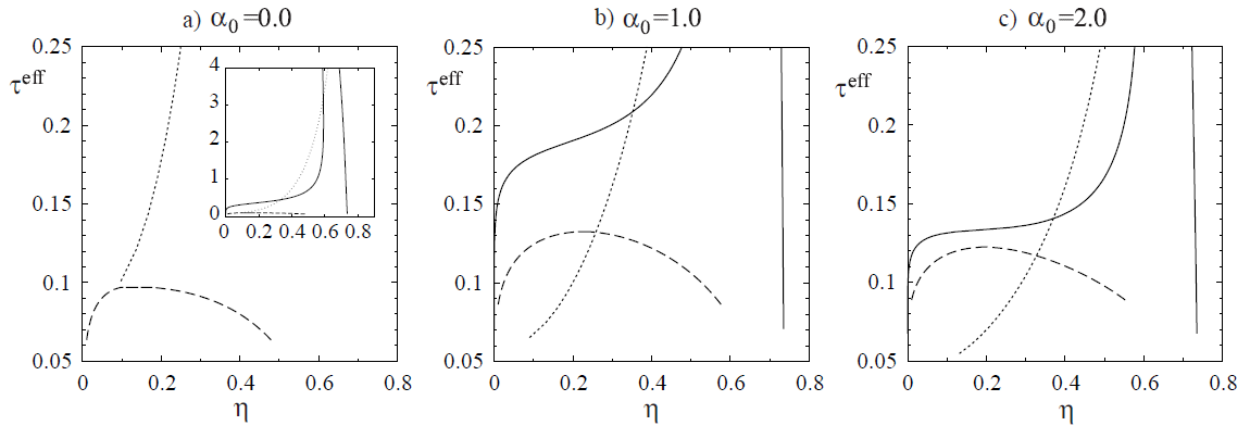

Figure 2.2: *Phase diagrams obtained for the same overall virial coefficient B_2, but with short-ranged attraction progressively being replaced by long-ranged ones. Gelation may arise below the (dotted) percolation line. As short-ranged atttractions dominate, the (metastable) fluid-fluid critical point is seen to lie in the region where gelation may interfere, thus impeding an acceleration of the crystallisation process due to critical fluctuations. It is freely accessible, however, if a significant part of the attractivity is provided by long-ranged forces.*

Percolation and gelation The question we have set out to address was how gelation is expected to interfere with crystal nucleation. However, gelation is a complex process, and even determining the microscopic nature of the gel structure is not a simple matter since it is formed out of thermal equilibrium. Rather than discussing gelation as such, one can make the assumption that it corresponds to a space-spanning structure. Thus gelation requires *percolation*.

The criterion for percolation to occur in a system of sticky hard spheres is known from the work by Chiew and Glandt [33],

$$\tau_{SS} \leq \frac{1 - 2\eta + 19\eta 2}{12\,(1-\eta)^2} \tag{2.9}$$

and the corresponding percolation line is also shown, as a dashed line, in Fig. 2.2. Note that the criterion (2.9) is not expected to vary significantly in the presence of additional long-ranged attractions, which would not have a significant effect on the structure of the fluid; this has indeed been shown to be the case even for electrostatic long-range interactions [106].

The main observation is that, as the attractiveness is progressively shifted from the short range to the long range, the percolation line moves towards higher densities. The key point, however, is the position of the fluid-fluid critical point with respect to the percolation line: it falls into the percolation zone when only short-ranged attractions are present. In contrast, it moves out of the percolation domain as the long-ranged contribution is increased.

Conclusion We can now interpret this result in the context of experiments on colloidal suspensions as well as on protein solutions. One should first remark that long-ranged forces must expected to be present, to a certain extent, in all such systems. This is particularly true for proteins, for which the interactions are very complex indeed. For colloids, however, the typical experimental approach is to perform *index matching*, which consists in producing the colloidal particles in such a way that their optical index is very close to the aqueous environment: this is done in view of light scattering experiments, which allow to penetrate into the bulk of the suspension only if the occurrence of multiple scattering can be limited. But this also amounts to suppressing the attractive, long-ranged dispersion forces.

Consequently, the presence of long-ranged attractions are one element which distinguishes experiments on proteins from those on colloids. The above considerations suggest that their effect may be to liberate the fluid-fluid critical point from the zone of percolation, for which one may expect gelation to occur. Accordingly, the critical fluctuations, which can help nucleation of a crystal, could be exploited for protein solutions, but not for (index-matched) colloids. And gelation is indeed seen to interfere in colloids, but not in proteins. Although this argument cannot rule out other explanations (such as polydispersity, directional attractions, etc.), the presence of long-ranged forces thus indeed constitutes one coherent explanation for the differences observed in experiments.

2.2.2 Fluid-fluid coexistence of 'patchy' particles

Reference to the original work:

> *"Fluid-fluid coexistence in colloidal systems with short-ranged strongly directional attraction"*
> *Norbert Kern and Daan Frenkel*
> *Journal of Chemical Physics 118, 9882 (2003)*

Another, arguably very important, feature of proteins is that their interactions are not typically isotropic, but must be expected to have strongly directional contributions. Indeed, the complexity of their folded structure provides many reasons for this, such as non-uniform surface charges, hydrophilic or hydrophobic zones due to the section of the chain exposed at the surface of the protein, or the occurence of hydrogen bonds between specific parts of the amino-acid chains. The directionality is also relevant from a biological point of view, since they allow for key-lock like interactions which are omnipresent in biological processes. They also constitute another factor which must be expected to have an impact on the phase behaviour, and thus on crystallisation conditions. Previously, the interest in directional interactions has often been motivated by questions relating to structural details in water [77, 192], where hydrogen bonds play an important role. Today, one may also invoke complementary considerations, such as the possibility of realising the corresponding experiment, by confering directional interactions to colloidal particles [205, 207] or producing entirely new molecules with altogether innovative directional interactions [20].

We have therefore set out to devise a model which consists of hard spheres with an additional short-ranged attraction, limited to localised zones ('patches') on their surface. Each such patch α is described by its location on the sphere (parametrised through a unit vector $\hat{t}_\alpha$, and an opening angle δ), as indicated in the sketch (see Fig. 2.3). A particle can then carry n such patches which, for the sake of this study, we assume all to be identical.

We use a potential of hard spheres with a short-ranged square-well attraction, but which is limited to those orientations where (any) two patches face (see Fig. 2.3). Representing the orientation of a particle by $\tilde{\Omega}$, we have

$$u_{ij}(\vec{r}_{ij};\, \tilde{\Omega}_i, \tilde{\Omega}_j) = u_{ij}^{(hssw)}(r_{ij}) \;\cdot\; f(\tilde{\Omega}_i, \tilde{\Omega}_j) \quad . \tag{2.10}$$

for the interaction between particles i and j, thus factorising the radial and the orientational degrees of freedom. Here the radial interaction potential is as hard sphere square well (hssw)

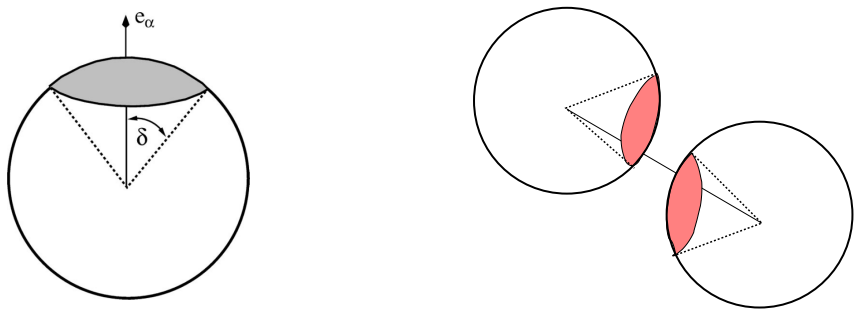

Figure 2.3: *Illustration of the geometry of an attractive patch and of the patch-wise attraction. Each particle carries patches on its surface. The corresponding solid angle is characterised by the (half) opening angle δ. An attractive interaction arises whenever two particles have facing patches, i.e. if the vector $\vec{r}_{ij} = \vec{r}_i - \vec{r}_j$ joining their centres passes through some patch on both particles.*

potential with a cutoff at $\lambda\sigma$:

$$u_{ij}^{(hssw)}(r) = \begin{cases} \infty & \text{for} \quad r < \sigma \\ -\epsilon & \text{for} \quad \sigma \leq r < \lambda\sigma \\ 0 & \text{for} \quad \lambda\sigma \leq r \end{cases} \quad . \tag{2.11}$$

The 'patchy' orientational part is taken to be

$$f_{ij}(\hat{r}_{ij}; \tilde{\Omega}_i, \tilde{\Omega}_j) = \begin{cases} 1 & \text{if} \begin{cases} \text{both} & \hat{e}_\alpha \cdot \hat{r}_{ij} \leq \cos\delta \quad \text{for some patch } \alpha \text{ on } i \\ \text{and} & \hat{e}_\alpha \cdot \hat{r}_{ij} \leq \cos\delta \quad \text{for some patch } \beta \text{ on } j \end{cases} \\ 0 & \text{otherwise} \end{cases} \quad . \tag{2.12}$$

The role of the angular modulation function $f(...)$ thus is to limit the attraction to those relative orientations where particles i and j have two patches facing each other. The decoupling between radial and angular degrees of freedom is convenient, and in particular allows to establish an analytical expression for the second virial coefficient.

A choice has to be made as concerns the patch distribution on the particles. We have chosen to study distributions among those which preserve a certain degree of symmetry: those of n=2 patches on opposing sides, n=4 patches in a tetrahedral arrangement and n=6 patches with a cubic symmetry. For each of these we vary the degree of directionality, by varying the patch size until they touch (thus excluding overlapping patches). We also consider the role of the attraction range, juxtaposing results for $\lambda = 1.5$ and $\lambda = 1.25$. In order to compare the different patch geometries on a common footing we define the *surface coverage*

$$\chi = n \ \sin^2\left(\frac{\delta}{2}\right) \quad , \tag{2.13}$$

indicating which fraction of the surface is covered by attractive patches.

Computational approach: Gibbs ensemble and parallel tempering Here we have set out to study the effect of directionality on the fluid-fluid coexistence, using Monte Carlo simulations. A well-adapted tool is the Gibbs ensemble method [69, 179, 180], which consists in simulating two boxes at once. In addition to the Monte Carlo moves for particle displacements one then allows for a stochastic exchange of both volume and particles (while keeping the *total* volume and particle number constant). This exchange equalises both pressure and chemical potential between the two boxes. Therefore, if the overall density is chosen within the coexistence

region, this procedure leads to coexisting fluids of different densities, one in each simulation box. Since this circumvents the appearance of an interface, it greatly limits the impact of finite size effects and the method is therefore ideally suited for mapping out the fluid-fluid binodal.

We have used the Gibbs ensemble method, which has worked well as long as the attraction range was not too short and the directionality was not too pronounced. Otherwise the equilibration process became very slow and did not allow to achieve equilibrium within in a reasonable simulation time. To address this problem, we have resorted to regular NVT Monte Carlo simulations, for which one can accelerate equilibration using the method of *parallel tempering*. It consists in simulating, in parallel, several copies of the system, each one at a slightly different temperature ($T_1 < T_2 < T_3 < ...$). In addition to the regular Monte Carlo moves, regular attempts are made to swap entire configurations between adjacent temperature levels i and j, which are accepted with a Metropolis-like probability [76]

$$p = \min(1, e^{-(\frac{1}{T_i}-\frac{1}{T_j})\ (E_j-E_i)}). \tag{2.14}$$

where $E_j - E_i$ is the energy difference between the two configurations at temperatures T_i and T_j. The idea is that this can help the system to evolve towards equilibrium, especially when this requires passing through energetically unfavourable configurations, which typically correspond to long-lived states at low temperatures. The exchange between temperature levels essentially allows to stochastically promote configurations to higher temperatures where they evolve more easily, such that they eventually return to their initial temperature level as a statistically independent configuration. The rule given by equation 2.14 is designed to guarantee detailed balance, and thus to respect thermal equilibrium [56, 69, 76].

Fluid-Fluid coexistence curves The simulation results show that the fluid-fluid critical temperature decreases as the attraction range is reduced, or as the surface coverage decreases. Both results are expected, and are consistent with the difficulties in equilibrating the configurations indicated above, which arise at lower temperatures. The critical density is found not to vary significantly. For a given range, the coexistence curves collapse onto a master curve when plotted in terms of the rescaled units of T/T_c and ρ/ρ_c. Its width depends on the attraction range (as expected, see [192]), but neither a variation in patch number nor in surface coverage destroys this universality.

However, when relating the fluid-fluid critical temperature to the corresponding virial coefficient (or, equivalently, the corresponding 'stickiness' parameter as defined by Eq. (2.8), one sees that particles with 'patchy' interactions do deviate significantly from those with isotropic attractions. Consequently, the fluid-fluid transition is no longer characterised by its virial coefficient as soon as the surface coverage falls below 60 or 70%, as is illustrated in Fig (2.4). The critical virial coefficient is *lowered* by directionality (it becomes more negative), which reflects the fact that more attractivity is necessary to achieve phase separation. This is consistent with the observation that an additional loss in configurational entropy must be overcome as the fluid is formed.

This is an important observation, since it clearly shows that one cannot hope to use the second virial coefficient as a guide to targetting the fluid-fluid critical point in a system with strongly directional attractions.

It is furthermore interesting to remark that these deviations are stronger for short attraction ranges, in the sense that they appear already for higher surface coverages, i.e. closer to the

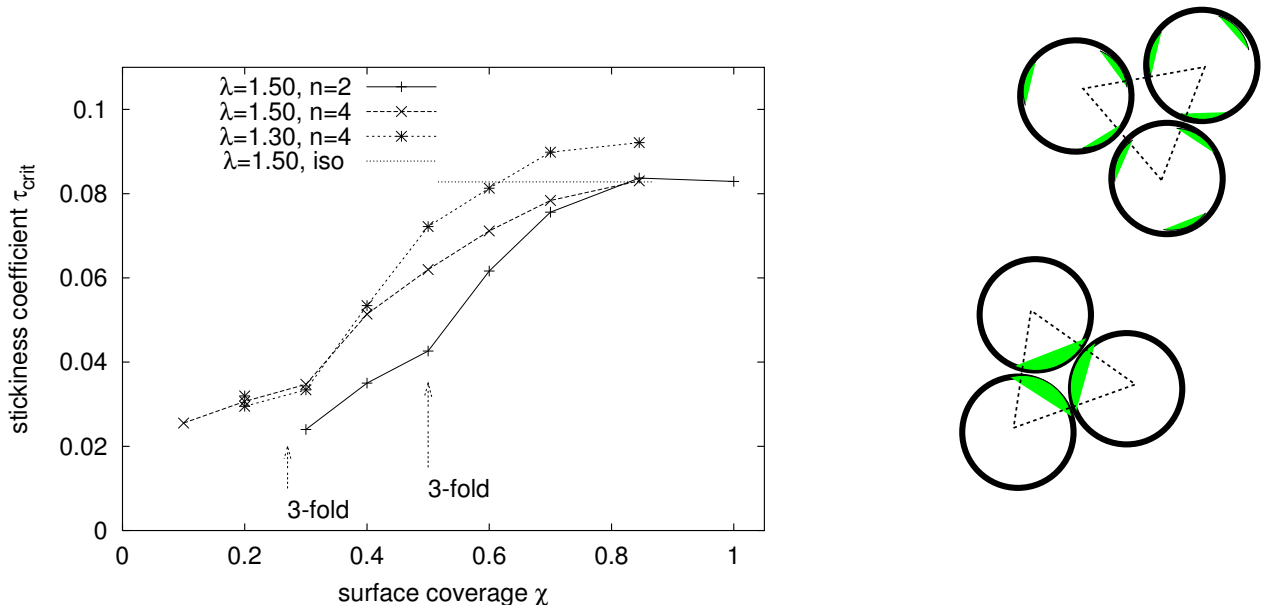

Figure 2.4: *Stickiness coefficient corresponding to the fluid-fluid critical point for spheres with 'patchy' attractions, here in a tetrahedral arrangement on the particle surface (n=4) and for two patches at opposing poles (n=2). Two values for the attraction range λ are considered. As the patches become smaller, the critical point is no longer characterised by the virial coefficient (directly related to the stickiness coefficient); rather, a higher stickiness (smaller τ) is required to achieve fluid-fluid coexistence. The points where the behaviour changes significantly corresponds to those patch sizes below which there are no longer any three-particle bonds, as shown in the sketch.*

isotropic case. As the interactions become very strongly directional, however, the range of the attractions is no longer important: instead, it is now the patch *geometry* which governs the behaviour, despite an identical surface coverage rate. Thus, even in the limit of very short-ranged attractions, knowing the surface coverage of the patches is no longer sufficient to predict the fluid-fluid transition.

2.3 Follow-up

Significant progress has been made, by many contributors, since the work summarised above.

Gelation has been studied in great detail, and many of the associated phenomena have been put onto a microscopic basis. In particular, the idea has been put forward that their long-lived metastable states may be viewed as 'attractive glasses' [18, 42, 67]. These contrast with the commonly studied glasses with strongly repulsive interactions, such as excluded-volume constraints. Repulsive glasses arise as fluids are so strongly compressed that particles can no longer efficiently explore configuration space, as would be required for the system to evolve into equilibrium. For attractive gels, this slowing down is due to the short-ranged attractions, and also leads to exceedingly long-lived metastable states. In particular, such *dynamically arrested* states have been seen to give rise to a logarithmic decay of density correlation functions (rather than the usually observed stretched exponentials) [175]. There is now a huge body of work analysing such slow, non-ergodic dynamics. Experimentally, such low-density glasses have indeed been produced in the form of *colloidal gels*, based on the depletion attraction [150].

The role of the attraction range has also been explored in various ways. A combination of

short-ranged attraction and long-ranged *repulsion* has been advocated as a way to encourage longer bond life times, which would thus stabilise a physical gel [175]. In a sense this is complementary support to the argument made above, stating that long-ranged attraction hinders the formation of a gel.

The interest in patchy interactions has soared since the time of the contribution summarised above, for a variety of reasons. One important aspect continues to be their relevance to protein interactions, a point we will briefly return to below. Another reason is the fact that intererest-ing fundamental questions have been identified, to which patchy systems provide an additional angle: gelation, the formation of so-called 'empty liquids', spinodal decomposition, etc. A final reason, of utmost importance, is the fact that it has become possible to experimentally produce colloids with strongly directional attractions, and thus many of the questions related to patchy attractions designed in a particular way are becoming experimentally relevant. The idea of *self-assembly* is a major point here, which involves all of these questions and obviously has a huge potential for applications.

The patchy model introduced above has been widely used by many authors, and complemented by other models. Many aspects of its physics have been explored, in particular by Sciortino and co-workers, who have established full phase diagrams. These include, as a special case, the concept of *Janus particles*, which are essentially spherical particles carrying two patches, each of which covers half of the surface. This is an interesting limit, since it eliminates additional parameters (number of patches, patch orientations, opening angles), but still retains much interesting physics [131, 176]. But even the fully general patchy model has been studied in great detail, including the solid phase (or rather, depending on the interactions, several solid phases) [80, 166].

The alternative model encountered most often consists in defining attractive *sites* on the surface of the spherical particles, between which simple interactions are defined. The Lennard-Jones potential is often used with a suitably adjusted range: the sticky spots therefore interact isotropically, and the directionality in the interactions between particles is due to the positioning of the spots only. Remarkably, Zhang [207] have been able to produce a system with such sticky spots in the laboratory.

Maximum valency models are another way of mimicking some (but not all) effects of directionality. In these models particles are subject to strictly isotropic interactions, but are limited to establishing no more than a given number of bonds. They have been shown to help to achieve open, low-density metastable structures [175] reminiscent of a gel. Zaccarelli et al. [206] have furthermore shown that the fluid-solid coexistence is weakened in a limited-valency model. This is interesting, since it makes it possible to study the low density gels without running into phase coexisence at the same time. In particular, they have exposed a difference with respect to glasses: whereas all wavelengths are non-ergodic in high-density glasses, this is only true for large wavelengths in a gel-like low-density glass.

Several aspects of the fluid-fluid coexistence in systems with patchy attraction have been clarified. Tavares et al. [188] have shown that particles must have at least three patches for a liquid-liquid coexistence to be present. In one line of thought the question of *empty liquids* has been brought up: the way the fluid-fluid critical point evolves suggests that it may be possible to maintain fluid-fluid coexistence down to arbitrarily small volume fractions: [19]. Experimental confirmation that this should indeed be possible has been provided recently [171].

In terms of protein crystallisation, many contributions have been made recently by Charbonneau and co-workers, based on patchy models. They have exploited biological databases

in order to establish $\lambda = 1.1$ and $\cos^{-1}(0.89) \approx 27^o$ as a reasonable choice for the range of attraction and for the size of a patch if one wishes to mimic typical proteins [71]. Using these parameters they have then explored various aspects of the phase behaviour. One line of work was to incorporate the fact that most proteins do not have the strong symmetries imposed above. This is modeled [72] by randomising both the interaction strength of the patches and the patch positions (subject only to compatibility with an orthorhombic crystal structure, which turns out to be the most commonly observed structure in monomeric proteins. The observation is that this variability in patch positions tends to decrease T_c (which one can attribute to the fact that it decreases the entropy of the liquid). The asymmetry furthermore favours the growth of a single cluster, rather than having several micro-clusters which then re-arrange. Strong variability in the patch bonding energies has been seen to favour a long-lived percolating state (the 'gel'), and thereby hinder crystallisation. All in all, one can say that disorder in the bond geometry has been shown to have a rather weak effect, or at least so as long as it maintains the compatibility with the crystal structure, whereas the patch *interaction energy* is the more important parameter. In particular, Fusco et al. have shown that the Wilson B_2 criterion (specifying the crystallisation window in terms of the virial coefficient) is necessary, but not sufficient for crystallisation.

Very recently, a different approach to studying protein-protein interactions has been put forward. It goes beyond the schematic description via patchy interactions, by calling upon *multiscale simulations*. Such a procedure has been devised by De Simone et al. [178], who are interested in a particular family of proteins (hyperthermophilic rubredoxins). These have a closely packed core, and are thus reasonably well represented by a 'hard sphere'. Molecular Dynamics is then used with a detailed force resolution, based on structural details of the protein. The results are then compared to those of a patchy model (the one introduced above, but allowing for attraction energies to vary from one patch to another). The authors thus show that mapping onto hard spheres with anisotropic short-ranged attractions ('patches') is successful for the case of rubredoxin. Other results include the observation that a protein crystallises more easily if it has many (albeit weaker) patches, rather than having only a few strongly attractive patches. The study has also been able to explore the effect of structural defects in this particular protein. Interestingly, it has shown that even small changes (such as mutations in single amino-acids) can lead to significantly modified protein-protein interactions.

The drawback of this approach is of course that it cannot be used for predictive modelling, since it requires a rather detailed knowledge of the structure as input. It does, however, confirm that the modelling approach via patchy interaction potentials, even in a rather schematic fashion, can make valid contributions towards understanding the crystallisation behaviour of real proteins.

Chapter 3

Foams: structure

3.1 Tour d'horizon

Foams are those fascinating structures which form by simply stirring a little detergent in water, thus creating a volume filled of bubbles separated by films. From an academic point of view they are interesting in many respects, since they constitute a conceptually rather simple soft-matter system which shows a tremendous range of interesting phenomena. These range from the local rules (which determine its static geometry through energy minimisation), the global structure (also involving the topology of the ensemble of bubbles), to its time evolution via coarsening (due to gas exchange and fusing bubbles), drainage of liquid through an existing structure (involving highly non-trivial hydrodynamic phenomena), to its physico-chemical parameters (which can affect the hydrodynamics in rather subtle ways), to rheology (i.e. the flow behaviour of an entire foam). Foam physics therefore involves many fields of expertise, and all of them contribute additional understanding, but often also benefit from studying foams.

In addition to this academic motivation, one has to be aware that foams also find a huge number of applications, since their properties make them suitable for many different fields. Some of these are: domestic products such as cosmetics and food stuffs (for their relatively stable structure achieved with cheap ingredients), fire fighting (for very quickly yielding a huge amount of foam from very little material), nuclear decontamination (for rinsing the polluted material into a very small amount of liquid), oil production (for sweeping out porous structures), engineering (for producing strong metallic structures with comparatively very little weight) and so on and so forth. Many of these applications rely on particular features of a particular type of foam, and many of them still pose challenges to fundamental understanding.

For a physicist, foams are an intriguing system since they constitute a well-defined visco-elasto-plastic system. They are essentially defined on a macroscopic (millimetric) scale, and thermal fluctuations as such play no role. An intriguing feature is the fact that one can formulate a rather simple description of the *structure* of foam, based on mathematical idealisations, to which one can then add more evolved physical features as required. In this introduction we will recall the most fundamental points, having in mind liquid foams, such as those produced in a bubble bath as mentioned above. Dynamical features and flow will be the subject of the following chapter.

Foam structure in 2d The key to understanding foams, or at least their static structure, resides in surface tension: in essentially all situations, all structural features are ultimately due to surface tension effects.

This point is made most easily in a 2d space, where the geometry is flat and thus simple. It appears useful to make them the first example for introducing foam physics. Many terms are used interchangeably between 1d and 2d foams, and somewhat inaccurately, which is at first confusing but ultimately convenient. Here we shall make an effort to use the proper wording both for 2d and 3d foams, in order not to create any ambiguity in the vocabulary.

By a 3d foam we mean a space-filling ensemble of gas-filled bubbles, each having a certain volume, separated by surfaces which correspond to liquid films, subject to a surface tension. A 2d foam may be envisaged as being a special case of a 3d foam with a translational invariance along the third spatial dimension, or it may be seen as a strictly 2d structure, embedded in a 2d space (as mathematicians would do). In the first picture we speak of bubble volume and film area, and the physical parameters are the gas pressure in the bubbles and the surface tension in the films. In the second picture this becomes bubble *area* and film *length*, and the physical parameters are the 2d gas pressure P_{2d} (i.e. a force per unit length, in 2d) and the films are subject to a *line tension* σ_{2d} (i.e. an energy per unit length). Fig. 3.1 sketches an example, which will be useful for the following discussion. More precisely this defines what we mean by a *dry foam*, since it does not retain any finite volume of water in the films or in their intersections.

Confusion may arise from the fact that, in the picture of a translationally invariant foam structure, the points where films meet also define line-like objects (in the third spatial dimension), which are referred to as *Plateau borders*. These are obviously entirely distinct objects from the lines separating 2d bubbles, but experimental realisations of quasi-2d foams require producing a foam squeezed between glass plates, in which case the situation is more complicated. We discuss the simple case, strictly 2d foams, before returning to the subtleties involved in their experimental realisation.

A (strictly) 2d foam thus consists of bubbles separated by films, which carry a line tension. This then directly implies Laplace's law, which relates the pressure difference across a film to its curvature:

$$\Delta P_{2d} = \sigma_{2d} \frac{1}{R} \ . \tag{3.1}$$

Consequently, it is immediately clear that all films must have constant curvature, i.e. be arcs of circles (or rather, for a physicist, the surfaces produced by translating arcs of circles along the 3rd spatial dimension). This is one of the main rules for an equilibrium foam structure, known as *Plateau's rules*, here stated for a 2d foam.

The other Plateau rule, for the 2d case, is that films meet in groups of three, and at those points (called *'vertices'*) they form an angle of 120 degrees between them. This is again based on surface tension effects. Indeed, higher order vertices are energetically unstable. To see this we might envisage a 4-fold vertex, as illustrated in Fig. 3.2. It quickly becomes clear, however, that the total line length in the structure having all four bubbles meet in one point is *larger* than a configuration where we have two 3-fold vertices. Thus any 4-fold vertex is intrinsically unstable, and will be reduced into two 3-fold vertices. Furthermore, each of these films is subject to a line tension and therefore exerts a pulling force onto the vertex. Since the surface tension is the same in all three films, the vertex is bound to displace until it reaches the configuration of equal angles which ensures its mechanical equilibrium. Note that the pressures of adjacent bubbles are not generally equal, but this does not affect the equilibrium angles, since the vertex is a point-like object and thus pressure forces do not enter the balance.

Another element which is most easily illustrated in 2d is the role of *topological changes*.

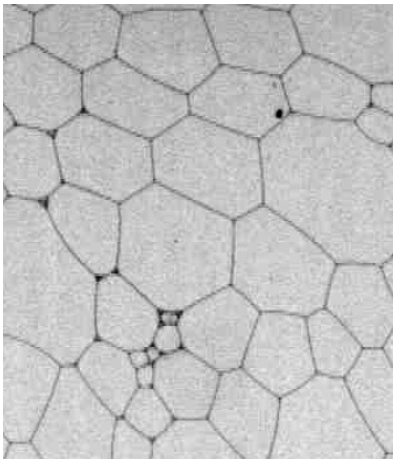

Figure 3.1: *Example of a 2d foam structure illustrating how bubbles fill space, subject to Plateau's laws (here in their 2d variants). The image has been obtained by R. Delannay and I. Cantat (Rennes).*

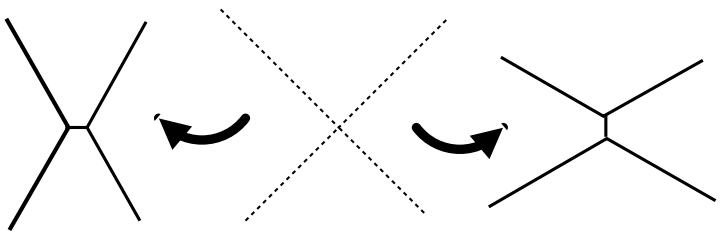

Figure 3.2: *Illustration of an unstable 4-fold vertex in a 2d foam. Plateau's laws require that, in equilibrium, films meet in threes, forming equilibrium angles of 120 degrees. Accordingly, a 4-fold vertex dissociates into two 3-fold vertices, which can form in two ways according to how the new edge is spanned, leading to different topologies. The 4-fold vertex may be seen as the intermediate step in the neighbour-swapping process illustrated in Fig 3.3.*

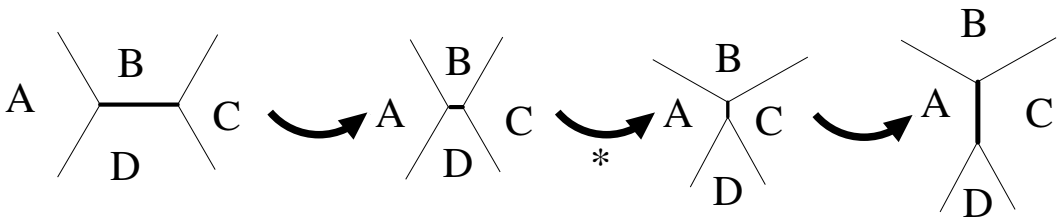

Figure 3.3: *Illustration of a T1 topological change. As the length of the edge between adjacent bubbles B and D reduces to zero, a 4-fold vertex would arise (labelled by a star). The latter being unstable, a new edge must develop in order to restore two 3-fold vertices, adjacent to bubbles A and C. This change of vicinity relations is known as a T1 neighbour swapping process.*

This is related to the statement made above concerning the instability of a four-fold vertex. We can make the concept explicit in the following example where a regular foam structure is successively deformed, in this case illustrated by a shear deformation (see Fig. 3.2). To see the topological change we focus on two bubbles which are neighbours through a common edge. But as the edge length reduces to zero a 4-fold vertex is created and, being unstable, separates into two 3-fold vertices. In this new configuration a new pair of bubbles become neighbours, whereas the initial neighbours are now separated.

This process is known as a *'T1' process*, or a 'topological change of type 1'. Other topological changes arise when an infinitesimally small bubble disappears and requires the connectivity of remaining edges to be re-defined, or when a film is ruptured and two bubbles join [199].

Dry foam structures in 3d It now remains to generalise these results to 3d foam structures. Here we are dealing with bubbles having a pressure and a volume, and they are separated by films which are subject to a surface tension. Again, no explicit water content is present in this description.

First of all, Laplace's law now reads

$$\Delta P = \sigma K \ , \qquad \text{with} \qquad K = \frac{1}{2}\left(\frac{1}{R_1} + \frac{1}{R_2}\right) \ . \tag{3.2}$$

where K is the *mean curvature* of the 2d surface corresponding to the film and σ represents the surface tension of a *film* (and not the interfacial tension γ due to the water-air interface, which will become important below and which is roughly half this value).

The equilibrium rules now become

- Bubbles are separated by films, which are of constant mean curvature, set by by Laplace's law through the surface tension and the pressure difference between adjacent bubbles.
- Films separating the bubbles meet in pairs of three, locally forming an angle of 120 degrees between them; their line of intersection is called a *Plateau border*.
- Plateau borders meet in pairs of four, locally forming a tetrahedral angle (of 109.5 degrees); the point-like structure of their intersection is called a *vertex*.

The latter rule again follows from equilibrium mechanics. These statements are known as *Plateau's laws*. Topological changes are more complex to visualise in 3d, but are equally present.

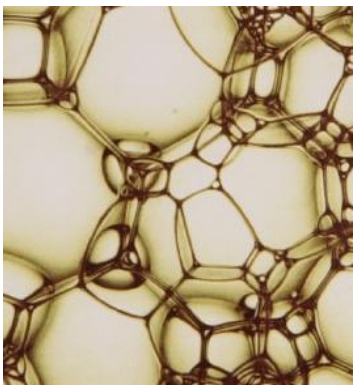

Figure 3.4: *Example of a 3d foam structure illustrating how bubbles fills space. The films separating the bubbles meet in line-like Plateau borders. In equilibrium the structure is subject to Plateau's laws. Image by M. Boran (Dublin).*

Minimum energy structures The problem of determining a foam structure thus amounts to minimising the surface energy, i.e. the total film area between bubbles (we focus on the 3d case here). The solution is obvious for a single bubble (which of course assumes a spherical shape), but it is non-trivial already for the case of a *double-bubble* if the bubbles do not have identical volume [98], and becomes highly complex for a large number of bubbles.

Part of this complexity is of course the fact that one needs to find a minimum in a high-dimensional space, which is always a difficult undertaking. There is, however, an additional aspect in the question of collectively minimising the foam structure, in that it must involve varying both the overall bubble geometry *and* the topology. Some exact results are known for regular bubble structures, with all bubbles having identical size. Thus the minimum energy structure of a 2d foam is a hexagonal arrangement of bubbles, with all straight edges: this result may appear intuitive, but has been proven rigorously only in 2001 by Hales [89]. The equivalent of this structure in 3d would be a space-filling structure of identical icosahedra, which is known as a *Kelvin foam*, after Lord Kelvin who postulated it in 1887 [190]. It turns out, however, that a slightly lower energy is achieved by the *Weaire-Phelan* structure, in which two types of bubbles intervene which, while having identical volume, carry different pressures. That this is an energetically preferable structure has been shown using numerical methods, and in particular Ken Brakke's Surface Evolver program [26]. For any more complex structures, and in particular those with unequal bubble sizes, the results become invariably complex.

Elastic moduli Elastic constants corresponding to any particular strain can be deduced directly as the linear term of the associated energy increase. For simple shear the elastic modulus G is given [199] by the relation

$$G = \frac{1}{4A} \left. \frac{d^2 E}{d\epsilon^2} \right|_{\epsilon=0} . \tag{3.3}$$

The only relevant energy being a surface energy, it follows that the elastic moduli are proportional to the surface tension γ.

Coarsening Let us also point out that we have assumed the volume of any bubble to be given. Mathematically speaking this corresponds to a constraint which is to be imposed during the minimisation process. Physically speaking, it amounts to excluding the gas exchange between bubbles across films. Depending on the physico-chemical properties of the foam, this

is often indeed a very good approximation on the time scale of experiments.

If, however, gas can be exchanged across the films, then one is dealing with a phenomenon of *coarsening*. One may take the rate of volume exchange between adjacent bubbles to be given by Fick's law, i.e. proportional to the pressure difference (and thus to the edge curvature) and of course to the film area. Denoting the permeability of the film κ it is then easy to show [199] that, for the 2d system maintaining 120 degree angles at the Plateau borders, the rate of change for the area A_b of a bubble b obeys

$$\frac{dA_b}{dt} = \frac{\pi}{3}\,\kappa\gamma\,(n_b - 6)\ , \tag{3.4}$$

where n_b is the number of sides to the bubble b. This is known as *Von Neumann's law* [196] for coarsening.

In the following we shall maintain the bubble volume constant, which thus excludes any coarsening process. Nevertheless, considerations along these lines will become useful in the following chapter when we shall introduce the viscous froth model for foam dynamics.

Wet foams The above description is obviously a simplification, which consists in describing the foam structure as if it were composed of soap films only, without any actual liquid content: this idealisation is known as a *dry foam*. The actual liquid content of a foam is measured in terms of the *liquid fraction*, defined as

$$\phi_{liq} = \frac{V_{liquid}}{V_{tot}} = \frac{V_{liquid}}{V_{liq} + V_{gas}}\ . \tag{3.5}$$

In two dimensions, at moderate but non-zero liquid fractions, the liquid is located primarily in the vertices (recalling that these are in fact Plateau borders in the third spatial dimension). Remarkably, the *decoration theorem* [198] states that any such structure in two dimensions can be thought of as a dry foam structure, the Plateau borders of which have been 'decorated' with the corresponding liquid content, and the decorated sample remains an equilibrium structure (albeit with slightly modified bubble volumes).

In three dimensional structures, liquid is essentially present in the (line-like) Plateau borders and, to a lesser extent, the (point-like) vertices. No generalisation of the decoration theorem is known. Nevertheless, the way in which one can formally conceive the dry limit in three dimensions is one of the topics to be discussed as an example below.

Drainage Gravity acts on the fluid contained in the Plateau borders and in the junctions, which causes liquid to *drain* through the network of Plateau borders. In *free drainage*, this will continue to remove liquid from the upper regions of the foam, until a local equilibrium between gravity and capillary forces is established throughout the sample. This asymptotic state is characterised by a gradient in liquid fraction. Another scenario is that of *forced drainage*, where water is continually added at the top of the foam. In this way one can establish a stationary state, where liquid drains at a steady rate through an otherwise stationary foam structure.

The question of how the liquid fraction varies with the height [157] in the asymptotic state of free drainage can be established by the local force balance on a slice through a Plateau border (here considered to be vertical). Note first that the liquid fraction ϕ_{liq} is proportional to the cross-sectional area $A(z)$ of the Plateau border, at any height z:

$$\phi_{liq}(z) = c\,A(z) = c'\,r^2(z) \tag{3.6}$$

where c and c' are geometrical constants and r is the radius of curvature of the sides of the Plateau border (see Fig. 3.8). As the cross-sectional area varies with the height there is an imbalance in the force due to hydrostatic pressure, which must compensate the weight of the liquid:

$$-\rho g\, A\, dz = p(z)\, dA(z) \ , \tag{3.7}$$

and thus, using the Young-Laplace law to relate the pressure to the local Plateau border radius ($p = p_{gas} + \gamma/r \approx \gamma/r$, the latter equality restricting the validity to the zones where the foam is still sufficiently dry, such that the Plateau border radius remains sufficiently small). This yields a differential equation for the Plateau border area $A(z)$ as a function of the vertical position:

$$dA = -\frac{c\rho g}{\gamma}\, A^{3/2}\, dz \tag{3.8}$$

and thus

$$A(z) = \left(\frac{2\gamma}{c}\, \frac{1}{c'' + \rho g z}\right) \ . \tag{3.9}$$

The constant c'' is subtle (one would expect it to be determined by matching the liquid content at the height where the foam floats on the bulk water, but here the foam is no longer sufficiently dry for the formula to hold, see [199]).

In *forced drainage* [193, 199, 201] the fluid is no longer static, and thus the force balance must also account for viscous forces. Again for a single vertical Plateau border, the simplest argument assumes that the liquid cannot flow at the boundary corresponding to the film. This is not strictly true, since the film constitutes a free interface, but it will hold if the surface viscosity of the film is sufficiently high. Then we are dealing with Poiseuille flow, for which the viscous force at the boundaries is given in terms of the average flow velocity $\bar{u}$ (averaged over the Plateau border area A). For a slice of height dz the force balance between the viscous and gravitational forces reads

$$f\, \eta_{liq} \bar{u}\, dz = \rho_{liq} A g\, dz \ , \tag{3.10}$$

where η_{liq} is the bulk viscosity of the fluid, and f is a geometric factor accounting for the shape of the Plateau border, which can be determined at least numerically. This directly yields

$$\bar{u}(z) = \frac{\rho g}{f\, \eta_{liq}}\, A \ . \tag{3.11}$$

This relation can also be interpreted as Darcy's law, viewing the Plateau border as a porous medium.

From liquid conservation we can furthermore write the flow rate Q as

$$Q = A\, \bar{u} = \left(\frac{\rho g}{f\, \eta_{liq}}\, A^2\right) \ , \tag{3.12}$$

and this directly implies $Q \sim A^2$. The flow rate imposed in an experiment thus directly sets the liquid fraction as

$$\phi_{liq} \sim \sqrt{Q} \ . \tag{3.13}$$

This scaling is an important result, and can be verified in experiments.

At this stage it remains to determine the variation of the liquid fraction with height, and to show that the intuition one may have of a homogeneous liquid fraction, and hence constant Plateau border cross sections, indeed yields a stationary state. We indicate the argument, since

it is full of physics, and will be useful for the following section. It proceeds by admitting, for the moment, that $A(z) = c\,r^2$ may vary. Then, the vertical derivative of the Laplace relation (Eq. 3.2) for the pressure drop across the Plateau border film is

$$\frac{\partial}{\partial z} p_{liq} = \frac{\partial}{\partial} p_{gas} + \frac{\partial}{\partial z} \frac{\gamma}{r} \ , \tag{3.14}$$

where γ refers to the liquid-gas interfacial tension (roughly half the surface tension, $\gamma \approx \sigma/2$). There is no significant gas-pressure gradient in a homogeneous foam (but see the discussion in the following section). Thus eliminating the Plateau border radius r in favour of its cross section A readily yields

$$\frac{\partial p_{liq}}{\partial z} = \frac{1}{2} C \gamma a^{-3/2} \frac{\partial A}{\partial z} \ , \tag{3.15}$$

which underlines that a vertical pressure gradient in the liquid directly results from the variation of the Plateau border size.

The complete force balance between gravity, viscous forces and the liquid pressure gradient now becomes

$$\frac{\partial p_{liq}}{\partial} A = \rho g\, A - f \eta_{liq} \frac{Q}{A} \ , \tag{3.16}$$

which correctly reduces to the simpler force balance above (Eq. 3.10) for a Plateau border of constant area. From this one can isolate an expression for the flow rate $Q(z)$ in terms of the cross-section $A(z)$ and its derivative $\frac{\partial A}{\partial z}$.

One can now call upon volume conservation via the continuity equation,

$$\frac{\partial A}{\partial t} + \frac{\partial Q}{\partial z} = 0 \tag{3.17}$$

and average over all orientations of Plateau borders in a foam [193], to establish what is known as the *foam drainage equation*:

$$3\eta_{liq}\, f \frac{\partial A}{\partial t} + \frac{\partial}{\partial z} \left(\rho_{liq} g A^2 - c\gamma \frac{\sqrt{A}}{2} \frac{\partial A}{\partial z} \right) = 0 \ . \tag{3.18}$$

Recall that c and f are purely numerical constants related to the Plateau border geometry. Interestingly, this equation admits a solution corresponding to a wetting front propagating like a solitary wave [193]. The simplest solution, however, is one of a homogeneous Plateau border size (and hence constant liquid fraction) throughout the sample, as was indeed the point to be made.

The above description of foam has been shown by the Dublin group to hold for experiments, including the scaling $\phi_{liq} \sim Q^{1/2}$. On the other hand, another set of experiments, performed by scientists in Harvard [114] was clearly incompatible with these results and pointed to a power law $\phi_{liq} \sim Q^{\alpha}$ with an exponent of $\alpha \approx 1/3$.

Importantly, the above model has taken into account the Plateau borders *only*. This would appear reasonable, since most of the liquid is contained in those channels, whereas the junctions only contribute a higher order term to the liquid fraction. On the other hand, all the liquid draining through the Plateau borders must also cross the junctions where they intersect. Consequently there is another contribution to the viscous forces, attributable to the junctions. Its relative importance turns out to depend on the *surface viscosity* of the films: if this is sufficiently low, there can be surface flow in the liquid-air interfaces, and we are then dealing with

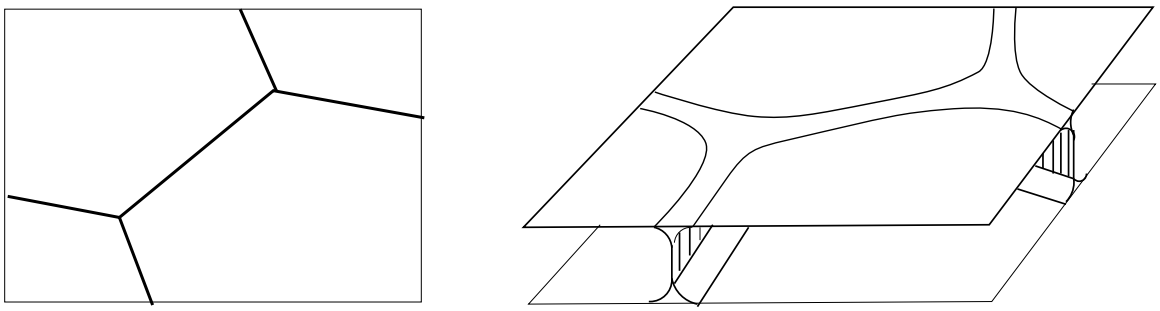

(a) Top view (b) Side view

Figure 3.5: *Illustration of the Plateau border geometry in an experimental realisation of a 2d foam, as bubbles are confined between two parallel glass plates. Films span the space between the glass plates and, in the top view (a), define the lines separating the bubbles. The side view (b) shows that each of these lines in fact corresponds to two Plateau borders, one at each plate. Each of these corresponds to three films meeting, one spanning the gap and two more corresponding to the bubble boundaries against the plates (which are strictly speaking only half-films, since they only involve one water-air interface). An ambiguity in terminology thus arises: in the top view, the lines separating two bubbles correspond to (double) Plateau borders, but they also correspond to the films separating the bubbles. Having a 2d foam in mind, it is thus more appropriate to refer to them as films. At the vertices where these films meet, they form 120 degree angles, as is appropriate for a 2d foam. A vertex corresponds in fact to another (very short) Plateau border, perpendicular to the glass plates. These geometrical aspects are important if one is interested in flow in this 2d geometry, which implies sliding of the plate-bound Plateau borders over the glass surface (see next chapter).*

plug flow (rather than Poiseuille flow) in the Plateau borders. It turns out that dissipation is dominated by the junctions, and in this case an exponent of $\alpha = 1/3$ can be deduced [114]. Experiments with direct control over the surface viscosity have confirmed that both exponents characterise opposing limiting cases [53]. The physico-chemical details can thus play a major role in drainage.

Quasi-2d foams A comment is in order to avoid confusion between the terminology in 2d and 3d foams. The simplest way to think of a 2d foam is in terms of a translational invariance of the structure, say in the z direction. All bubbles would then be infinite in this direction, and their projection onto the xy-plane yields a strictly 2d foam as it was introduced above. Consequently, the lines separating the 2d bubbles in this setup indeed represent the 2d films. However, the vocabulary becomes ambiguous in that the *vertices* in the 2d projection actually correspond to *Plateau borders* in the 3d foam, which run parallel to the z direction. A first difficulty in terminology is thus due to the fact that one may speak of the edges in a 2d foam as being subject to a line tension, but one can also be tempted to refer to a surface tension, having the underlying 3d foam in mind.

In addition, further confusion arises when one is dealing with an experimental realisation of 2d foams, achieved by confining bubbles between parallel glass plates which are separated by a distance small compared to the bubble size (see Fig. 3.5 for an illustration). In this case the (flattened 3d) bubbles are still separated by films subject to a surface tension, which project onto lines subject to a line tension (although this is only approximately true, since there may well be a curvature also in the z direction of the films). The (2d) vertices still correspond to Plateau borders running (roughly) in the z direction, but there are now other Plateau borders

where a film meets the glass plates. Consequently, the (2d) vertices also correspond to (3d) vertices, joining a vertical Plateau border with three Plateau borders, at the top and bottom plates, respectively. We will focus on this geometry in the following chapter on dynamics and flow.

3.2 Selected publications

The following pages discuss two contributions to aspects of foam structure, both related to the presence of liquid. The first argument considers the effect of the weight of the liquid, as a simple example of an applied force, and discusses the implications this has for simple 2d foam structures. Instabilities observed experimentally in foams are one point of interest. The second argument concerns the link between wet foams and dry foams, and in particular asymptotic expansion arguments as to how the dry limit is approached in foams. The analysis points to a somewhat surprising correction in terms of a (negative) line tension to be applied to the dry foam skeleton, which may lead to instabilities in numerical models.

3.2.1 Foam structure: 'loaded' foams

Reference to the original work:

"Loaded foam structures"
Denis Weaire, Norbert Kern and Guy Verbist
Phil. Mag. Lett. 84(2), p. 117 (2004)

By the concept of a 'loaded' foam we mean a foam structure subject to external forces acting on its vertices and/or on its Plateau borders. Probably the simplest example is a foam with small but non-negligible liquid content, which is subjected to a gravitational force. In this case one can resort to discussing a dry foam backbone and introduce the necessary corrections due to the external forces. Here we consider the simplest example, which is a 2d honeycomb structure, gravity acting in the plane of the foam.

In the case of a 2d foam the liquid content would be present at the vertices, and its weight would produce an external force $\vec{W}$ acting on a each vertex. We analyse the effect on a regular honeycomb lattices. In the following discussion we focus on the most instructive case where the loading force is applied parallel to one of the symmetry directions of the honeycomb lattice. In this case, analytical arguments allow to clearly expose the essence of the physics. One can easily generalise to loading in an arbitrary direction [200], but the essential conclusions remain unchanged.

Unit cell and structural deformation The hexagonal (honeycomb) structure we focus on in order to illustrate the effect of gravitational loading can be constructed by periodically replicating a unit cell involving two vertices. In our case the argument can thus be made based on two vertices constituting this unit cell, which is conveniently chosen as illustrated in Fig. 3.6.

We can distinguish two mechanisms. Firstly, the weight acting on the vertices modifies the force balance between the line tensions of the three films attached to the vertex. Consequently, we can no longer expect angles of 120 degrees. Secondly, if the ensemble of the foam is to remain at rest, the overall weight force must be balanced. This is naturally achieved by a gradient in the bubble pressures: the bubble pressures cannot remain uniform, as is the case

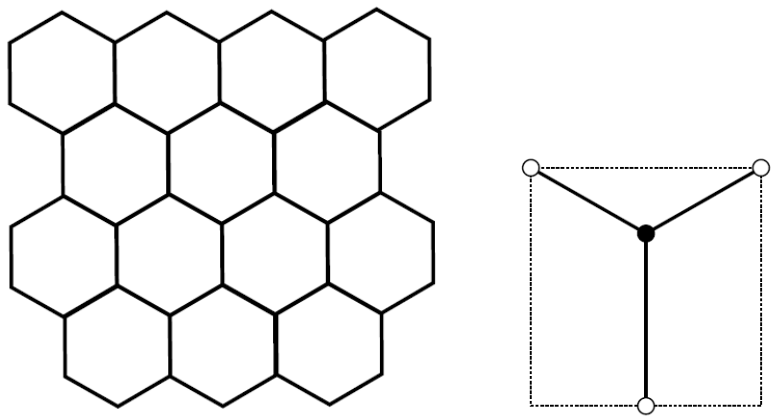

Figure 3.6: *Illustration of a convenient choice for the unit cell in loaded foams having a periodic honeycomb structure. It consists of two non-equivalent vertices, the one in the center and the one at the cell boundaries (where each of the indicated vertices contributes to three unit cells). As loading is introduced, the geometry of the entire structure can be deduced from the local equilibrium conditions at both of these vertices.*

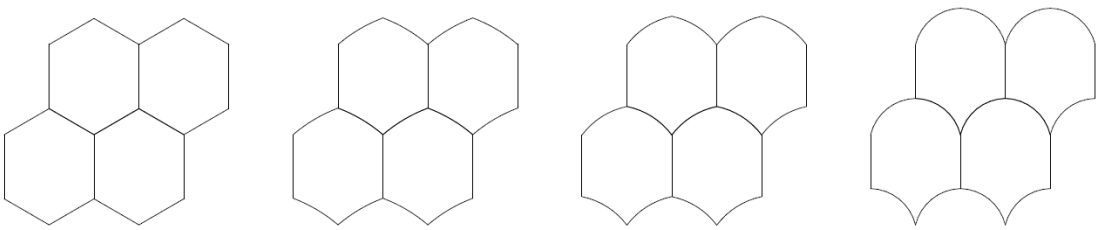

Figure 3.7: *Effect of loading on a 2d hexagonal foam, the loading force being applied downwards, i.e. coinciding with one of the symmetry directions of the hexagonal cells. The structures shown are those corresponding to a loading parameter* $W/\sigma = 0$ *(no loading), then* $W/\sigma = 0.3$, $W/\sigma = 0.6$ *and finally* $W/\sigma = 0.95$. *At the critical value* $W^*/\sigma = 1$ *the surface tension can no longer support the loading force, and the structure collapses. Picture as in [112].*

for a honeycomb structure in the absence of loading.

According to Laplace's law (Eq. 3.1) this goes hand in hand with bending the films. Their shape are easily determined: they remain arcs of circles, their curvature being set by the pressure drop between bubbles, according to Laplace's law. Unlike for the honeycomb lattice before loading, the two vertices in the unit cell are no longer equivalent, and must thus be distinguished in the model. At both of them the external force $\vec{W}$ must be balanced by the pull of the line tension. Parametrising the geometry in terms of two angles, θ and ϕ, as in Fig. 3.6, the equilibrium condition reads

$$\cos\theta = \frac{1}{2}\left(1 + \frac{W}{\sigma}\right) \tag{3.19}$$

$$\cos\phi = \frac{1}{2}\left(1 - \frac{W}{\sigma}\right) . \tag{3.20}$$

From this, all other variables, such as the positions of the vertices, the film radius and hence the pressure differences can be deduced. The resulting deformations are represented, for various loading forces, in Fig. 3.7.

Instability Probably the most intriguing observation, already apparent from the force balance equations, is that no equilibrium structure exists for loading beyond $W^* = \sigma$: there is a threshold beyond which the honeycomb structure must become unstable. This is particularly interesting for example in the context of wet foams. We make contact with the liquid fraction by recalling that the (2d) vertices correspond to Plateau borders perpendicular to the plane of the (2d) projected foam. Thus the load force (per length L, in the perpendicular direction, of a Plateau border) is

$$W = \frac{\rho_{liq}\, V_{liq}\, g}{2L} = \rho_{liq}\, g\, \phi_{liq}\, A \tag{3.21}$$

where A is the size of a unit cell and the factor of 2 in the denominator accounts for the fact that the liquid in a unit cell is shared between two vertices. The stability threshold thus corresponds to a liquid fraction of

$$\phi^*_{liq} = \frac{\sigma}{\rho_{liq}\, g\, A}\ ,$$

which turns out to be of the order of 10 % for bubbles of the size of a a square centimetre. The effect is thus seen to be relevant, and the threshold is further reduced for larger bubbles.

Relevance for drainage One interesting question is whether this mechanism may play a role in the instability which arises in a foam undergoing forced drainage. In this situation the (stationary) liquid content may achieve 20 %, suggesting that the effect of instability due to loading may be a relevant mechanism. On the other hand, what is typically seen in experiments is an instability via the formation of convective rolls [99].

To exploit the above intuition we must first make contact with a 3d foam. Here, the weight of the fluid acts on the (3d) vertices and, mainly, on the Plateau borders. This implies that the angles between films meeting at the Plateau borders deviate from the 120 angles. This in turn imposes film curvature, reflecting the presence of macroscopic gas pressure gradients, as in the 2d case.

A first point to be made is that this directly affects the drainage rate. To see this, we consider a vertical Plateau border, as in standard drainage theory (see the summary in the introduction above). Recall that the drainage equation (Eq. 3.18) has a stationary solution corresponding to a constant liquid fraction throughout the sample for stationary forced drainage, implying a constant cross section of a (3d) Plateau border. Note, however, that the drainage equation has been established assuming the absence of a gas pressure gradient: this implied that, in the stationary state, in order to have a constant Plateau border radius there could not be a pressure gradient in the liquid. Here, however, this is no longer true, and the pressure gradients in gas and liquid must go hand in hand. The gas pressure gradient can readily be evaluated on a mesoscopic scale, considering a bubble as a buoyant body in the surrounding foam. The archimedian relation

$$\nabla P\, V_{cell} = 2\, W = 2\, \rho_{liq} \phi_{liq} V_{cell}\, g \tag{3.22}$$

must hold, expressing that the buoyancy force must compensate the weight of two vertices per unit cell. It follows directly from the Laplace relation (Eq. 3.2) that there must be a corresponding pressure gradient in the liquid:

$$\nabla P = 2 \rho_{liq}\, \phi_{liq}\, g\ . \tag{3.23}$$

The gravitational force draining the liquid is reduced by this amount, which can be incorporated into standard drainage theory by substituting gravity according to

$$g \longrightarrow (1 - \phi_{liq})\, g\ . \tag{3.24}$$

The effect of the pressure gradient in the liquid due to loading thus is to *reduce* the drainage rate and, since the liquid fraction in forced drainage can approach 20%, the correction can indeed be significant.

The second, yet more crucial point concerns the instability which may arise in a foam as the drainage rate, and hence the liquid content, is increased. One can analyse how the threshold scales with the bubble size R. On one hand, for the instability due to gravitational loading, the criterion $W = \sigma$, using $W \sim \phi R^2$, implies that $\phi^*_{grav} \sim 1/R^2$. On the other hand, the threshold for convection is known [99] to scale as $\phi_{conv} \sim 1/R$. Hence one deduces that the instability due to loading may be expected to pre-empt convection for large bubble sizes.

3.2.2 Foam structure: the dry limit

Reference to the original work:

"Approaching the dry limit in foam"
Norbert Kern and Denis Weaire
Phil. Mag. 83, 2973-2987 (2003)

The idealised idea of a 'dry' foam, with vanishing liquid content in the Plateau border (as well as in the junctions between them and, even more so, in the films), is clearly a useful concept. It is this picture which allows to regard the structure as consisting of films which meet according to Plateau's laws, implying that all the physics is due to surface tension effects, or at least so concerning the static structure of foams. This picture is what makes much of foam physics so esthetically pleasing, and also establishes many contact points with rigourous mathematics on minimal surfaces, tilings of space, and other related mathematics [185].

The question addressed here is how the 'dry' limit comes about, starting from bubbles in a liquid from which the liquid is progressively removed. This process first yields a 'wet' foam, in which a significant amount of liquid remains. The dry foam then corresponds to the limiting case where all liquid has been drained away. The 'dry' limit considered concerns the regime where only an infinitesimal amount of liquid is left in the foam.

Expansion parameter based on osmotic pressure A useful notion is the *osmotic pressure* Π as defined by Princen [155, 155–157]. It can be illustrated by thinking of a sample of foam sitting on top of a liquid reservoir. Imposing a pressure p_{liq} in the reservoir will push liquid into the foam, but ultimately the process will stop. The difference between the external pressure in the surrounding air and the liquid pressure must thus be balanced by a pressure contribution from the foam itself,

$$\Pi = p_{ext} - p_{liq} \ . \tag{3.25}$$

Unlike the osmotic pressure in thermodynamics it is not of an entropic nature, but reflects the fact that capillarity naturally pulls water into the foam. Said the other way round, a (negative) external pressure p_{ext} must be applied to pull the liquid from the foam, since this leads to progressive deformation of the bubbles and thus implies a cost in surface energy. The pressure in the liquid p_{liq} is uniform in a static foam. The key observation here is that a vanishing liquid fraction ϕ_{liq} requires an *infinite* osmotic pressure:

$$\lim_{\Pi \to \infty} \phi_{liq} = 0 \ . \tag{3.26}$$

For any given Plateau border, the geometry of which is sketched in Fig. 3.8, the Laplace equation relates the liquid pressure to the gas pressure in each of the adjacent bubbles i, and

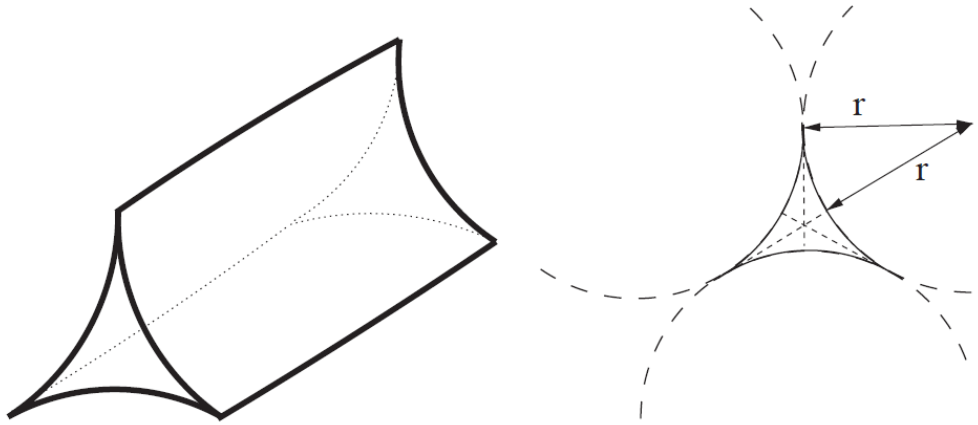

Figure 3.8: *Schematic illustration of the Plateau border geometry in an (almost) dry foam. Its cross-section is delimited by three circular arcs, with a curvature such that the surface tension force at the water-gas interface matches the pressure drop (Laplace's law). In principle Plateau borders do not need to be straight, and the curvature setting the surface tension force is the mean curvature of the interface. In the dry limit, however, the perpendicular radius r of the Plateau border is seen to go to zero: any Plateau border can thus be considered to be locally straight in the dry limit.*

the bubble pressures p_i must remain finite in the dry limit. Consequently, the dry limit is characterised by a (negatively) diverging liquid pressure, in agreement with the idea that the Plateau border radii must vanish in the dry limit. The notion of a diverging osmotic pressure thus promises to provide a useful approach for formalising this limit.

Indeed, in the dry limit the osmotic pressure must dominate as compared to the pressure drop p_{ij} between any neighbouring bubbles i and j. We thus must have

$$\Delta p_{ij} = \frac{2\gamma}{R_{ij}} \ll \Pi \ , \tag{3.27}$$

where R_{ij} characterises the typical radius of curvature of the bubbles. Using the average bubble size $\langle R \rangle$ to provide an upper bound for the radius of curvature, we thus conclude that in the dry limit the parameter

$$\epsilon = \frac{r}{R} = \frac{\gamma}{\Pi \langle R \rangle} \tag{3.28}$$

is a suitable small parameter. One can thus conceive an *expansion*, close to the dry limit, in terms of the appropriately non-dimensionalised *inverse* osmotic pressure.

Liquid fraction From the geometry of a Plateau border (which can be taken to be straight in the present limit) it follows directly that the liquid fraction scales as

$$\phi_{liq} \sim \epsilon^2 \sim \Pi^{-2} \ , \tag{3.29}$$

which is an important result. It shows that there is a subtlety in using the liquid fraction itself as a way of parametrising the approach to the dry limit: if one wishes to do so, the first contribution which should be accounted for in an expansion is of order $\phi_{liq}^{1/2}$, and the linear contribution in ϕ_{liq} is already a second-order term.

Note also that the contribution of the junctions to the liquid content, which can be expected to be of order ϵ^3, is neglected here.

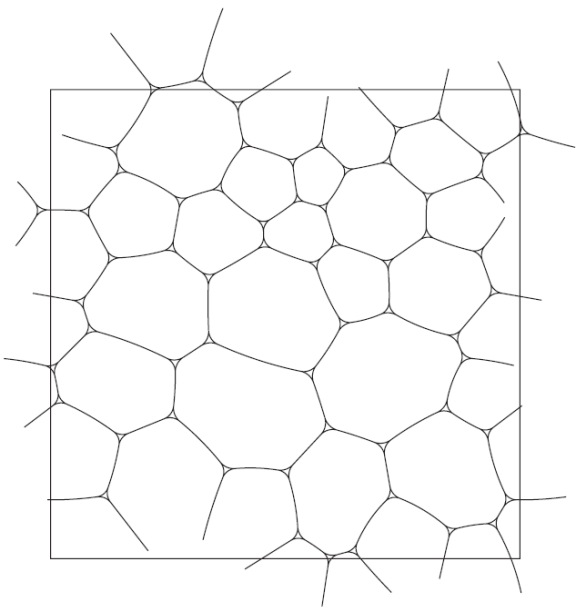

Figure 3.9: *Illustration of the notion of 'decorating' a 2d dry foam backbone with a small but finite liquid content. The theorem says that an equilibrium structure with a finite liquid content may be constructed from a 'dry' backbone structure, by replacing the kinks at the vertices where films meet at 120 degree angles by arcs of circles. A rigourous generalisation to 3d structures is not straightforward. Figure as in [112].*

Negative line tension Another implication concerns the question how the liquid content in the Plateau border affects the energy in the foam. If we use the limiting dry foam backbone as a reference value, adding a finite liquid content in the Plateau borders *reduces* the energy: this is a direct consequence of the fact that less interfacial area between liquid and gas is present in this 'decorated' backbone (see Fig. 3.9). This difference can be quantified, again from straightforward geometry [112], and relating it to the liquid content reveals that the leading term scales as

$$\Delta E_{\phi_{liq}} \sim -\epsilon \, l_{\mathrm{PB}} \sim -\sqrt{\phi_{liq}} \, l_{\mathrm{PB}} \ , \tag{3.30}$$

where l_{PB} is the total length of the Plateau borders in the structure. We are thus lead to consider a somewhat surprising correction to the energy of a dry foam backbone: for any finite liquid content, we must add a contribution which can be described as a *negative line tension* T, and which scales as $\sqrt{\phi_{liq}}$.

One is thus lead to wonder to which extent such a negative line tension might compromise the established results for the structure of foams. There clearly is no modification of the dry structure as such, since the line tension vanishes in this limit. But an effect may in principle arise for close-to-dry foams, like they are used in experiments. To this end, we consider the line tension corresponding to a liquid fraction of 35 %: in this extremely wet foam a description in terms of a dry foam is no longer applicable, but it does provide an upper bound on what can reasonably be expected.

Energy minimisations via Evolver simulations would appear appropriate but require thinking through a subtlety: a negative line tension will tend to reinforce ondulations of an otherwise straight Plateau border. Indeed, a stability analysis in terms of Fourier modes [112] readily shows that this leads to a somewhat unusual instability: perturbations grow without limit for wave lengths *below* a certain threshold. As concerns real systems, this is an artefact in that the corresponding length scale is small compared to the Plateau border radius, which in a real

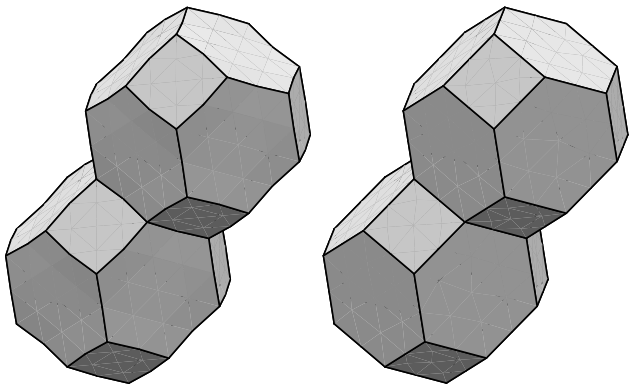

Figure 3.10: *Illustration of the effect of a (deliberately overestimated) line tension on a Kelvin structure: the line tension used here is the positive equivalent of what would correspond to a liquid fraction of 35%, which is clearly no longer close to a dry foam. Note that a positive tension is used to appreciate the effect while avoiding numerical instabilities. Even at these unrealistically high values for the line tension the structure is only weakly modified. Figure as in [112].*

system would effectively introduce a cutoff and suppress this instability. Nevertheless, it must be avoided in simulations, for example by limiting the numerical refinements of the line-like Plateau border.

In order to appreciate the importance of the correction to the structure, Fig. (3.10) shows the effect of an extreme *positive* line tension, corresponding (in modulus) to a liquid content of $\phi_{liq} = 35\%$. The structural changes on a Kelvin structure (see Fig. 3.10) can thus be expected to be rather limited.

Elastic shear modulus There is nevertheless an indication that it may be important to account for a negative line tension, if one is interested in the (elastic) *shear modulus*. The latter can be taken to be

$$G = \frac{d}{d\alpha^2}\frac{E}{\langle V \rangle} \ , \tag{3.31}$$

where α is the shear angle. This will now involve a correction due to the presence of the liquid content:

$$G = G_{dry} + \Delta G(\phi_{liq}) \ . \tag{3.32}$$

The leading term in the correction has heretofore been taken to be *linear* in the liquid fraction (see the full relation in [183]), as appears to have been confirmed by experiments [6, 134].

However, in the light of a negative line tension and the scaling introduced above, one would expect a leading order correction of the form

$$\Delta G(\phi_{liq}) \sim \sqrt{\phi_{liq}} \ , \tag{3.33}$$

which would result in a much larger correction. This is not necessarily in contradiction with the experimental results: the square-root behaviour would dominate for very small liquid fractions, but these are notoriously difficult to achieve in experiments, since film rupture becomes omnipresent. Nevertheless, there is a conclusion to be drawn if the experimental data for various liquid fractions are used to extrapolate to the 'dry' value of the elastic shear modulus: in the fitting procedure one should account for the square-root term due to the line tension, since otherwise the extrapolated G_{dry} may be significantly underestimated.

3.3 Follow-up

The concept of gravitational loading has been picked up by Embley and Grassia, who have introduced various generalisations in order to explore its impact on real 3d foam structures, using both analytical arguments and numerical structure calculations based on the Surface Evolver [26]. Considering a single Plateau border they have included the variation of the cross section along the border in order to determine the structural deformation of the underlying dry skeleton. Transverse loading forces are shown to lead to 'sagging'. Longitudinal loading forces are transmitted along the Plateau border and affect the balance on vertices, deflecting them from their equilibrium position and causing deviations from the tetrahedral angles. The local elastic properties are seen to be modified, making the structure locally softer in the former case and locally stiffer in the latter [59]. Too strong a loading leads to collapse, just as in the 2d case. These results have then been shown to be robust as the constraint of liquid conservation is introduced, albeit with an increased stability threshold [58].

The presence of a negative line tension in foams has been directly confirmed in experiment. Géminard et al. [87] have performed a detailed analysis of the shape of a Plateau border delimiting a circular film, held up by catenoid-shaped soap films. They have shown that there are significant deviations from the 120 degree Plateau equilibrium angles, and that these are well explained by a negative line tension due to the effects described above.

Fortes and Teixeira [68] have revisited the dry limit for simple bubble structures in a theoretical work. They argue that it is not straightforward to generalise the decoration theorem to 3d. This is because, in wet ('decorated') 2d structures, one can extrapolate the interfaces between bubbles into the decorated vertex, to see that they always meet in one point: the position of the vertex in the dry foam (before decoration). These extrapolated films are furthermore seen to meet at their equilibrium angle of $\pi/3$. In 3d, this is in no way obvious (and possibly not true, also given that it is not quite clear how one is to perform this extrapolation). However, Fortes and Teixeira show that the construction holds for very simple examples of 3d structures, such as a double bubble. Even in this simple scenario the angles deviate form their equilibrum value. However, in these cases the deviations can be explained in terms of the (negative) line tension introduced above.

Chapter 4

Foams: dynamics and flow

Essentially all applications using foams require making them flow, whether it be during preparation (such as for producing metal foams or for fire fighting purposes) or during the application itself (such as for oil recovery or nuclear decontamination). We are thus no longer dealing with a foam structure which is stationary, but it evolves over time. One consequence is that Plateau's equilibrium rules need no longer apply and must be revisited. The required modifications are not always straightforward, since they call upon many different effects, ranging from local hydrodynamics in the liquid to global collective relaxations due to topological changes. The following pages attempt to provide a very brief overview over those aspects of foam dynamics, before addressing two examples.

4.1 Tour d'horizon

One way of looking at foams, on a macroscopic level, is to consider them as complex fluids. One then has to acknowledge the various facets of their behaviour: elastic response, viscous dynamics and plastic deformations. One interesting aspect of this system is that one can attribute these features of the global behaviour to particular processes and local effects, at the scale of the bubbles or below.

Rheology A flowing foam is characterised by its visco-elasto-plastic behaviour. On a 'macroscopic' level, considering an entire foam sample with many bubbles, a yield-stress fluid may be used as a simplified rheological description. One commonly used constitutive relation is the *Herschel-Bulkley* relation for the shear stress S

$$S = S_{\text{yield}} + \eta_{\text{plastic}}\, \dot{\epsilon}\nu \ , \tag{4.1}$$

where $\dot{\epsilon}$ is the shear rate, S_{yield} is the yield stress, η_{plastic} is the so-called *plastic viscosity* and ν is an exponent. The simplest variant is a *Bingham fluid* [199], for which the constitutive relation is linear ($\nu = 1$). Both the yield stress and the plastic viscosity depend on the liquid content. In particular, the yield stress drops drastically at a critical value for the liquid fraction, a phenomenon which is also known as the *rigidity loss transition* [24].

Elasticity: surface tension The elastic response is directly due to surface tension effects: deforming a foam structure from its equilibrium (minimum energy) structure requires an external force, in order to supply the energy necessary for increasing the film area. If the amplitude of the perturbation was not too large (see below), the foam thus spontaneously returns to its equilibrium structure as the external stress is released. Surface tension hence accounts for the quasi-static response of a foam, or at least so for small deformations.

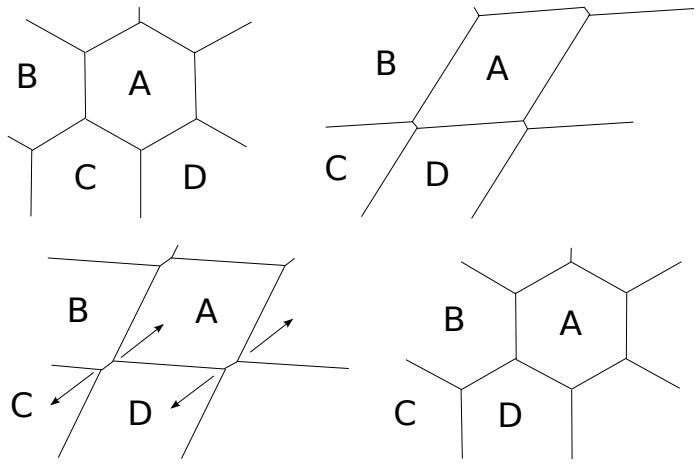

Figure 4.1: *Illustration of the role of neighbour swapping (T1) processes as a foam is sheared, here shown for a regular honeycomb structure. It may be viewed as a process in which an edge length progressively vanishes. This leads to an (unstable) fourfold vertex, which thus spontaneously separates into two threefold vertices. As a consequence, the neighbourship relations have changed. In a disordered foam structure this amounts to plasticity. Figure as in Princen [154].*

Plasticity: topological changes The above description must be refined if the deformations become sufficiently large. This is easily seen for a honeycomb structure undergoing shear. As the shear amplitude increases quasi-statically, the length of one of the edges goes to zero (see illustration in Fig. 4.1). At this point a fourfold vertex is formed, which is unstable and initiates a T1 process (see the previous chapter, and in particular Fig. 3.3). Even if the shear strain is reduced afterwards, the structure then cannot relax back to its initial state. For the simple example of a honeycomb structure, due to its periodicity, the new equilibrium structure is of course equivalent to the initial one. However, this is not true in a general structure. Thus the occurrence of T1 processes constitutes the end of the elastic regime and implies a plastic deformation.

Viscosity: dissipation Real-world deformations typically will not take place in a quasi-static fashion, and thus one must also consider dissipation effects. There are several sources for these. One of them is the in-plane flow of soap films as they expand or deform. This essentially invokes the *surface viscosity* of the films, as it has already been seen to play a role in drainage processes (see previous chapter). Depending on the physico-chemical properties of the detergents this effect may be very important or entirely negligible [53]. The other source of dissipation is the evolution of Plateau borders. As they adapt to the changes in structure, liquid must re-distribute along the Plateau border network. This becomes particularly relevant in the experimental situation of a foam confined between glass plates, where any rheological deformation requires Plateau borders to slide over the glass plate, giving rise to non-trivial hydrodynamics [29]. Both surface viscosity at the liquid-gas interface and the bulk viscosity in the liquid may contribute. In contrast, the bulk dissipation due to the flow of gas within the bubbles, is typically negligible.

In the simplest scenario, the bubble boundaries in a 2d foam can be attributed a dissipation force of the type

$$F \sim v^{\nu} \ , \tag{4.2}$$

where F is the viscous force, v is the velocity with which the bubble boundary moves, and ν is an exponent allowing for a potentially non-linear relation. This will be exploited further in the following, and we will refer to Eq. (4.2) as the *pressure-velocity relation.*

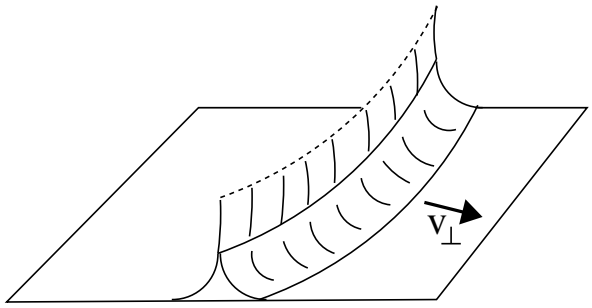

(a)

Figure 4.2: *Sketch of a Plateau border sliding across a glass plate, as in the experimental realisation of a 2d foam (see Fig. 3.5).*

Quasi-static flow Understanding dissipation is obviously a major factor if fast changes arise, i.e. in the presence of high flow rates or high shear rates. One might be tempted to conclude that, in the opposite case of very slow flow processes, dissipative effects would not play a role. However, this is *not* entirely true. Indeed, as concerns the mechanical relaxation of a perturbed geometry, the structure can adapt to external changes. If these are infinitesimally slow, this process does not involve significant dissipation. This amounts to a (quasi) instantaneous relaxation, maintaining the foam in mechanical equilibrium at all times. This quasi-static regime can thus be adequately modelled by solving for the minimum energy structure at every instant in time.

However, the approach fails as soon as topological changes take place. As discussed in the previous chapter, a neighbour-swapping T1 process is in fact a singular event: an edge retracts to zero length at some point in time leading to an unstable four-fold vertex. This, however, necessarily creates a structure which is *not* in mechanical equilibrium. As the fourfold vertex dissociates into two threefold vertices which separate in order to re-establish the equilibrium following Plateau's rules, this is *not* a quasi-static process. Indeed, we will highlight the associated singular dynamics in the following. It thus becomes clear that, through the singular T1 events, dissipative effects *always* interfere - a fact which is entirely neglected in the quasi-static flow model.

4.2 Selected publications

The following discussion will focus on analysing the behaviour of a flowing foam in a 2d geometry, which significantly simplifies the description, the modelling and also the experimental setup required to confirm the theoretical results. We first discuss in some detail the dissipation mechanism in the flow of a foam over a glass plate, as it can be exemplified experimentally in an even simpler geometry. We then show how one can construct a simplified model for the flow of a 2d foam, taking into account all the aspects discussed above.

Here we neglect bulk dissipation within the bubbles, as well as surface viscosity effects, and concentrate on the bulk dissipation due to hydrodynamic effects within the Plateau borders. The focus will be on quasi-1d and quasi-2d geometries. These are particularly well suited to understanding the role of the container walls, i.e. the motion of plateau borders over the glass plates, a process which necessarily intervenes in an experimental setup.

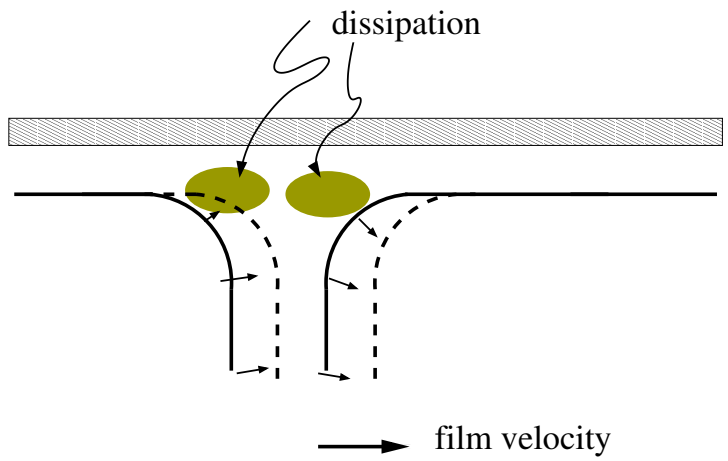

Figure 4.3: *Illustration of flow in a Plateau border sliding over a glass plate, shown in a cross-section, perpendicular to the film. Far from the Plateau border, no flow takes place in the liquid film along the wall. Velocity gradients, and therefore dissipation, arise mainly in the highlighted zone.*

4.2.1 Dissipation in 2d foams

Reference to the original work:

> *"Dissipation in foam flowing through narrow channels"*
> *Isabelle Cantat, Norbert Kern and Renaud Delannay*
> *Europhys. Lett. 65, p. 726-732 (2004)*

In the context of dissipative mechanisms the 2d scenario is particularly interesting due to the simplifications it introduces, both for the dissipative processes themselves as well as for modelling the foam dynamics. Indeed, in a 2d foam one can attribute the dominant contributions to the motion of Plateau borders located at the confining glass plates. We refer to Fig. 4.2, which points out how every film separating two 2d bubbles corresponds to two Plateau borders. In the equilibrium situation these meet at angles of 120 degrees, like in a strictly 2d foam. The fourth Plateau border, perpendicular to the plates, essentially translates without involving flow within the fluid.

The overall situation concerning the hydrodynamics is thus sketched in Fig. 4.3, illustrating that the sliding of a Plateau border leads to a flow pattern which must respect the no-slip boundary conditions. In typical 2d soap froths the bubbles measure of the order of at least a centimeter, whereas the glass plates are separated by a few millimeters. The Plateau borders are yet much smaller than this, and the velocity gradients thus are important. The zones of highest dissipation arise at the regions where the film is peeled off the plate (upstream) and where it is deposited back onto the plate (downstream) [29].

One central question for understanding the impact on rheology is to understand the relation which determines the pressure gradient required to make a Plateau border advance at a given speed. One may assume a power law

$$\Delta p \sim V^{\alpha} \ . \tag{4.3}$$

The process being complex (for example since the Plateau borders also deform in response to being pushed), nonlinearity ($\alpha \neq 1$) is to be expected.

It has been shown theoretically [29, 94] that, for low capillary numbers $\mathrm{Ca} = \eta V/\sigma \ll 1$ (η

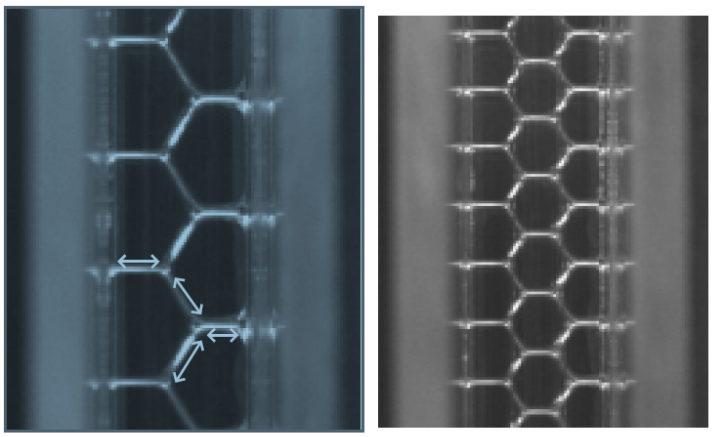

Figure 4.4: *Regular monodisperse foam structures within cylindrical tube. The simplest structure (not shown) has a bamboo-like topology, where bubbles line up along the tube, separated by films which span the entire cross-section. For smaller bubble sizes one finds the 'staircase' structure shown here, and progressively more complex variations involving several strings of bubbles alongside each other.*

being the bulk viscosity of the liquid and σ the interfacial surface tension), the scaling given by Eq. (4.3) is expected to be obeyed with an exponent $\alpha = 2/3$. A simple experimental setup, devised by E. Cantat and R. Delannay in Rennes, has allowed us to confirm this relation, and has furthermore suggested that it is the motion of the Plateau borders *perpendicular* to their orientation which provides the dominant contribution to dissipation.

The procedure consists in creating a foam in a tube-like plexiglass channel, having a diameter comparable to the bubble size. In the simplest case this results in a bamboo-like structure of bubbles, or in progressively more complex but regular bubble trains (see Fig. 4.4). The advantage of this bamboo geometry, in some sense closer to a 1d arrangement, is that it involves only identical, circular Plateau borders. As the tube, which is open below, is then plunged into a container of water, the hydrostatic pressure pushes the entire structure up into the tube, requiring the Plateau border to slide upwards along the glass wall. Filming the process with a high-speed camera allows to measure both the depth of immersion of the structure, from which both the driving hydrostatic pressure and its velocity can be deduced. The result is shown in Fig. 4.5, from which one deduces that a power law relation with an exponent of 2/3 is indeed appropriate.

In the above analysis the coefficient of proportionality is of course linear in the total length of the Plateau borders gliding over the glass surface. Further information is obtained from considering slightly more complex structures, which involve various columns of bubbles disposed in a regular fashion within the tube (see Fig. 4.4). These now involve both ring-like Plateau borders, which are oriented orthogonally to their direction of motion, and Plateau borders at an angle, which therefore move with both a perpendicular and a parallel component. Decomposing each Plateau border into these components then shows that the data is well described if only the orthogonally projected Plateau border lengths are taken into account: it is indeed the *perpendicular* sliding of Plateau borders over the glass plates which dominate dissipation.

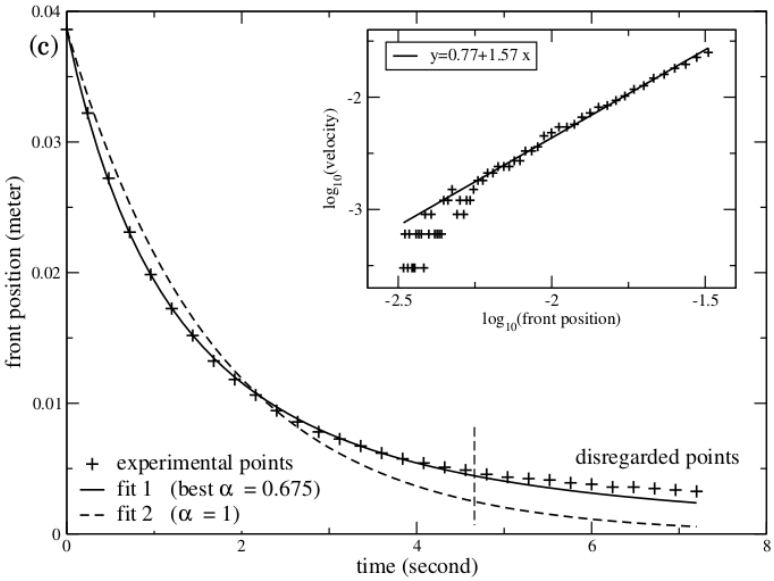

Figure 4.5: *Example of an experimental results showing the velocity-pressure relation, as they are obtained for simple regular structures within a tube. The tube is partially plunged into a water-filled basin at time $t = 0$. The graph shows the position of the bubbles in the tube as a function of time, as they are pushed upwards by hydrostatic pressure. The best fit is a power law of the form of Eq. 4.2, with an exponent of $\nu = 2/3$, as expected. Also shown, for comparison, is the result expected if the pressure-velocity relation were linear.*

4.2.2 The viscous froth model for a 2d foam

Reference to the original work:

"Two-dimensional viscous froth model for foam dynamics"
Norbert Kern, Denis Weaire, Aengus Martin, Stefan Hutzler, and Simon J. Cox
Phys. Rev. E 70, 041411 (2004)

We now return to quasi-2d foams, confined between two parallel glass plates. Formulating a model for the dynamics of such a 2d foam is a first step towards understanding the rheology of foams in general. Restricting the debate to a 2d system is an obvious simplification, both in terms of topological complexity and concerning the dissipation mechanisms. Nevertheless, even these simplified 2d systems are known to display an entire range of interesting phenomena, for example as one makes trains of bubbles flow through fairly narrow channels [51]. In that setup it has been shown that one can use the channel geometry to split bubble trains, make them cross, reunite them, etc, by provoking topological changes as required: applications in the spirit of 'lab on a chip' technology spring to mind [97, 186]. Many phenomena can be understood in terms of surface tension effects and quasi-static flow, others cannot. One such example is the case of a two-fold bubble train being pushed around a bend, see Fig. 4.6. One observes in experiments [51] that the inner bubble train becomes the leading one, by way of a controlled sequence of topological changes. Intriguingly, quasi-static flow is *not* sufficient to explain this effect.

In this section we set out to formulate a model accounting for dissipation in such flowing 2d foams.

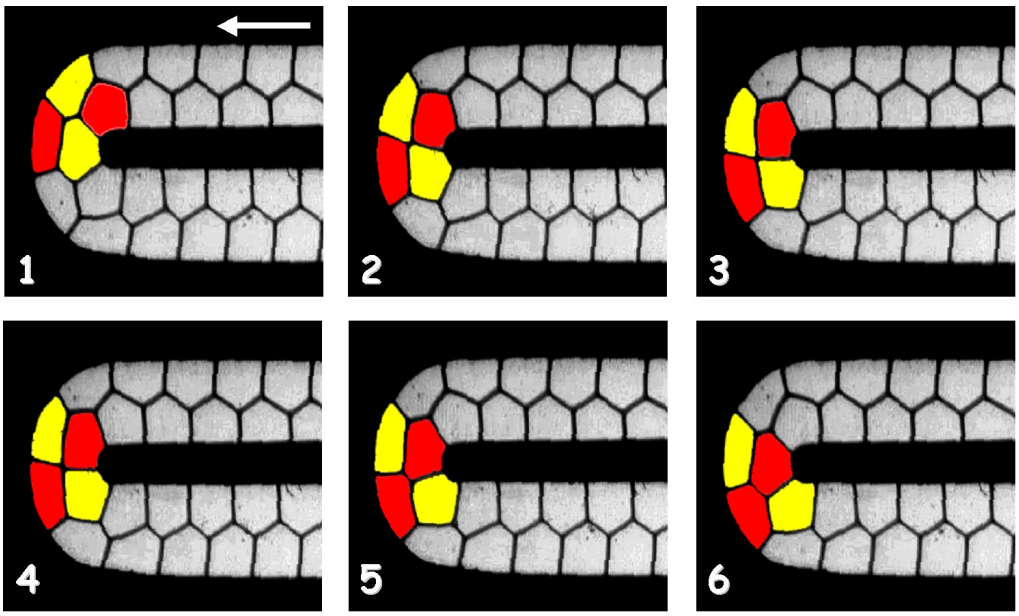

Figure 4.6: *Bubble trains pushed around narrow bends constitute an interesting experimental setup, which shows many relevant phenomena. Here we illustrate a T1 process (figure from [51]). The viscous froth model developed here establishes that this process crucially relies on dissipation, without which no topological change would occur.*

Viscous froth model The viscous froth model [108] may be seen as a framework for modelling the dynamics of the flow of 2d foams. It is, however, a more general model, which can be arrived at by formulating generalisations to various starting points and provides a unified point of view, and thus accommodates elements of various physical mechanisms, as we shall discuss below.

The defining relation for the model is the force balance on an element ds of a Plateau border, as it slides over the glass plates, which we take to be a generalisation of Laplace's law taking into account dissipation effects:

$$\lambda\, v(s) = \Delta P_{bb'}(s) - \gamma\, K_{bb'}(s)\ . \tag{4.4}$$

Here b and b' refer to a neighbouring pair of bubbles. v is the velocity of the Plateau border (or, more precisely, its component normal to the element ds) and λ is a friction coefficient. γ stands for the interfacial (line) tension and $K_{bb'}$ for the curvature of the film separating bubbles b and b', and $\Delta P_{bb'}$ is the pressure drop across this film.

The essential statement thus is that the friction force on the Plateau border segment ds must cancel the driving force, due to the pressure gradient and the elastic surface tension. This is an overdamped motion, neglecting inertia, which is a very good approximation.

The dissipation relation has been simplified to a linear relation, taking the drag force to be proportional to the velocity of the film segment. This amounts to assuming a coefficient of α=1 (rather than 2/3) in the relation 4.3 discussed above. This considerably simplifies setting up the numerics, but the simplification is not essential and a different exponent could be implemented. Another implicit assumption it only the velocity $v(s)$ component *normal* velocity of the Plateau border matters, as appears indeed justified based on the experimental results discussed in the previous chapter.

Generalisations and limiting cases The viscous froth model, as introduced above, can be viewed as using the ideal soap froth, corresponding to a quasistatic equilibrium to which a viscous drag force has been added. This is how we have motivated the model. At the same time, it may be seen as a generalisation of a domain growth model [202], initially formulated for the growth of domains in metal [139]. For those systems there is no relevant pressure, which is thus added by the present model. Finally, one may also think about pressure driven coarsening [196], as discussed briefly in the introduction to the previous chapter, to which surface tension effects have been introduced.

The relative importance of these effects can be appreciated in terms of the associated time scales:

$$\begin{aligned} T_\lambda &= \frac{\lambda R^2}{\gamma} && \text{(structural relaxation)} \\ T_\kappa &= \frac{R^2}{\kappa\gamma} && \text{(coarsening)} \\ T_{\dot\zeta} &= \frac{1}{\dot\zeta} && \text{(shear)} \end{aligned} \tag{4.5}$$

where R is a typical length scale characterising the structure, such as the average bubble size, and $\dot\zeta$ is an applied shear rate.

Coarsening dynamics It is worth pointing out that the Von Neumann law (Eq. 3.4) for the coarsening dynamics of an ideal soap froth can be generalised to account for the effect of viscous drag. In this case one can show [202] that the rate of change of the area of a bubble b follows

$$\frac{dA_b}{dt} = \frac{\pi}{3}\frac{\kappa\gamma}{1+\lambda\kappa}(n_b - 6) \ , \tag{4.6}$$

and thus the ratio $\lambda/\kappa = T\lambda/T_\kappa$ is seen to be the relevant dimensionless parameter which interpolates between Von Neumann law in the limiting cases of an ideal soap froth and Mc Mullin's law, which is the equivalent for grain growth. Eq. (4.6) thus constitutes the generalised Von Neumann's law interpolating between those cases in the full viscous froth model.

Quasistatic limit Note that the time scales defined above in particular provide an argument as to when the quasistatic model for rheology is recovered. First of all, the time scale of coarsening has to be slower than that attributed to shear. But also, for the dynamics to be 'slow', the structural relaxation after T1 must be fast compared to other structural changes, such as those imposed by the shear rate.

Implementation The numerical implementation is based on a discretisation of the Plateau border network. It must include topological bookkeeping to keep track of the vicinity of bubbles, films and film segments, which represents a considerable coding effort. Forces on discretisation points can be calculated in a finite element-like fashion to include all contributions to Eq. (4.4). They are complemented by two additional, somewhat technical procedures.

One element is the displacement rules for the vertices. It is based on the fact that the films meeting at a vertex maintain an angle of 120 degrees, *despite* the presence of viscous forces. This may appear surprising at first sight, but is readily seen by looking at an infinitely small control volume around a vertex: as it vanishes, only the interfacial tension remains, whereas the viscous contributions disappear. The rule for displacing the vertices is thus to maintain the appropriate angles, for which analytical solutions are available [85]. The novelty in the

dynamics with respect to the quasistatic, ideal soap froth therefore lies in the fact that there no longer is any requirement for the films to be arcs of circles.

The other technical point concerns the variation of bubble volumes. In principle, for the purpose of rheology as discussed above, this variation is required to be zero. But a more general procedure can be devised to include coarsening effects, for which the variation of bubble volumes is given by the generalised Von Neumann relation stated above (Eq. 4.6). This is the point where the linear viscous drag relation (Eq. (4.3 with $\alpha = 1$) simplifies the procedure: in this case, Eq. (4.6) tells us how all areas vary, which leads to a self-consistency condition in terms of a matrix equation for the bubble pressures. One can thus impose the bubble pressures as to achieve the desired area change. If coarsening is to be excluded, the same procedure provides numerical stability on the bubble volumes.

In addition to the smooth part of the dynamics, topological changes must be handled during time evolution. In the absence of coarsening this amounts to the T1 processes, which can be handled by defining a minimum value for the length of a film, beyond which a neighbour swapping process is attempted. It is thus an energetic criterion, applied locally at the vertex, which triggers the (infinitesimal) topological change, following which the structure then evolves according to viscous froth dynamics.

There are technical aspects to the implementation which are required to keep the numerical procedure well-defined, smooth and stable; full technical details are reported in [108].

Neighbour swapping and film rupture Two test cases are well suited for showing the effect of singular topological events, as they would not appropriately be handled in the quasistatic, ideal soap froth model, as discussed above.

One is the rupture of a film, as indeed it arises commonly in dry foams, and which can also be provoked in experiments. In this case one sees that a relaxation process ensues, in which the former vertices, i.e. the points which used to be connected by the ruptured film, move apart (see illustration in Fig. 4.7). One confirms [108] that their distance increases in a square-root fashion, indicating in particular an initially singular motion at these points, as is expected from the rules for the vertex motion. The time scale for this structural relaxation is set by $T_\lambda = \lambda R2/\gamma$ (see Eq. 4.5).

The second case is a T1 process, achieved by preparing an equilibrated configuration with one edge having close to zero length, illustrated in Fig 4.8. As soon as the neighbour switching is performed on this essentially fourfold vertex, the structure becomes unstable and relaxes by developing a new edge. The length of this edge initially increases following a square-root law, again reflecting the singular nature of the topological change. Asymptotically, the new equilibrium configuration is achieved through an exponential relaxation process.

Importance of the model The viscous froth model for 2d foams has thus been seen to lend itself to a numerical implementation, and provides valid results for the topological changes above, including estimates for time constants of the subsequent relaxation process. Nevertheless, the above examples are mere illustrations of our implementation. The main point is not that one can reproduce isolated topological changes, but that the time interval following these singular events is handled by the model. This is an important difference with respect to any quasi-static description, where any topological change is followed by an *instantaneous* relaxation to equilibrium. As discussed above, the out-of-equilibrium relaxation following these

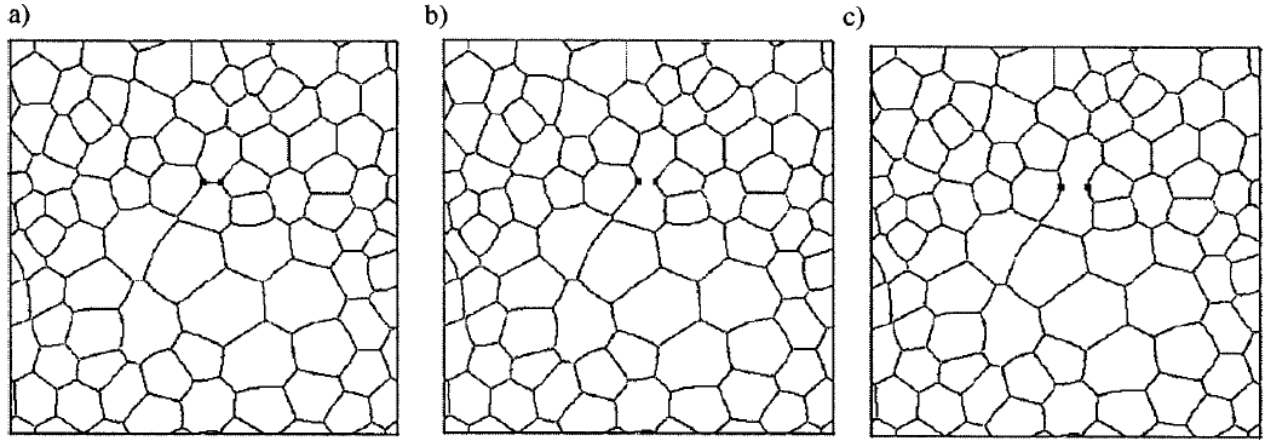

Figure 4.7: *Simulation of a film-rupture event in a film. The foam structure evolves according to viscous-froth dynamics. As a consequence, the distance between the points where the vertices of the disappeared edge used to be located grows in a square-root like fashion, thus representing the singular nature of the perturbation.*

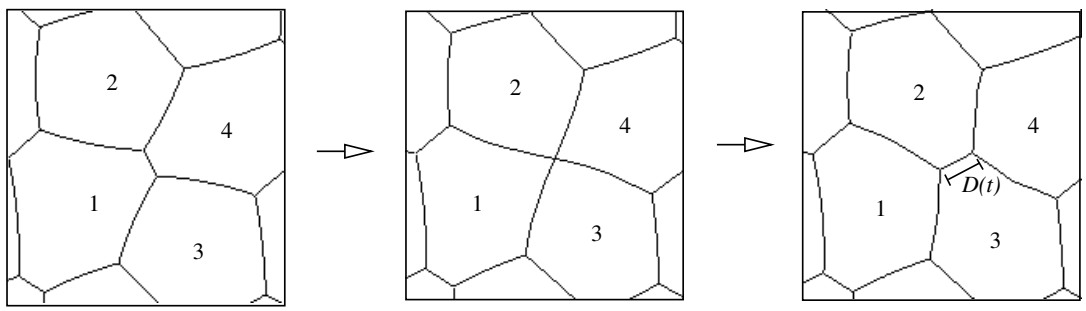

Figure 4.8: *Dynamics of a foam structure following a T1 event. At first (left) bubbles are inflated/deflated as required to produce a zero edge length, implying an (unstable) 4-fold vertex (middle). The foam then evolves according to the viscous froth dynamics (right). Note in particular that the angles between films quickly return to the 120 degree equilibrium values, which remain valid even in the presence of dissipation. Films, on the other hand, are no longer required to remain arcs of circles. Here too, the new edge grows in a square-root fashion, reflecting the fact that the topological change constitutes a singular event.*

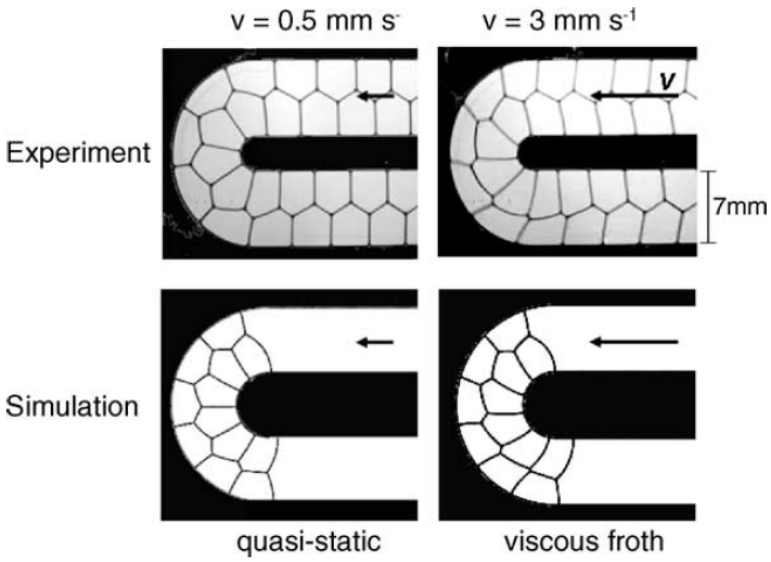

Figure 4.9: *Full results on a bubble train being pushed around a bend. For low velocities the experimental observations are well represented by quasistatic results, whereas the viscous froth model is required to reproduce deviations for higher velocities. Most interestingly, the viscous froth model correctly predicts the occurrence of a T1 topological change as the bubble trains are pushed around the bend, which is absent in the quasi-static dynamics.*

events can intrinsically not be handled by a quasi-static model. This is where the viscous froth model innovates, since it allows to resolve this singular time interval. In particular, this will resolve the ambiguity concerning the order of events in avalanches of T1 processes, as they can arise in rheological situations [1, 102–104].

Application to neighbour switching in a channel bend A nice illustration of the relevance of the viscous froth model has been provided based on the setup of bubble trains flowing along channels, which we have briefly touched upon in the introduction. We consider the example of a bent channel, around which a double train of bubbles is pushed. In order to incorporate the constraints due to the channel walls, the viscous froth implementation has been ported to the Surface Evolver program by S. Cox [38], exploiting its facilities to this effect. The results show that the viscous froth model indeed has the potential to explain many of the observations. This is illustrated in Fig. 4.9, highlighting the role of the viscous drag specific to the viscous froth model. One sees that pushing the bubbles very slowly around the bend, corresponding to the case of a quasi-static description without friction, the double row of bubbles is pushed around the bend 'as is', undergoing deformation but without any topological changes taking place. As viscous drag becomes important (i.e. for higher velocities), however, a neighbour swapping process is provoked, which amounts to topologically promoting the inner bubbles one step ahead of the outer bubbles. Such a T1 process takes place successively whenever a new bubble pair passes this critical area, and the resulting advance maintained as the bubble train is pushed further around the bend. This correctly reproduces the experimental observations performed at different flow velocities.

4.3 Follow-up

The work on dissipation as bubbles move through narrow tubes has been pushed further by Dollet and Cantat [49], who have experimentally studied the case of higher velocities for the

bubble trains. They show that ultimately the high velocities lead to the bursting of films or to unsteady motion. However, these experiments have also shown that this only occurs at a relatively high speeds (of the order of meters per second), and that the Bretherton law holds up to these surprisingly high velocities. The line of work touched upon above, where the channel geometry is used to manipulate, order, separate or recombine bubbles and bubble trains has been summarised in a further publication [51]. It has since been re-visited in the somewhat more applied vision of a 'lab on a chip' technology [97, 186], where many of our original setups are represented.

The viscous froth model has been used by Barry, Weaire and Hutzler [14] in order to investigate shear-localisation (initially reported by Debrégeas et al. [45]). In particular, they have established a correspondence with a continuum model. The Herschel-Bulkley exponent (ν in Eq. 4.1) has been estimated as 1/3, as is compatible with experimental data.

Green et al. [85] have applied the viscous froth model to a *lens* bubble, consisting of only three films and one vertex, pushed through a channel. Their analysis quantifies the deformation of the bubble as a function of driving pressure or flow velocity, and highlights the differences with quasi-static motion. Most interestingly, they show that the expected stationary solution only holds up to a threshold in the driving velocity, beyond which a topological change is triggered through a non-stationary process. Their very careful analysis of this simple scenario has also led to various technical improvements of the implementation, in particular concerning the numerical precision and the spatial and temporal resolution. Ultimately this results in extending the time scales which are accessible in simulations of a viscous froth.

Other dissipative processes have been considered, which may intervene in foam rheology and would require the model to be generalised. For example, Cantat [30] has explored the effect of Gibbs elasticity, in this case on a 2d foam. This amounts to acknowledging the fact that the films can grow or shrink during the flow process, which requires the surface concentration of surfactant to adjust. Assuming this to be the slowest process, they have shown that this type of dissipation leads to a Herschel-Bulkley law for the foam constitutive relation, with an exponent differing slightly from other models. However, this work has adopted the so-called *vertex model*, in which all films are straight lines [144]. Thus the full detail of the bubble geometry is not represented, and in particular the Plateau rule on equilibrium angles cannot be respected. Nevertheless, these simulations provide an additional angle to the question of dissipation in a 2d foam, which could in principle be implemented to extend the viscous froth model.

An entirely different approach to simulating a viscous 2d foam has been exploited very recently by Kähärä, Tallinen and Timonen [105]. In their simulations the bubble boundaries are represented through discretisation points, which evolve in a molecular-dynamics like fashion, subject to specially designed forces. These include the pressure force, as well as viscous forces, similar to the viscous froth model. The novelty here is that the discretised shape is that of the *gas-liquid interface*, i.e. *half* a film: *two* such lines, which repel each other through elastic forces, resolve the interfaces of the liquid film with both adjacent bubbles. In this sense the model attempts to combine the features of a viscous froth with that of Durian's bubble mechanics [54, 55]. In this way it is possible to resolve structures with a finite liquid content, and one may hope that extending simulations including viscous effects beyond dry foams would eventually become possible.

Chapter 5

Active transport on quasi-1d structures

5.1 Tour d'horizon

The interest in 1d, or quasi-1d, active transport can be motivated from many points of view. Some of these directly originate from fundamental theoretical physics (such as out-of-equilibrium statistical physics), from real-world applications (such as traffic or crowd control), from communication issues (such as internet routing protocols) or from biological questions (such as cytoskeletal transport based on molecular motors). The latter example is particularly suitable for introducing the essential ideas, in that it can be conceived, with quite little simplification, as a rather direct realisation of a completely abstract and generic lattice process, of which it is often said that it constitutes for non-equilibrium physics what the Ising model is to equilibrium physics. We shall therefore use the example of molecular motors to motivate and introduce the model. We then review its main features, and in particular the resulting collective behaviour. This will lay the basis for discussing, in the following sections, the various contributions to this domain in terms of simple models. In particular these concern branched structures and networks, before returning to discuss the interest of the approach with respect to intracellular transport (see [28] for a recent review of this topic).

Molecular motors as 1d active 'particles' Molecular motors are complex protein molecules, which are ubiquitous in living cells. They come in several families (dynein, kinesin and myosine, for the molecular motors producing linear motion), each of which features several variants of similar (from out point of view) molecules. The conformations taken by these proteins typically allow to distinguish several parts: a docking region for binding other bio-molecules (the 'cargo'), a central part (the 'body') and one or two, according to the type of motor, elongated strands ('heads') which can bind to track-like bio-polymers (see sketch in Fig. 5.1).

By 'tracks' we mean long, rather stiff biopolymers which, in the right conditions, self-assemble from identical building blocks which are themselves globular proteins. The structurally simplest case is that of actin fibers, in which actin monomers assemble to a long chain-like molecule, rather like a long polymer chain. These have a bending rigidity which confers them a persistence length of the order of 15 μm. Microtubules are a somewhat more complex example, where tubulin dimers assemble to form long chains, several (typically 12) of which gather to form a bundle resembling a hollow cylinder. As a consequence the microtubule fibers are more rigid, which is reflected in their larger persistence length (of the order of a few millimetres). Both actin filaments and microtubules, along with another type of biomolecules (the 'intermediate filaments') are present in eukaryotic cells. These cells typically assemble larger structures from such filaments, either by bundling or by criss-crossing and interlinking them. Together with the lipidic cell membranes, these structures largely contribute to the mechanical

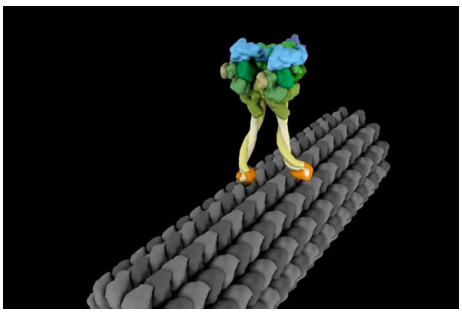

Figure 5.1: *Illustration of a motor protein, here dynein, moving along a microtubule. The typical elements are a rather compact 'body' with two flexible 'heads'. These can successively attach to the microtubule, always further ahead, thus making the motor 'walk' along the (polar) filament. Each step occurs stochastically, and consumes energy in form of ATP (or GTP). The body of the motor protein also serves to anchor a cargo, for example a vesicle or an organelle, which is pulled along and thus undergoes active transport. Filaments are typically populated by many motors, such that their interaction becomes an issue, making their stepping dynamics a collective process. Image from the website of Harvard Medical School [174].*

properties of a cell. Another important structural property of these filaments is that they are *polar*, i.e. they come with an orientation, which is of course important for directing the transport processes.

Molecular motors bind to these tracks, according to biological specificities (myosin walks on actin filaments, dynein and kinesin bind to microtubules). The particular feature of the motors resides in the fact that they can take on various conformations, which correspond to various degrees of structural deformation and also to various affinities with respect to biochemical interactions. Certain changes of conformation can release the binding to the supporting filament. Others can bind molecules of ATP (adenosine-triphosphate) and exploit its hydrolysis to ADP (adenosine-diphosphate) as a source of energy. Each such hydrolysis liberates an energy of the order of $10\,k_BT$. The molecular motor can then undergo a *cyclic* succession of these conformations which, using the energy provided by ATP to pull the molecular motor (and its biological cargo) one step forward along the track. One molecule of ATP is consumed in each such step, and the forward motion is more or less of a fixed step size (of the order of several nanometres to several tens of nanometres).

TASEP: the model To a physicist's eye, striving to neglect all biological complexity and biochemical details, we are thus dealing with the simplest possible non-trivial active transport process: we have a 1d structure, in which 'particles' move stochastically (whenever a motor catches a molecule of ATP) under energy consumption (ATP hydrolysis). It then steps ahead one site on a regular lattice (reflecting the periodic structure of the underlying biofilament). The only complication which arises in this process is the condition of excluded volume, i.e. the fact that two motors cannot bind simultaneously to the same lattice site. This model is known as a *Totally Asymmetric Simple Exclusion Process (TASEP)*, and it is graphically summarised in the sketch provided in Fig. (5.2).

Formally, the model can be written in terms of a master equation

$$\frac{dn_i}{dt} = \gamma \left[n_{i-1} \left(1 - n_i\right) - n_i \left(1 - n_{i+1}\right) \right] \ , \tag{5.1}$$

where $i = 1 \ldots L$ identifies the position on a lattice of size L and $n_i \in \{0, 1\}$ indicates whether a given site is empty or occupied by a motor. γ is a rate constant, which sets the probability

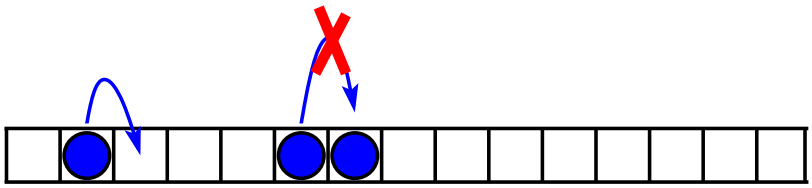

Figure 5.2: *Sketch illustrating the Totally Asymmetric Simple Exclusion Process (TASEP). Particles stochastically attempt to hop to the next site on a lattice, in a predefined direction. The hop fails whenever that site is already occupied.*

with which a given motor will attempt a forward hop within the time interval dt. This can also be written in terms of the net current resulting from particles leaving site i and those entering from site $i-1$:

$$\frac{dn_i}{dt} = J_i - J_{n-1} \ , \tag{5.2}$$

where the current leaving site i is

$$J_i = \gamma \left(n_i \left(1 - n_{i+1} \right) \right) \ . \tag{5.3}$$

As to describing actual molecular motors, this model is obviously a crude simplification, and many assumptions may be questioned. Is the distribution of ATP in the surrounding solution homogeneous, as to justify an entirely equal stochastic motion for any motor? Is the step size strictly constant? Does it correspond to precisely one lattice site, reflecting the size of the monomers? Can the motor really step in one direction only? Can the excluded volume condition on a single binding site be used when there is a cargo present? What is the role of intermediate states in the cycle of configurational changes? Etc., etc. All of these questions (and many more) deserve to be raised, all of them are of biological importance, and a significant number of studies have been performed to address certain of these issues. At the same time, the answer to these questions is typically specific, and may differ from one motor to another, from one track to another, from one cell to another or even from one stage in the cell cycle to another. As physicists, this is clearly not what we want to be concerned with at first, but we would rather start by understanding a 'purified' (translate: entirely oversimplified) model such as TASEP, before entering any more specific issues. This is what we will discuss in the following. It turns out (see the discussion below), maybe against all odds, that the TASEP indeed provides a valid starting point for describing the motion of molecular motors. In particular, it helps to unravel the collective effects which are crucial phenomena in this type of transport process, including those in real biological systems [127].

Fundamental physics and applications The simplicity of its defining rules makes TASEP also a paradigmatic model for out-of equilibrium transport, just like the Ising model constitutes a paradigm for equilibrium phase transitions (for recent reviews see [34, 132, 133]). TASEP has received considerable attention also from this point of view, and the exact solution is known [46]. It has since been studied using various techniques, such as the matrix product method [21,47,48], large deviation theory [44], the Bethe ansatz [43,81,93]. The resulting phase diagram is well studied by many authors, such as Derrida et al. [47], Schütz and Domany [73], Kolomeisky and Straley [118], amongst others.

In terms of applications TASEP, and a variety of related models based on stochastic lattice gases, have been recognised as useful to a whole spectrum of topics. These include the motion of pedestrian and crowd control [5], vehicular traffic [36] (where the stochastic motion is typically replaced by a synchronised update rule), spintronics [164], information flow on the internet

or on wireless networks [182], amongst others. We shall return below to the applications of TASEP in the biological realm.

TASEP on a ring: current-density relation A mean-field analysis of TASEP is very straightforward indeed, and reveals much of its behaviour. On a closed ring (periodic boundary conditions) the average current can be deduced from Eq. (5.3), noting that it is necessarily constant along the track (due to particle conservation). We thus have, in a mean-field spirit,

$$J = \gamma\, \rho\, (1 - \rho) \tag{5.4}$$

where ρ is the overall particle density, obtained from the number of particles N and the number of lattice sites L as $\rho = N/L$. The argument uses the *local (averaged) density*, on site i, defined as

$$\rho_i = \langle n_i \rangle \ , \tag{5.5}$$

which thus amounts to the probability of having site i occupied by a particle, and we have used homogeneity ($\rho_i = \rho = const$), due to the periodic boundary conditions. In this simple mean-field argument cross-correlations between neighbouring sites have been neglected by assuming

$$\langle n_i\, n_{i+1} \rangle \approx \langle n_i \rangle\ \langle n_i + 1 \rangle = \rho_i\, \rho_{i+1} \ . \tag{5.6}$$

It is remarkable, however, that the parabolic density-current relation $J(\rho)$ given by Eq. (5.4) has been shown to also be the *exact* result [47, 48] for TASEP.

The origin of the non-monotonic current-density relation lies, of course, in the excluded volume interaction between particles. It immediately reveals several important features. One is the fact that there is a symmetry with respect to half-filling ($\rho = 1/2$), such that $J(\rho) = J(1-\rho)$. This in fact reflects a particle-hole symmetry: particles hopping forwards follow rules entirely analogous to those of holes hopping backwards. A direct consequence is the fact that any particular current can be sustained by two different densities. This suggests that two segments of these two complementary densities can *coexist* in a stationary state. This observation will be useful in the following.

TASEP on a finite segment: density profile ρ_i The full spectrum of features of the TASEP emerges as boundaries are introduced. This requires defining particle injection and extraction, which is done via additional boundary rates. Thus a particle is injected into the first site, if this is empty, at a rate α. Similarly, a particle on the last site of the segment is extracted at a rate β. On a mean-field level this is equivalent to introducing two reservoir sites, one with particle density α at the entry and another one with particle density $1-\beta$ at the exit.

The first remarkable result is that, in the stationary state, the density along the segment is still constant, except for boundary regions. This is not entirely trivial: stationarity necessarily requires a uniform current ($J_i = J = const$), but not *a priori* a constant density, as was the case for a closed ring. One way to establish the fact that the density profile ρ_i (representing the average density as a function of the position i along the segment) is constant relies on analysing the current conservation condition as given by Eq. (5.3). Reading it as a recurrence relation for the occupation number n_i it becomes, in a mean-field approximation,

$$\rho_{i+1} = 1 - \frac{J}{\gamma}\, \frac{\rho}{n_i} \ . \tag{5.7}$$

We are thus dealing with a discrete dynamical system, which has two fixed points at

$$\rho^*_{\pm} = \frac{1 \pm \sqrt{1 - 4J/\gamma}}{2} \ , \tag{5.8}$$

ρ_-^* being unstable and ρ_+^*being stable. Thus no fixed points can exist corresponding to currents $J/\gamma > 1/4$, as was to be expected from the current-density relation. Furthermore, whatever the initial value for the map (the entry density ρ_1 at the first site), the density profile ρ_i asymptotically reaches $\rho_i \longrightarrow \rho_+^*$ as $i \longrightarrow \infty$, and one can show that this occurs on a typical length scale which does not depend on the segment length (in fact only a few sites). This proves that the density profile is asymptotically constant for a sufficiently large segment, and that the asymptotic density is independent of that at the entry site.

It is, however, important to realise that this is not the only scenario. Indeed, the discrete map given by Eq. (5.7) can also be established 'backwards', iterating from the exit density towards the entry site. In this case one finds asymptotic convergence towards ρ_-^* at the entry site, i.e. the particle-hole symmetric scenario in reverse direction, the asymptotic density being independent of that at the *exit* site. Not also that we have necessarily $\rho_-^* \leq 1/2 \leq \rho_+^*$, which is why the corresponding regimes are denominated 'low density' and 'high density', respectively.

Juxtaposing these two behaviours provides a first glimpse of the fact that we are dealing with a *boundary controlled* process, as we shall discuss now.

TASEP: boundary induced phase transitions We have established that, except for a boundary effect, we are essentially dealing with a constant density profile. We can now call upon further mean-field arguments to establish complementary intuition. Indeed, from the above discussion we know that we must distinguish several phases for the stationary transport regime:

- A *high density (HD)* regime, for which the bulk density is equal to the density at the exit, and thus set to $\rho_{HD} = 1 - \beta$ by the exit reservoir. The corresponding current is, $J_{HD} = \beta\,(1 - \beta)$, from Eq. (5.4).
- A *low density (LD)* regime, for which the bulk density is set by the entry reservoir density α. The corresponding current is $J_{LD} = \alpha\,(1 - \alpha)$.
- A *maximum current (MC)* regime, for which the current is at its maximum value, $J_{MC} = \gamma/4$. This occurs at half-filling ($\rho_{MC} = 1/2$).

These different regimes are usually presented in terms of a 'phase diagram', mapping out the occurrence of each of these regimes in a two-dimensional 'phase space' corresponding to the entry and exit rates α and β. This is presented in Fig. (5.3). We can thus complete the above list to

- HD: $\beta < \alpha$ and $\beta < 1/2$ (exit-limited flow)
- LD: $\alpha < \beta$ and $\alpha < 1/2$ (entry-limited flow)
- MC: α, $\beta > 1/2$ (bulk-limited flow)

Here we have highlighted that, as established above, in each of these regimes the density ρ is the parameter which characterises transport. In LD, current and density are set by the entrance density: we are dealing with an *entry limited* current. In contrast, in HD we are dealing with *exit limited* transport. For the MC phase, however, nor the entry rate α nor the exit rate β have an effect on the flow: this is the *bulk-limited* regime, where particles can essentially enter and exit freely, but it is their hopping from one site to the next which becomes the limiting process.

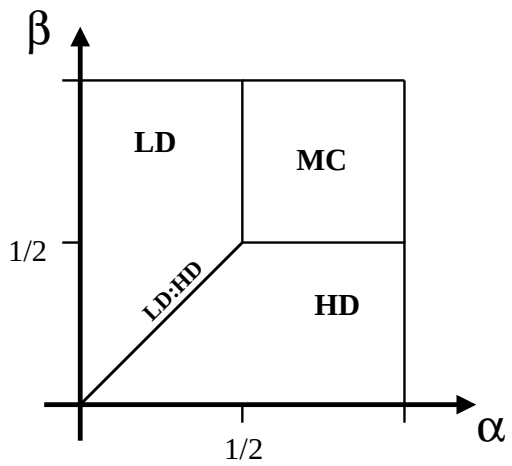

Figure 5.3: *Illustration of the 'phase diagram' for TASEP on a single segment. According to the in-rate α and the out-rate β, one finds a low density (LD) phase, a high density (HD) phase or a maximal current (MC) phase. The line LD:HD indicates a coexistence of both phases on the same segment, corresponding to a first order transition.*

Terming the respective regions in parameter space 'phases', as one would have done for an equilibrium system, suggests pushing the interpretation further by considering 'phase transitions' between the corresponding regimes. Acknowledging the important role of the entry and exit rates, we are thus dealing with *boundary-induced phase transitions*, a term coined by Krug [120] and now well adopted [93, 151]. The somewhat loose denomination in terms of 'phase transitions' is widely used, but refers of course to bifurcations concerning the stationary solutions, rather than implying any features of equilibrium phase transitions. Nevertheless, the analogy is in fact very useful. We can thus consider how one crosses from one of the LD or HD regions into the MC regions. A straightforward analysis based on the mean-field results shows that the (bulk) density ρ and the current J vary continuously and with a smooth first derivative, as the boundaries of the MC phase are crossed. This is reminiscent of a second order transition. In contrast, as one crosses the line $\alpha = \beta$ from the LD to the HD regions, both density and current evolve with a discontinuity in their first derivative, suggesting a first-order 'transition'.

Domain walls The analogy with a first-order transition is further strengthened by recalling that the density corresponding to a given current is double-valued: in principle, two values for the density can sustain the same current. This is a key observation. One can thus envisage a segment consisting of a LD zone followed by a HD zone, the two separated by an interface. And one can show, based on a description in terms of partial differential equations [48, 70], that this is indeed a viable solution corresponding to a soliton, often referred to as a *domain wall*. The HD phase then corresponds to the case where this domain wall has been pushed right towards the exit, whereas the LD phase corresponds to it being pushed to the entry. The transition line $\alpha = \beta$ on the other hand, for α, $\beta < 1/2$, is the borderline case. Here the interface can persist in the bulk. It thus leads to a *coexistence* of a LD and a HD phase on the same segment, again reminiscent of coexistence of two phases in the same sample, as in first-order phase transitions.

In this coexistence phase, the position of the domain wall is set by the total number of particles in the system: this determines how large the HD zone can be, and needs to be. In an open segment on the other hand, coupled to reservoirs, the domain wall position fluctuates. Through a collective process it can thus diffuse throughout the segment, albeit on a much larger

time scale than that associated with particle motion. The domain wall motion, including its diffusion coefficient, can be characterised by what is known as *domain wall theory* [118].

Stochastic simulations of TASEP It is important to critically examine any results which are established based on mean-field arguments, and this can be readily done using computer simulations, which are very straightforward for TASEP. They consist simply in representing N particles on a lattice of L sites, which undergo stochastic hopping events. For TASEP, the procedure is close to what one would do in Monte Carlo simulations:

- randomly pick a site $i \in [0, L]$, thus allowing for an extra site ($i = 0$) which represents the entry reservoir
- perform the associated random process:
  - if $i = 0$: with probability α, insert a particle onto the entry site $i = 1$ (provided the latter is empty)
  - if $i = L$: with probability β, remove the particle from the exit site L
  - otherwise (i.e. if $i \in [1, L-1]$): move the particle from site i (if any) to site $i+1$ (provided the latter is empty)
- sample whatever observable one is interested in over this chain of configurations

Performing $L+1$ such (attempted) moves corresponds to one cycle, which serves as basic time scale (in units of $1/\gamma$). Counting the number of successful moves then directly allows to deduce the particle current, and averaging the occupancy on a given site i yields the average density ρ_i on this site.

This scheme is the conceptually simplest procedure, but can of course be optimised (for example by directly picking particles, rather than the sites, which are potentially empty). It can also be generalised to other models, for example to include particle absorption/desorption. In this case it may also prove useful to use a continuous-time algorithm [107] as a variant.

Biological relevance of TASEP We have introduced TASEP above as a simplified model for describing the stochastic active motion of molecular motors. Initially, however, it has been introduced by MacDonald et al. [130] in the context of *protein synthesis*. For a protein to be 'expressed', the corresponding sequence in the DNA chain must be converted into a protein molecule. This is done by synthesising a corresponding sequence of amino-acids, but this step does in fact not happen directly on the DNA. Instead, a messenger-RNA (m-RNA) chain is produced in a first step which codes the complementary structure to the DNA chain, i.e. for each nucleic acid in the original DNA blueprint the complementary nucleic acid is placed in the m-RNA chain (*transcription*). It is this chain which is then, in a second step, 'read' and translated into protein chains (*translation*). This is achieved by *ribosomes*, themselves complex proteins, which step along the m-RNA chain and synthesise the protein sequence as coded by the m-RNA. In this process, too, 'particles' (ribosomes) stochastically step along a linear structure, with a regular step size, and subject to an excluded volume condition. It is this analysis which has prompted MacDonald et al. [130] to formulate the TASEP.

At the first level of detail, as introduced above, the model also describes the motion of molecular motors (for recent reviews see [35], but also [34]). It has the great merit of establishing a connection between the (simple) microscopic motion of individual motors and the (potentially complex) collective behaviour in molecular transport along actin fibers or microtubule filaments.

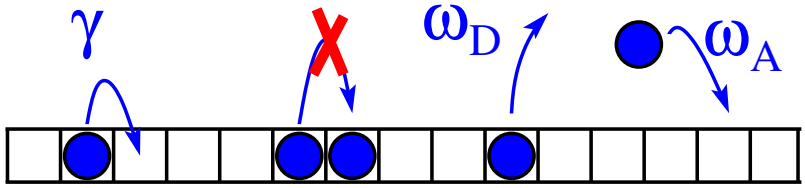

Figure 5.4: *Schematic illustration of the Totally Asymmetric Simple Exclusion Process with Langmuir Kinetics (TASEP-LK). It amounts to a TASEP, but in which particles can also detach from the filament (rate ω_{off}), or can adsorb from the bulk (rate ω_{on}). The bulk concentration is taken to be uniform and constant.*

One may thus wonder how realistic this description is in view of the many drastic simplifications introduced above. Very recent work [161] has confronted predictions to experimental results in various situations, concluding that a valid description is obtained once one acknowledges the fact that molecular motors have a finite *processivity*, i.e. that they do not run indefinitely along a track, but will ultimately unbind. This feature had been explored by Parmeggiani and Frey [146, 147] in a model known as *TASEP-LK*, where LK stands for *'Langmuir kinetics'*. In this model particles can be exchanged with a surrounding reservoir where they are assumed to be present in a homogeneous concentration. They stochastically undergo binding and unbinding events, in the same spirit as the Langmuir absorption process [123], hence the name of TASEP-LK. The mathematics of these models are rather more involved than those of TASEP, even on a mean-field level.

TASEP-LK: the model and a brief review of its phenomenology The model of TASEP subject to a Langmuir adsorption/desorption process has been introduced and solved by Parmeggiani, Franosch and Frey [146, 147]. It generalises TASEP by additionally letting motors detach from each site (with a detachment rate ω_{off}), but also allows for an empty site to catch a molecular motor from a surrounding bulk reservoir (attachment rate ω_{on}). On its own this Langmuir process would establish an average density of

$$\rho_{Langmuir} = \frac{K}{1+K} \tag{5.9}$$

where K characterises the ratio of adsorption and desorption rates:

$$K = \frac{\omega_{on}}{\omega_{off}}, \tag{5.10}$$

and this is the density one expects for TASEP-LK on a ring. On an open segment, however, the local equilibrium due to the Langmuir kinetics can be modified due to to the transit of particles actively hopping along the filament. The current among the filament thus need not be conserved, and the density profile no longer needs to be uniform (like in TASEP), but it can vary linearly along the segment, due to the particle exchange process operating along the filament. Nevertheless, one can still distinguish high density and low density phases, and it is still possible to achieve coexistence of these two 'phases' on the same segment. The MC phase is replaced by a Langmuir phase, where the density is no longer half-filling, but rather it is directly set by the exchange process: it turns out to be the same density that one would find on an independent site in contact with a reservoir, ρ_{Langmuir} given by Eq. (5.9).

The mean-field phase diagram [146, 147] is simplest in the particular case of equal on- and off-rates (K=$\omega_{on}\omega_{off}$=1), in which case it remains very reminiscent of that of TASEP. The major difference is that the coexistence phases are now extended phases, which occupy a surface

in the (α, β) plane, rather than being confined to a line. This case is illustrated in the middle column of Fig. 5.5, as a reference for discussions in the following.

Most of the phenomenology is already apparent from this particular case. There is one additional parameter which sets the ease at which the exchange takes place, which is conveniently chosen as

$$\Omega = \frac{\omega\, L}{\gamma} \ . \tag{5.11}$$

This is a dimensionless measure for the ratio of the time it takes an isolated motor to cross the filament ($L\,\frac{1}{\gamma}$) and the time it takes for a motor to detach ($1/\omega$). The parameter Ω thus measures the importance of the exchange with the bulk. Its inverse $1/\Omega$ characterises the fraction of the segment which a single (isolated) motor would cover before detaching. Note that this parameter does not only depend on microscopic rates, but also on the length of the segments.

The corresponding phase diagram is shown in Fig. 5.5. We see that the coexistence phases progressively dominate as the exchange parameter Ω is increased, involving the matching of two mathematically different solutions in different regions of the segment. Such the LD-HD coexistence is present, as in standard TASEP, but it now corresponds to an extended phase occupying a finite region in the (α, β) parameter plane (contrary to what is seen in standard TASEP, where the coexistence is limited to a line). However, in TASEP-LK it is localised at a particular position, and no longer diffuses freely over the entire length of the segment.

In addition, further 'extended phases' arise as a LD-MC and MC-HD phases, in which there is coexistence between LD (or HD) sections with a MC phase. In the HD and LD phases, the density profile is linear along the segment, its slope directly set by Ω. In contrast, the MC phase has a homogeneous density profile at a value of $\rho = K/(1+K) = 1/2$. Note also that an extended region in parameter space sustains a three-fold coexistence, LD-MC-HD.

The general case, $\omega_{off} \neq \omega_{on}$, is mathematically more complex [147], but it is governed by similar physics. It requires two parameters, which could be chosen by defining separately $\Omega_{off} = \omega_{off} L/\gamma$ and $\Omega_{on} = \omega_{on} L/\gamma$, but it is more convenient to use the (dimensionless) combinations

$$K = \frac{\Omega_{on}}{\Omega_{off}} \qquad \text{and} \qquad \Omega = \frac{1}{2}\left(\Omega_{off} + \Omega_{on}\right) \ . \tag{5.12}$$

Thus K indicates to which extent the particle attachment is faster than the process of particle detachment, whereas Ω characterises the overall exchange with the bulk reservoir.

As an example, the phase diagram for $K = 1.5 > 1$ is sketched in Fig. (5.5). Essentially, the LD phase is progressively disfavoured. This is a consequence of the fact that, for $K = 1.5$, particle attachment is faster than detachment, which disfavours low particle densities. As soon as the exchange, characterised by Ω, is sufficiently efficient, the HD phase is entirely eliminated, and remains present only as a coexistence phase. The other difference to be pointed out is that the MC phase indicated in the phase diagrams is actually a modified MC phase, the density of which is set by the Langmuir process as $\rho_{\text{Langmuir}} = K/(1+K)$, which is thus larger than the half-filling density of 1/2 corresponding to the MC phase in TASEP. Full mathematical details and a full discussion of the phase diagrams are given in the work by Parmeggiani et al. [147]. Note also that it is sufficient to consider $K > 1$, since a symmetry can be established which allows to deduce the corresponding phase diagram for the inverse parameter $K' = 1/K < 0$.

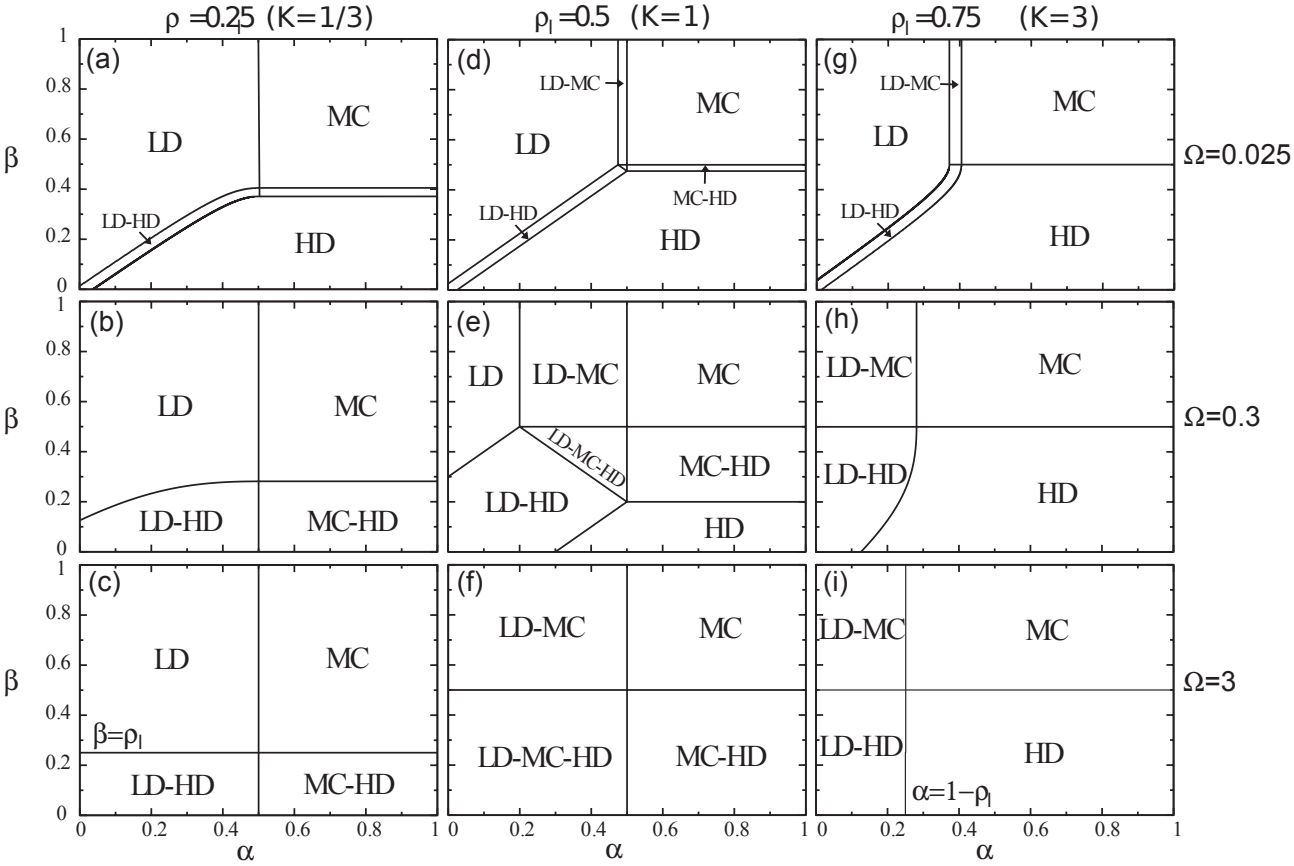

Figure 5.5: *Overview of the mean-field phase diagrams for a single segment of TASEP-LK. The exchange parameter Ω increases from top to bottom. The middle column (d-f) corresponds to the case of equal attachment and detachment rates ($K = \omega_{off}/\omega_{on} = 1$).*

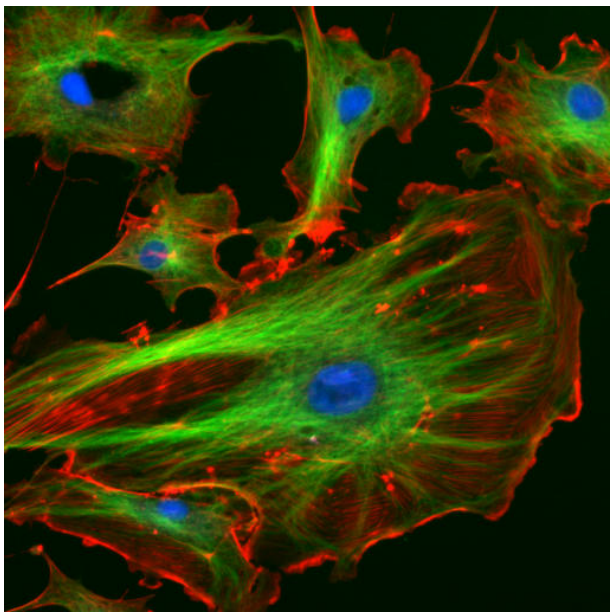

Figure 5.6: *Example of a cytoskeleton, comprising both actin filaments (red) and microtubules (green). The cell nucleus is shown in blue. Note that the structure is in fact dynamic, and its re-organisation plays an important role in the cell division process. Image from [137], available at [138].*

5.2 Selected publications

The active, motor-protein driven transport mechanisms introduced above play an important role in biological cells. One aspect, which as been explored very little heretofore, is the fact that the fibers along which the transport takes place are in fact highly interconnected. Microtubules are known to cross-link due to special cross-linking proteins (so-called MAPs, *microtubule-associated proteins*) which create a junction by fixing them close together. Actin fibers can also cross-link, or even branch their actual structure (due to proteins called called *Arp complexes*). The resulting network of fibers is the scaffold of what is known as the *cytoskeleton*: see Fig. (5.6) for an illustration allowing to appreciate its complexity. This compound plays an important role also for the structure, elasticity and active shape adaptation of cells [2, 95]. In the context of intra-cellular transport, the interconnections modify the transport, and we must understand the role of the network connectivity. The work discussed in the following is motivated by this question, and attempts to provide insight into active transport on branched structures or on networks. It is also worth pointing out that networks of microtubules or of actin filaments can now be produced in laboratory conditions [152, 165, 172], with some degree of control on the network geometry.

Having in mind the picture of a cross-linked network, we will often refer to *junctions* as a synonym of the term *vertex* used above.

5.2.1 TASEP on structures of branched filaments

Reference to the original work:

> *"Understanding totally asymmetric simple-exclusion-process transport on networks: Generic analysis via effective rates and explicit vertices"*
> *Ben Embley, Andrea Parmeggiani, and Norbert Kern*
> *Phys. Rev. E 80, 041128 (2009)*

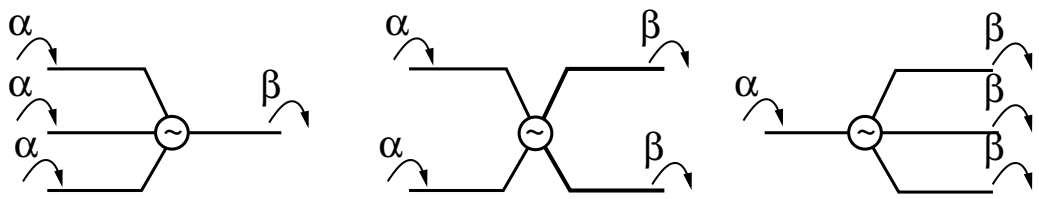

Figure 5.7: *Illustration of all variants of a 4-fold vertex: a V(3:1), i.e. 3 incoming and one outgoing segment; a V(2:2), i.e. 2 incoming and 2 outgoing vertices; a V(1:3), i.e. 1 incoming and 3 outgoing vertices.*

The first question to ask is how one can go about generalising the study of TASEP to a system of branched filaments. Only a few studies had addressed these questions [27, 158] for particular structures, such as a segment with a double-section in its middle or a 3-fold vertex. Furthermore, they did not tackle the questions in a way which would be easy to generalise to other topologies. We have thus first set out to analyse TASEP on a regular honeycomb structure of segments [60], and then to address generic elements (4-fold vertices of any type), developing a systematic procedure for treating a general topology. We will do so on a mean-field level: to our knowledge, there is currently no exact solution available for TASEP involving any branched topology, and even for simpler systems in equilibrium branching continues to pose a formidable challenge for exact methods [39].

Junction site and effective rates Four-fold vertices come in three kinds, which we will name V(1:3) for '1-in-3-out', V(2:2) for '2-in-2-out' and V(3:1) for '3-in-1-out'. They are schematically represented in Fig. 5.7. We limit the discussion to having all incoming/outgoing segments equivalent (i.e. identical in-rate α for all incoming segments, and identical out-rate β for all outgoing segments of the vertex under consideration). We also assume, for the time being, that the particles leaving the vertex pick one of the outgoing edges at random, with equal probability (i.e. for now we do not allow *bias*).

We analyse the transport by singling out one particular site, which we attribute to the vertex v itself. It will be convenient to label quantities local to a vertex by a tilde, and thus the average occupancy on the site of vertex v site is noted $\tilde{\rho}_v$. The key observation is that it is this (average) density which sets the flow into and out of the vertex. Thus the mean-field current from a given incoming segment s into the vertex v is

$$J_{s\to v} = \gamma\, \rho_s^{(out)}\, (1 - \tilde{\rho}_v)\ , \tag{5.13}$$

which is proportional to the hopping rate, to the probability of having a particle on the last site of the segment s (noted $\rho_s^{(out)}$)), and the probability of having the vertex site empty, $1 - \tilde{\rho}_v$. Similarly, the current out of the vertex v into an outgoing segment s' is

$$J_{v\to s'} = \frac{\gamma}{c_v^{(out)}}\, \tilde{\rho}_v\, (1 - \rho_{s'}^{(in)})\ , \tag{5.14}$$

where $\rho_{s'}^{(in)}$ stands for the average occupancy of the first site of the outgoing segment s'. The factor $1/c_v^{(out)}$ accounts for the fact that any particle hopping out of the vertex site selects one of the $c_v^{(out)}$ outgoing segments, where $c_v^{(out)}$ is the *out-degree* of this vertex.

The above expressions for the mean-field current amount to saying that the vertex v plays the role of a reservoir for both the incoming and outgoing edges. Thus the incoming segments s receive particles from a reservoir of density ρ_v; equivalently, their effective out-rate is $\beta_{s'} = 1-\tilde{\rho}_v$.

Analogously, the outgoing segments s' are fed by a reservoir of density $\tilde{\rho}/c_v^{(out)}$; this is equivalent to attributing entry and exit rates to those segments. Thus we have

$$\begin{array}{lcll} \text{in-segment s} & : & \alpha_s = \alpha & , \quad \beta_s = 1 - \tilde{\rho}_v \\ \text{out-segment s'} & : & \alpha_{s'} = \dfrac{1}{c_v^{(out)}}\,\tilde{\rho}_v & , \quad \beta_s = \beta \ . \end{array} \tag{5.15}$$

These *effective rates* allow us to treat each of the segments separately, just as if it were a single TASEP segment, with its 'phase diagram' as established above. This also sets the current through each segment, via the relation $J_s = J(\alpha_s, \beta_s)$ established in the introduction, and the density as $\rho_s = \rho(\alpha_s, \beta_s)$.

Current conservation The only remaining step is to determine the vertex occupancy $\tilde{\rho}_v$, which can be done by imposing current conservation at the vertex:

$$\sum_{s\to v} J\left[\alpha, \beta_s = 1 - \tilde{\rho}_v\right] = \sum_{v\to s'} J\left[\alpha_s = \frac{\tilde{\rho}_v}{c_v^{(out)}}, \beta\right] \ . \tag{5.16}$$

We use $J[\alpha_{eff}, \beta_{eff}]$ to indicate the mean-field TASEP current as set by the *effective* entry/exit rates of the segment. In this example the sums are of course just a complicated way of representing the fact that there are $c_v^{(in)}$ identical contributions to the in-current, and $c_v^{(out)}$ identical contributions to the out-current. However, the explicit notation in Eq. (5.16) is more appropriate in view of generalisations to come.

Eq. (5.16) thus yields one (linear) equation for the vertex occupancy $\tilde{\rho}_v$, from which the mean-field currents and densities follow directly for the incoming and outgoing segments. With this procedure, which is entirely generic for any vertex topology, the analysis of a 4-fold vertex becomes straightforward.

One result which can be established is the effective 'phase diagram' of the composite vertex, as it is driven by entry rates α and exit rates β. This is shown the Fig. (5.10), where the notation LD:3HD, for example, indicates that a V(1:3) has its entry segments in HD and its three exit segments in HD phases. These have been confirmed directly by simulation [61], but we turn to other predictions which allow to confirm the mean-field results more quantitatively.

Periodic V(2:2) as an example Two directly predicted observables are the current J as a function of the entry/exit rates, or the current-density relation $J(\rho)$, as well as the junction occupancy $\tilde{\rho}$, which turns out to contain significant insight. We show this data, in Fig. 5.9. To be precise, we should state that it has been obtained for a periodic equivalent of the V(2:2), resulting from connecting the outgoing segments back into the incoming ones, as shown in Fig. 5.8. This is equivalent to a 2-fold loop sharing one vertex site, and corresponds to imposing the relation $\alpha = 1-\beta$ in the (α, β) plane (we avoid going into the discussion of strict periodicity vs. periodicity-on-average, see [60]). This mean-field prediction can be summarised and interpreted as follows:

- for small densities ($\rho < 1/3$) both segments are in a LD phase, and their current increases quadratically, following the corresponding relation $J(\rho)$ for a single segment,
- for high densities ($\rho > 2/3$) both segments are in the HD phase, with the corresponding quadratic decrease of the current,
- in the intermediate region ($1/3 < \rho < 2/3$) the mean-field prediction is a plateau, which corresponds to a LD-HD coexistence in both of the rings. Here the vertex acts as a bottleneck.

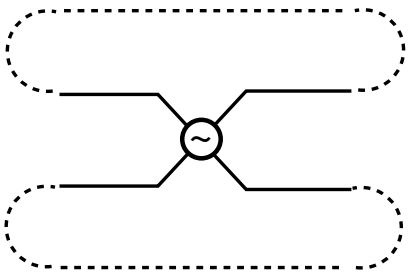

Figure 5.8: *Periodic system corresponding to a V(2:2). Whenever the entry and exit rates satisfy $\alpha = 1 - \beta$, a V(2:2) forms a system which is periodic on average, and most of its physics can be understood by studying a simpler system consisting of two TASEP loops having one shared site.*

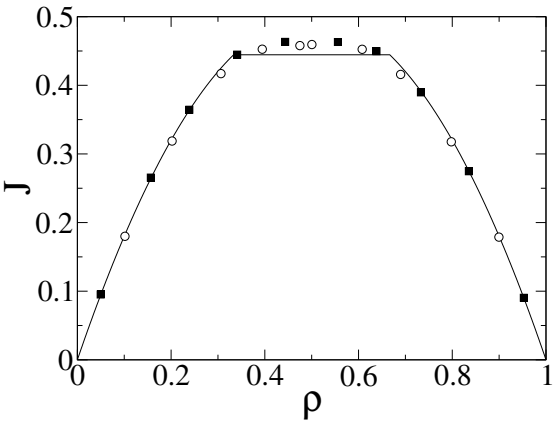

Figure 5.9: *Current-density relation of a periodic V(2:2), topologically equivalent to a double loop sharing a junction site. The line indicates the mean-field prediction, symbols are from stochastic simulations.*

The simulation data (symbols) confirm the mean-field prediction (continuous lines) exceptionally well, except for the plateau-region around half-filling, where the mean-field predictions slightly underestimate the current. This can be attributed to inter-segment correlations across the junction, as has been argued very recently by Baek et al. [9].

In fact, the most remarkable feature is not that the mean-field results require a correction in the density range corresponding to the presence of two LD-HD domain walls. Rather, it may seem surprising that, despite having a shared vertex which must be expected to act as a bottleneck for both rings, the (mean-field) current in the low and high density regimes is *exactly* what we would expect for two entirely independent rings with no junction. This is obvious for very low (and very hight) densities, but it is surprising for this to hold for densities as high as 1/3. A careful analysis shows that this is due to two cancelling effects. On one hand the vertex acts as a bottleneck, making it less likely for a particle to succeed a hop into the junction. On the other hand, particles pile up in front of the junction, and thus hops are attempted more often. It turns out [61] that the two effects *cancel*, right to the point where the LD-HD coexistence arises.

Another feature that emerges from this data is that the current-density relation $J(\rho)$ is particle-hole symmetric. This is not entirely surprising for the topologically symmetric V(2:2), but the microscopic aspects are in fact a little subtle: particles hopping forwards obey the same rules as holes hopping backwards, *except* at the vertex site, where the symmetry is broken due to branching. It nevertheless turns out that one can establish a generalised particle-hole symmetry for branched structures [61], which also covers the symmetric phase behaviour

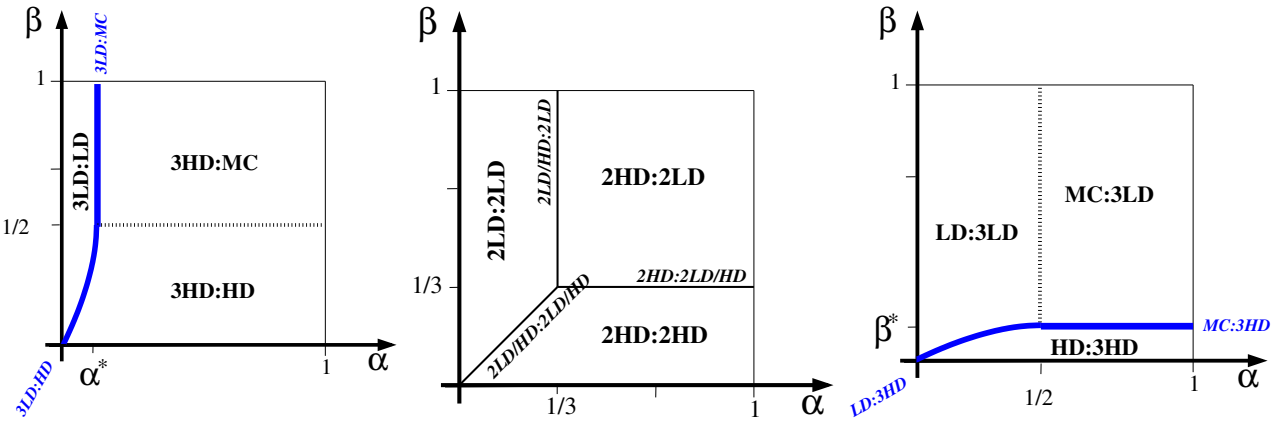

Figure 5.10: *Phases of a 4-fold vertex. Shown is a V(1:3), i.e. a vertex consisting of three incoming segments and one outgoing one, as well as a V(2:2) and a V(3:1). The phase diagrams of the V(3:1) and the V(1:3) are related by symmetry rules generalising the particle-hole symmetry in a single segment.*

between the V(1:3) and the V(3:1), shown in Fig. 5.10.

Bias at a junction As a test case for the generality of our approach, one may consider the above V(2:2) but with a bias at the junction: the jumps out of the vertex site take place giving preference to segment 1, say, with a ratio $\sigma_1 : \sigma_2$ (where $\sigma_1 + \sigma_2 = 1$, i.e. the overall jump rate is still set by γ). This scenario shows nicely that the approach is generic, since we can easily incorporate the bias into the effective rates of the segments. The in-rates for the two segments are most easily written thinking about the segments directly:

$$\begin{aligned} \text{segment } s_1 \quad &: \quad \alpha_1 = \frac{\sigma_1}{c_v^{(out)}}\,\tilde{\rho} \quad , \quad \beta_1 = 1 - \tilde{\rho}_v \ , \\ \text{segment } s_2 \quad &: \quad \alpha_2 = \frac{\sigma_2}{c_v^{(out)}}\,\tilde{\rho} \quad , \quad \beta_2 = 1 - \tilde{\rho}_v \ , \end{aligned} \tag{5.17}$$

whereas both out-rates remain unchanged, since they are independent of the bias.

Applying the condition of current conservation at the junction still closes the set of equations and yields the full behaviour of the system. The mean-field calculations become more tedious but remain straightforward. An example for the resulting flow is characterised in Fig. 5.11 for a bias of $\sigma_1 : \sigma_2 = 0.75 : 0.25$. They are confirmed, with rather small deviations, by microscopic simulations. Two remarkable features arise:

First of all, the current in the loop favoured by the bias is indeed higher than that in the other one, but only up to half-filling. For $\rho > 1/2$ it turns out that both branches carry the *same* current. This amounts to saying that, rather surprisingly, beyond this threshold the bias has no effect whatsoever. The explanation again resides in a cancellation of two terms, showing that the bias falls victim to it's own success: as more and more particles are pushed into the favoured branch, the occupancy at its entrance site rises, making it more and more difficult for further particles to enter. The inverse feedback takes place in the less-favoured branch, and beyond half-filling both currents become equivalent.

The other feature is that we are now dealing with *two* current plateaus. A first plateau, at around $\rho \approx 1/3$, corresponds to current saturation close to the maximum of the parabolic current, and is attributable to a LD-HD coexistence in the *favoured* loop. The other one, extending from $\rho = 0.5$ to about $\rho \approx 0.75$, is due to a LD-HD coexistence in the *less favoured*

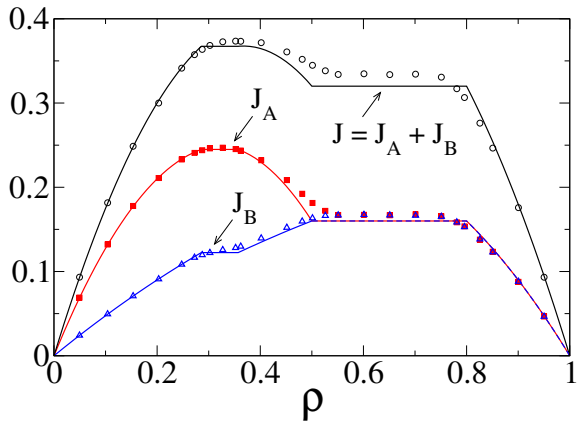

Figure 5.11: *Current-density relation for TASEP on a periodic V(2:2), in the presence of bias ($\sigma_A : \sigma_B = 75 : 25$). Shown are the currents through the individual loops, J_A and J_B, as well as the total current through the junction site ($J = J_A + J_B$).*

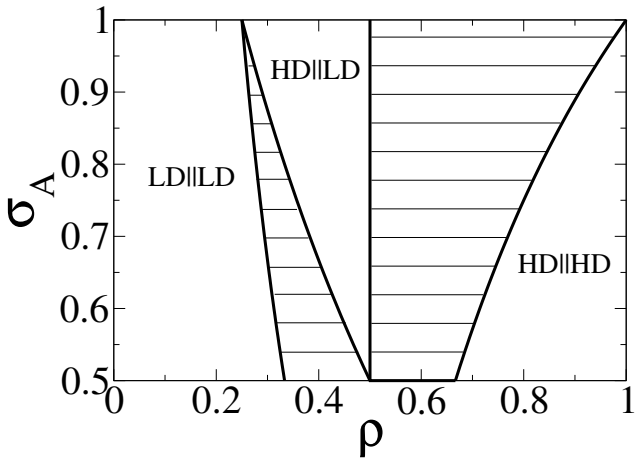

Figure 5.12: *Phases of the current plateaus for the current through a periodically closed V(2:2). For any given bias (σ_A, knowing that $\sigma_B = 1 - \sigma_A$) the diagram indicates which phases are present in the system. The hatched zones indicate LD-HD coexistence, the first one in the favoured loop, the second one in the other loop.*

loop. The mean-field equations reveal full details as to how these plateaus evolve as a function of the bias, as is represented in Fig. 5.12.

One major conclusion which can be drawn from the previous discussion is that the junctions play a major role in the flow. This suggests that introducing the (average) occupancy at the junction as an explicit variable, $\tilde{\rho}$, is a fruitful approach, and we shall exploit this further in the following. The example of a bias has furthermore highlighted the impact of junctions on the flow. This will also be explored further below, with a view towards experiments on molecular motors.

5.2.2 TASEP transport on a network

Reference to the original work:

"Totally Asymmetric Simple Exclusion Process on Networks"
Izaak Neri, Norbert Kern, and Andrea Parmeggiani
Phys. Rev. Lett. 107, 068702 (2011)

Having analysed the flow through a simple junction has shown us how to use the mean-field approach in order to address the question of branched structures, and has provided a glimpse of the behaviour one should expect. The subsequent challenge is of course to study a full network. We shall show that the method can easily be generalised and provides an efficient method for analysing large networks, far beyond the scale which would be accessible in stochastic simulations. At this point it does not appear useful to taylor the structure of the network as to represent any particular biological situation: high-resolution structural studies of the cytoskeleton are still rather recent [17, 66, 135] and may vary from one type of cell to the other, but also with the localisation within the cell and over time. Also, depending on the type of network one might be interested in (for example actin or microtubule networks) the nature of the junctions may require further thought (see below). For the moment, in order to develop our argumentation, we focus on *random* networks, which will allow us to expose the role of their topological features on the transport process.

Random networks In the following it will be necessary to refer to the connectivity of the network, and we adopt a pragmatic notation, as light as possible yet inspired by the mathematical literature on graphs. We thus refer to the nodes or junctions as *vertices*, represented as $\{v\} \in V$, where $|V|$ is the total number of vertices. Similarly, we refer to the (polar) filaments as *segments* $\{s\} \in S$; note that in graph theory they would be referred to as *(directed) links* or *edges*, but the name 'segments' anticipates the fact that they will be analysed in the same spirit as the single open segment for TASEP transport, discussed in the first section.

The connectivity of the resulting network is typically described by a *connectivity matrix* [12], but we do not need to define it explicitly here. It will be sufficient to observe that the topology of each vertex is characterised locally by its degree or *cardinal number* c. Since we are dealing with directed segments, we must distinguish the *in-degree* $c_v^{(in)}$ and the *out-degree* $c_v^{(out)}$, each of which counts the number of incoming/outgoing segments for a given vertex v, just as for the single vertex considered above.

A network for which all vertices have the same degree (and therefore $c_v^{(in)} = c_v^{(out)} \, \forall \, v \in V$) is called *regular*. By contrast, a network in which the vertices do not satisfy this constraint (the general case) are called *irregular* networks. Here we use *random networks*, which are described by the distribution from which the network instances are drawn or, equivalently, by the set of rules by which they are constructed.

A regular network of degree c can be thought of as a randomised version of a lattice. We start from a regular (cubic) lattice in c-dimensional space, which is a particularly ordered example of a regular network. Each vertex has then c incoming and c outgoing segments. By iteratively picking pairs a vertex at random and exchanging either two of their incoming or two of its outgoing segments, we ultimately obtain a randomised network in which any vertex is connected to any other vertex with the same probability, but which remains regular. This is also known as a *Bethe* network.

Irregular networks can be constructed from various rules. Here we consider *Poissonian* networks, which can be obtained by starting from a set of $|V|$ nodes without any segments. Each of the potentially present $|V| \times (|V| - 1)$ directed segments is then added with a finite probability. As a result one obtains a poissonian distribution for the vertex degrees [12]. In mathematics this would correspond to the Erdös-Renyi graph. Technically speaking, in order to avoid pathological contributions, we restrict our analysis to the *strongly connected component*, obtained by removing unconnected vertices or sub-graphs.

Numerical approach to solving TASEP transport on a network The goal is thus the following: once an instance of a network is drawn at random, we wish to determine the (steady state) transport features. It turns out that, once the problem is formulated as we have done in the introduction above, there is a straightforward numerical procedure to determine this stationary state. It is based on the particle count at a junction v which, in the mean-field approximation, reads

$$\frac{d\rho_v}{dt} = \sum_{s\to v} J[\alpha_s, \beta_s] - \sum_{s'\leftarrow v} J[\alpha_{s'}, \beta_{s'}] \ , \tag{5.18}$$

where the sums run over the segments entering ($s \leftarrow v$) or leaving ($s \to v$) the vertex v under consideration and $J[\alpha, \beta]$ stands for the single-segment mean-field current, as in the previous section. In the stationary state this reduces to the equation of current conservation, Eq. (5.16), which we must impose. Here the procedure consists in implementing this equation iteratively. Since the currents of a TASEP segment are given by Eq. (5.4), in terms of the effective rates (Eq. 5.17) set by the junction occupancies, we can rewrite this as

$$\frac{d\rho_v}{dt} = \sum_{v'\to v} J[\frac{\rho_{v'}}{c_{v'}^{(out)}}, 1-\rho_v] - \sum_{v'\leftarrow v} J[\frac{\rho_v}{c_v^{(out)}}, 1-\rho_{v'}] \ . \tag{5.19}$$

We can thus simultaneously modify the mean-field occupancy of all vertices v of the network according to this rule, until a stationary state is achieved. In this way we obtain the stationary transport state which simultaneously satisfies current conservation at all junctions. Convergence is typically fast as long as the vertex degrees are not extremely high, and the gain in performance with respect to particle-based simulations is obviously extremely interesting: rather than simulating particles on L sites for each segment, we simply have to solve for one variable per vertex, which is its (mean-field) average occupancy ρ_v. This is what has made it possible to investigate rather large networks.

Phenomenology of regular vs. irregular network topologies The simplest case to discuss is that of regular networks. For these the mean-field predictions are particularly simple, based on the observation that all vertices, and all segments, are topologically equivalent. Since inter-segment correlations are neglected by the approach we thus expect all vertices (and consequently all segments) to obey the same relations, which are in fact simply those of a V(c/2:c/2), i.e. a vertex with $c/2$ incoming and $c/2$ outgoing segments. The corresponding behaviour is a straightforward generalisation of the V(2:2) discussed above, and leads to the density-current relation

$$J(\rho) = \begin{cases} \frac{c}{(c+1)^2} & \text{for } \rho^* < \rho < 1-\rho^* \\ \rho(1-\rho) & \text{otherwise} \end{cases} \ , \tag{5.20}$$

where the density threshold setting the mean-field transition to the LD-HD coexistence phase (or shock phase, SP) is $\rho^* = 1/(c+1)$. This current-density relation is represented by continuous lines in Fig. 5.13. The correspondence with both numerical mean-field solutions outlined above (full symbols) and explicit particle-based simulations (open symbols) is excellent in the LD and HD regions (the plateau corresponding to the LD-HD coexistence region is not accessible by the numerical implementation, which assumes homogeneous segments).

The main physical observation within the mean-field picture is that the junction clogs up as the connectivity is increased, as was to be expected. The numerical approach is entirely validated, since the results coincide with the analytical mean-field predictions. As for the slight deviations on and close to the coexistence plateau, they allow to appreciate the effect of cross-segment correlations, as already concluded for the V(2:2). This has been elucidated very

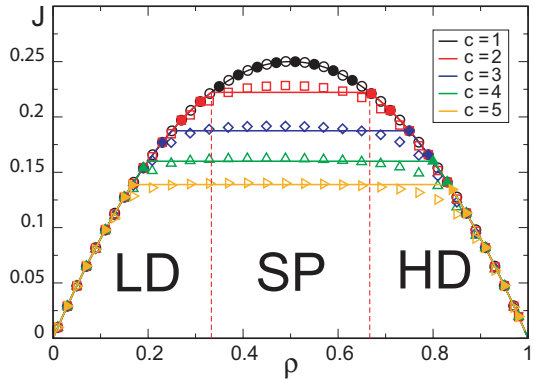

Figure 5.13: *Current-density relation for TASEP on a regular network. 'SP' refers to 'shock phase', an alternative term sometimes used for LD-HD coexistence. Solid lines are mean-field predictions, symbols are results from stochastic simulations.*

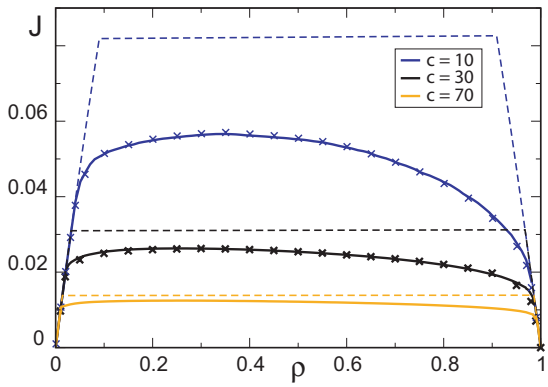

Figure 5.14: *Current-density relation for TASEP on a (poissonian) irregular regular network. Symbols are from stochastic simulations, solid lines are mean-field predictions, solved for using the iterative method presented in the main text. For comparison, the dashed lines indicate the mean-field prediction for a regular network with an equivalent vertex degree.*

recently by Baek et al. [9].

We now turn to the current-density relation for irregular, poissonian networks, which is non-trivial (see Fig. 5.14). Unavoidably the overall behaviour remains qualitatively similar: the current initially increases with density and then decreases again (due to steric exclusion), and the current drops as the connectivity increases. On the other hand, there no longer is a particle-hole symmetry. Accordingly, the optimal transport no longer occurs at half-filling, but at lower densities instead. There is no analytical mean-field prediction for this case, but directly comparing results from the numerical mean-field method and full simulations shows excellent agreement for all densities. The coexistence plateau, for which deviations occurred in the case of regular networks, is not present here.

Indeed, the absence of a coexistence plateau pinpoints the huge difference between the two types of networks. This is best illustrated in terms of a network containing very few particles (low overall density ρ), to which particles are added progressively. Initially, all segments are in a LD phase, irrespective of the network topology. As further particles are added, the density simply increases in each segment. The difference arises in the way the segments transit to the LD phase. In a regular network, there is a density threshold ($\rho* = 1/(c+1)$ at which the density of the segments becomes too high for a LD phase. Importantly, since all segments are equivalent, this point is reached *simultaneously* for all segments. On the other hand, at this point there are not yet enough particles for all segments to adopt a HD phase (which requires an overall density of $\rho > 1 - \rho^* = c/(c+1)$. This is of course similar to what happens in a single segment, and leads to the presence of a LD-HD coexistence ('shock phase') in *all* of the segments. Consequently, the current-density relation of a regular network reproduces the coexistence plateau. In contrast, in irregular networks, there is no unique point at which segments undergo the transition from LD to HD. Consequently, the *overall* current-density relation does not show a plateau.

This point of view is further illustrated in Fig. 5.15, which juxtaposes the distribution $W(\rho_s)$ of segment densities, i.e. the probability of finding segments with a (local) density ρ_s, for the regular and the irregular case. The example corresponds to an intermediate overall density ρ. It clearly shows that the regular network leads to a *monomodal* distribution, centered around the overall density ρ, and it is the *position* of this peak which increases as further particles are added. In contrast, for the irregular network the distribution of segment densities is *bimodal*, and it is the relative weight of the two contributing peaks which shifts towards the higher one as further particles are added to the system.

5.2.3 Active transport vs. diffusion

Reference to the original work:

> *"Modeling Cytoskeletal Traffic: An Interplay between Passive Diffusion and Active Transport"*
> *Izaak Neri, Norbert Kern, and Andrea Parmeggiani*
> *Phys. Rev. Lett. 110, 098102*

One important motivation for studying TASEP is its importance in Biology. Initially designed to account for the ribosome mediated transcription process [130], a whole variety of extensions and variations of TASEP has more recently been applied to modelling motor protein driven cytoskeletal transport, where molecular motors stochastically hop along bio-filaments such as microtubules or actin fibers. In particular, it has been shown recently that TASEP

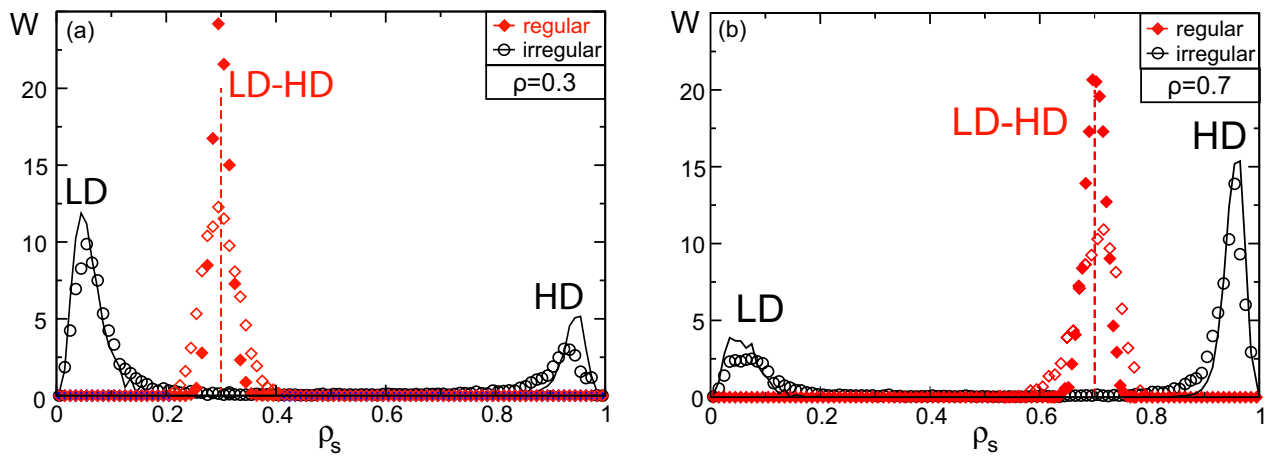

Figure 5.15: *Distribution of segment densities ρ_s on an irregular (Poissonian) vs. a regular (Bethe) network. (a) has been obtained for an overall density of $\rho = 0.3$, whereas (b) corresponds to the complementary density, $\rho = 0.7$. The black lines refer to numerical mean-field predictions, black circles to the corresponding stochastic simulations. The dashed lines labeled LD-HD indicate the location of the delta function predicted from analytical mean-field theory for the regular network, red symbols show results from stochastic simulations. Simulations for filled diamonds have run for longer, indicating that there is indeed a (slow) convergence to the delta-function like behaviour. Figure as in [141].*

transport subject to absorption/desorption kinetics (TASEP-LK, see [146, 147] is a valid description for transport by molecular motors.

One may thus wonder whether, in the context of TASEP transport on a network, any of the above results can be generalised to more complex models such as TASEP-LK. We shall see that this is indeed the case. Via this model we address the question of whether the active transport via TASEP-LK is able to maintain gradients in the cell, which is one of its crucial functions. As we shall show this is indeed possible, but the network topology has an important impact on how spatial inhomogeneities are promoted by the network.

The second aspect we focus on in this model is that it allows to gauge the effectiveness of active transport (along the filament) with respect to diffusion (in the bulk). This is because TASEP-LK implements an exchange with a bulk reservoir which is assumed to be *homogeneous* (the attachment rate in particular, but also the detachment rate, do not vary with the position). This amounts to assuming that the bulk density is homogenised as soon as a particle attachment or detachment has taken place. In this sense we are thus dealing with the limiting case of an infinitely efficient diffusion process in the bulk. We can thus use this extreme case to make our point that, despite a continuous exchange with the bulk, the active transport on the segments is still able to build up gradients in the particle density along the segments, and we will analyse the way in which this happens on a network.

Simulations and mean-field equations on a network The approach is identical to TASEP for both cases. In simulations, it suffices to implement the attempts to attach an additional particle to any site of the segment (which succeeds if this site is free) and to remove particles from any site of the network (which always succeeds), with the corresponding rates. The mean-field numerical procedure also goes through, where the current-density relation $J[\alpha, \beta]$ to be used in Eq. (5.18) is now that known for TASEP-LK [147]. Note that this is straightforward since, although the current is no longer necessarily constant along a given

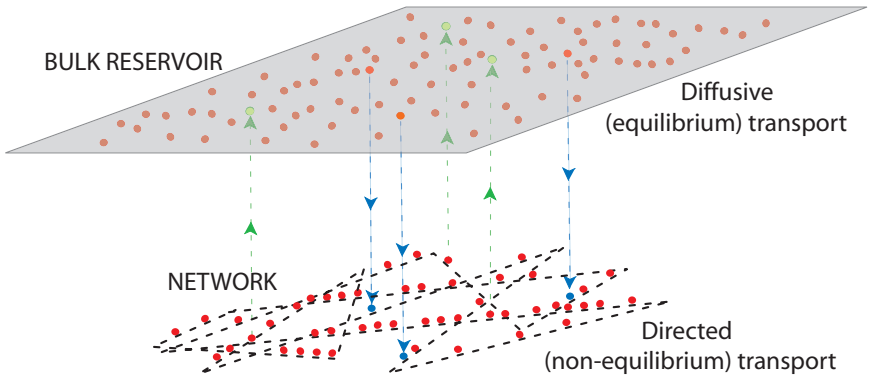

Figure 5.16: *Illustration of active transport vs. (infinitely fast) diffusion, as represented in TASEP-LK. Particles (motors) are exchanged between the segments and the bulk reservoir, which is taken to be maintained at a constant and homogeneous bulk density.*

segment, there still is current conservation at the junctions.

Effective rate plots for the network Here our goal is to study how the transport on the network takes place in the presence of an exchange with a bulk reservoir. To this end it proves useful to have a way to characterise the overall transport features of the network. We thus recall that the transport through a single segment s is entirely characterised by is effective entrance and exit rates, α_s and β_s, which allows to position the segment on the single-segment phase diagram. We can thus achieve a characterisation of the entire network by constructing a cloud of all points (α_s, β_s) representing all segments in the network.

In standard TASEP, the distribution of points in an effective rate plot depends on the topology only: for a regular network we expect them to coincide (since all segments are equivalent), whereas they are spread out for irregular networks (due to the locally varying connectivity). The distribution of points on the phase diagram then accounts for the overall state of the network, and the way how they evolve when parameters (such as the network connectivity) are varied.

This remains true for TASEP-LK, but in a more complicated scenario: varying the exchange parameter Ω changes both the distribution of state-points, but so makes the underlying single-segment phase diagram evolve. This is illustrated in Fig. (5.17). The main role of the exchange parameter Ω is seen to be to modify the underlying single-segment phase diagram, whereas it has little influence on how the (α, β) points are distributed in the phase space plane. We will now interpret these effective-rate plots on the scale of the network.

Inhomogeneities in the network The question we have raise is how spatial inhomogeneities arise due to active transport as opposed to the diffusive motion in the bulk. We will analyse this process by varying the exchange parameter Ω, which regulates the exchange with the bulk reservoir, for a given network connectivity. The picture emerges most clearly from the case $c = 10$ in Fig. (5.17).

In particular, we see that the points progressively retract to a zone close to the origin as the average vertex degree is increased. The role of the exchange parameter Ω on the other hand, is mainly to modify the underlying single-segment phase diagram. But it has little influence on the *zone* in the (α, β) plane into which segments fall (despite having an effect on the finer details of their distribution). The overall result of these two effects is to modify the

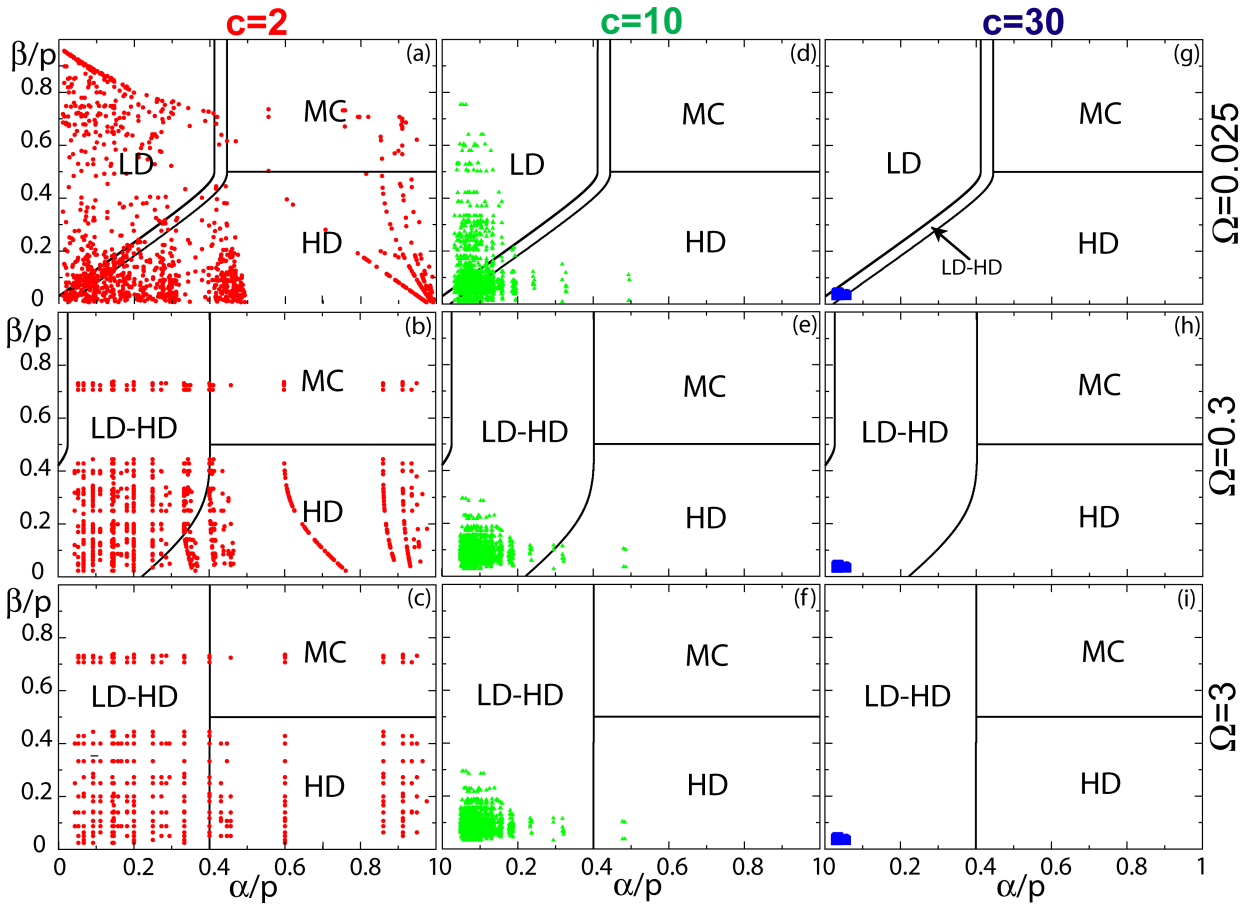

Figure 5.17: *Effective rate plots for a TASEP-LK network, for various Ω. The leftmost column shows a sequence of increasing exchange parameters Ω for a very weak exchange parameter, close to standard TASEP. TASEP-LK in the special case $K = 1$. The right column shows a similar sequence for non-equal attachment/detachment rates ($K = 1.5$).*

phases which are predominantly found in the network, and we shall exploit this in the following.

Reading the corresponding graphs from top to bottom, we first consider a weak exchange, i.e. a behaviour close to standard TASEP. The effective rate plot indeed confirms that the predominant phases are LD and HD. The MC phase is marginal or absent, which is due to the fact that only segments with more incoming than outgoing nodes can ever sustain a MC phase, and will only do so if the right conditions are met. The LD-HD, which corresponds to a zone of finite but still rather narrow extension in the (α, β) plane, accommodates only a few points: the number of segments in this phase is no longer zero (as it would be for TASEP), but it remains small. We refer to this regime as the *network regime*, since the main source of heterogeneity is on the scale of the network: we are dealing with an interconnected ensemble of segments which are either densely occupied (HD) or very sparsely occupied (LD).

The picture changes as the exchange parameter Ω is increased, and the LD-HD phase invades the single-segment phase diagram at the expense of the LD phase. By far the largest number of segments now shows coexistence, implying the presence of a domain wall within the segment. We thus term this the *segment regime*, since the spatial heterogeneities now arise within the segments.

Finally, when Ω increases even further, all segments are in the LD-HD phase. However, this is different from the previous case: the Langmuir kinetics dominates in this case, and imposes the Langmuir density $\rho_{Langmuir}$ onto each site. Note that this is not immediately obvious from the effective rate plot, but is due to another mechanism: the domain wall in the LD-HD sections is progressively shifted to one of the edges in this limit, thus ensuring that a larger and larger part of the LD-HD segments is effectively governed by the direct site-wise exchange via the Langmuir exchange process with the bulk. In this *site regime* (or *Langmuir regime*) any heterogeneities are thus limited to fluctuations from one site to another.

The different regimes of spatial heterogeneities are graphically summarised in Fig. 5.18.

Decoupling The widespread occurrence of the LD-HD coexistence phase has a direct consequence for the transport process on the network. Indeed, in this composite phase it is known that the in-rate α_s of a segment directly sets the density and current profile upstream of the domain wall, whereas the out-rate β_s sets the density and current profile downstream of the domain wall. This effectively makes it easier to satisfy the constraint on the current conservation at the vertices, since one of the bounding vertices has no effect whatsoever on the current. As soon as this decoupling occurs all over the network, as is expected for strong exchange parameters Ω, the problem greatly simplifies, and one can again obtain an analytical mean-field solution (see [142]).

5.2.4 Towards cytoskeletal transport: TASEP networks and beyond

Reference to the original work:

> *"Role of network junctions for the totally asymmetric simple exclusion process"*
> *Adélaïde Raguin, Andrea Parmeggiani and Norbert Kern*
> *Phys. Rev. E 88, 042104 (2013)*

The previous section has taken one step towards modelling biological active transport, by acknowledging the importance of the attachment/detachment process. Indeed, real molecular

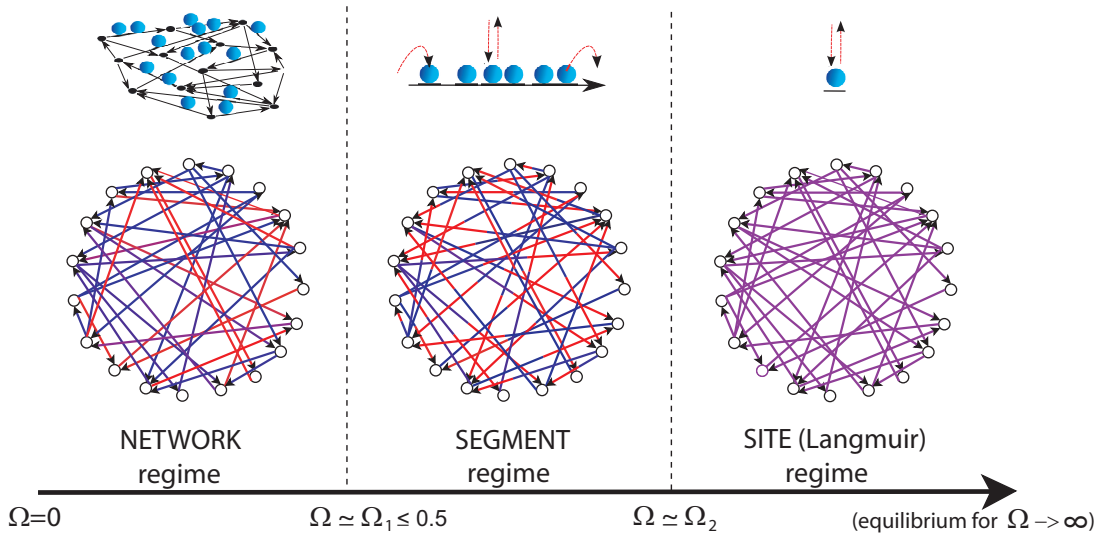

Figure 5.18: *Sketch representing the scales at which spatial heterogeneities occur. As long as the exchange with the bulk reservoir is weak, inhomogeneities arise at the network scale: individual segments are mainly either in the LD or in the HD phase. For intermediate exchange parameters the LD-HD coexistence phase dominates, and thus inhomogeneities arise within these segments. For a very strong exchange, an increasing part of the LD-HD segments becomes dominated by the exchange with the reservoir, ultimately limiting all heterogeneity to the level of individual sites.*

motors can (and will) detach stochastically from the filaments they 'walk' on. The exchange parameter Ω is related to the length an (isolated) motor is expected to move along the filament before detaching, and is thus closely related to what biologists refer to as the motor *processivity*. The recent validation of TASEP-based modelling for molecular motors has also included this ingredient [64, 136].

Other modifications may be necessary, such as taking into account the fact that molecular motors can also 'backstep', i.e. perform a backwards step from time to time. The importance of this varies greatly from one motor to another, but the phenomenon can be of considerable importance. In terms of modelling, this would suggest to build a model based on the *Asymmetric Exclusion Process (ASEP)*, also known as the *Partially Asymmetric Exclusion Process (PASEP)*, which incorporates separate rates for the forward and backward steps. The important message here is that, as we have shown [141, 148] the physics remains similar, and the method of solving numerically for transport on a network and analysing the result in terms of effective rate diagrams can easily be generalised.

Dynamics at the junctions Another crucial phenomenon, however, has not been considered at this stage: the behaviour of a molecular motor as it crosses a junction can of course be much more involved than the simple rule of picking an outgoing segment with equal probability. One element of this line of thought is that the junction site introduced above rather crudely represents in fact quite different scenarios, like a branching point in the structure (in actin fibers) or a crossing of filaments in contact or closeby (in microtubules). One may argue that the sub-structure of the filaments (e.g. the constituting protofilaments) should be taken into account: this is work well in progress [159].

In a first step we have approached the other side of the issue, consisting in a more complex dynamical behaviour of the particles crossing the junction point. It is known from experiments

[10, 170] that a number of different events can take place, according to the type of motor and the type of filament: motors have been observed to obey a different stepping rate at the junction (for example implying a delay before crossing the junction), to detach rather than enter the junction, but also to proceed preferentially to certain of the outgoing segments. We have explored the role of two effects, a modified stepping rate at the junction and a bias towards certain outgoing segments, in a schematic model consisting of one junction site which is shared between two (or more) segment loops. As discussed in the previous section for the symmetric 2-fold vertex V(2:2), the c loops sharing a common site is similar to the V(c:c), but implements a closed topology. This is technically a little simpler to study but provides the same physical insight.

Modified stepping rate at the junction: 'pumping' The modification of the model is simple here: it consists in attributing a different stepping rate, say $\tilde{\nu}\,\gamma$, to a particle at the junction site. Clearly a reduced rate must be expected to increase the bottleneck effect already present due to the shared site. The more interesting case is that of an *increased* stepping rate ($\tilde{\nu} > 1$) on the junction. We have termed $\tilde{\nu}$ the *pumping rate*, to reflect its locally increased throughput. One may imagine mechanisms which would bring about such an increased rate (due to regulation of the motor activity, for example, or due to the proximity of several segments which would increase the chances for the next motor to successfully project one of its heads for an outgoing step), but no specific mechanism is put forward at this point.

The interesting question here is whether, and to which extent, 'pumping' at the junction can help to overcame the bottleneck effect imposed by the shared site. The answer is clearly 'yes', which is easily seen within the mean-field picture for the system of c loops sharing one junction site. The effective rate at which particles attempt to leave a given segment (to enter the junction) is unchanged,

$$\beta = 1 - \tilde{\rho}\ . \tag{5.21}$$

The in-rate into the segment (coming from the junction), however, is modified to

$$\alpha = \tilde{\nu}\,\gamma\,\frac{1}{c}\ . \tag{5.22}$$

We thus see that a pumping 'neutralises' the bottleneck for $\tilde{\nu} > c$, and makes the segment enter a maximum current (MC) phase. This is confirmed by direct simulation (see Fig. 5.19). From the same figure we also see that pumping only affects the current in the density zone which corresponds to LD-HD coexistence. Furthermore, once the threshold $\tilde{\nu}^* = c$ is attained, additional pumping beyond this value is no longer useful. At this point the junction no longer plays the role of a defect, since it is evacuated as easily as any other site, and thus increasing the hopping rate on the junction alone is no longer useful: the current saturates at the value which would correspond to indepedent loops.

Combining 'pumping' and bias We have thus seen several ways in which the junction affects transport: as a direct consequence of sharing a site (see section 5.2.1), due to a bias giving priority to certain exiting segments (see section 5.2.4 for a 2-loop system, but see [160] for the general case), and via an active 'pumping' mechanism tending to accelerate the departure of motors out of the junction site (as discussed above). All of these have been analysed, in a mean-field framework, for an arbitrary number (c) of loops sharing a junction site. We now raise the question of the effects caused by simultaneously 'pumping' on top of an existing bias. The arguments are generic and can therefore be made for any number of loops, but it is more useful to focus on the case of only two loops ($c = 2$) in order to expose the new features.

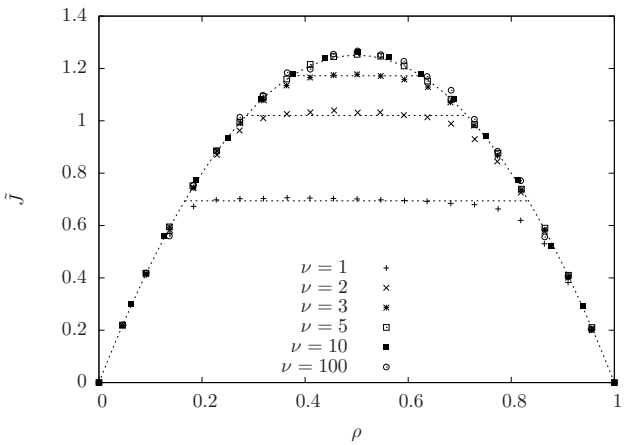

Figure 5.19: *Effect of 'pumping' on junction shared between $c = 5$ loops sharing a junction site. $\nu = 1$ corresponds to the regular hopping rate at the junction, whereas the latter is ν-fold increased for the other values. Pumping counteracts the bottleneck effect, until the threshold $\nu^* = c$ is reached. At this stage any additional pumping has no further effect on the current.*

We are thus dealing with three independent parameters: the bias $(\sigma_1 : \sigma_2)$, the pumping rate ν and the overall particle density ρ. Here we proceed by analysing a fixed bias, and then explore the effect of its variation in a second step.

Before addressing the full picture (Fig. 5.20) it is now useful to establish a point of view which looks at the system in terms of an increasing overall density ρ, as particles are progressively added to the system. The complexity increases in the following fashion (noting A:B the phases of the two segments):

- In the absence of both bias and pumping, we have seen that the system will pass through the phases

$$\text{LD}:\text{LD} \;\rightarrow\; \text{LD-HD}:\text{LD-HD} \;\rightarrow\; \text{HD}:\text{HD} \tag{5.23}$$

  since the coexistence occurs simultaneously in both loops.

- In the presence of bias (but no pumping) the sequence is

$$\text{LD}:\text{LD} \;\rightarrow\; \text{LD-HD}:\text{LD} \;\rightarrow\; \text{HD}:\text{LD} \;\rightarrow\; \text{HD}:\text{LD-HD} \;\rightarrow\; \text{HD}:\text{HD} \tag{5.24}$$

  i.e. the coexistence phase LD-HD arises first in the favoured loop, and later in the secondary one.

- In the presence of pumping (but no bias) the sequence depends on the pumping rate.

$$\begin{array}{lcccc} \nu<\nu^*: & \text{LD}:\text{LD} & \rightarrow & \text{LD-HD}:\text{LD-HD} & \rightarrow & \text{HD}:\text{HD} \\ \nu>\nu^*: & \text{LD}:\text{LD} & \rightarrow & \text{MC}:\text{MC} & \rightarrow & \text{HD}:\text{HD} \end{array} \tag{5.25}$$

  Thus, whenever the pumping rate is below the critical threshold, the sequence is the same as that in the absence of pumping (but with a reduced coexistence zone, see below). Above the critical pumping rate, however, the coexistence phase (LD-HD) is replaced by the restored maximum current (MC) phase.

In the general case, bias and pumping can be present simultaneously. The first point to notice is that now the criterion giving the critical pumping rate (for which the pumping neutralises the bottleneck of the junction), must be established separately for each loop. Reasoning

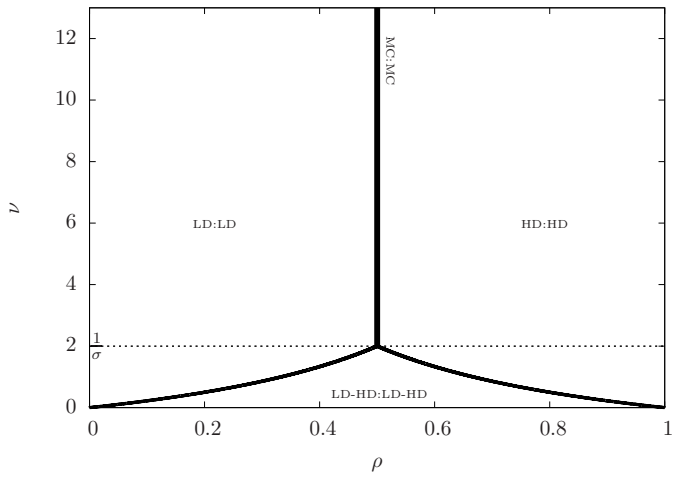

(a) No bias (0.5:0.5)

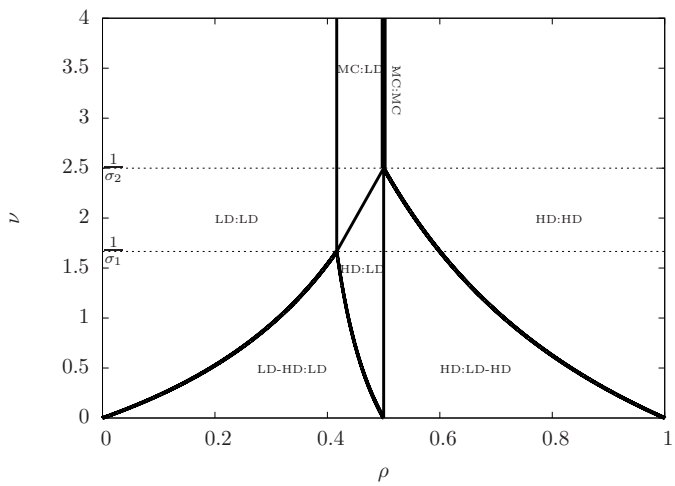

(b) Weak bias (0.6:0.4)

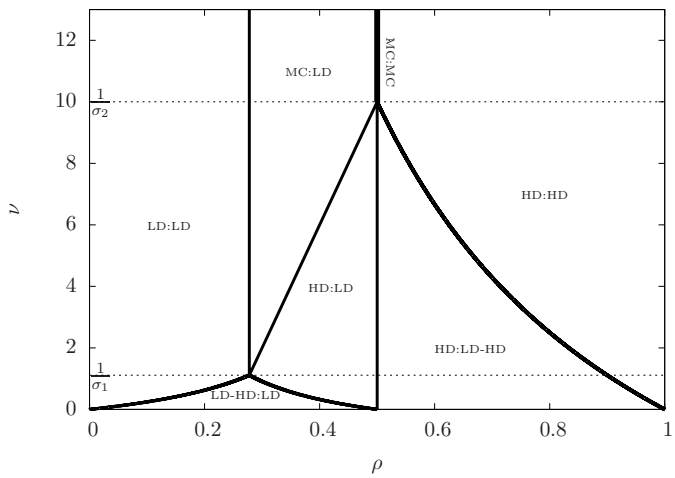

(c) Strong bias (0.9:0.1)

Figure 5.20: *Combined effect of bias and pumping, here for on a 2-fold loop sharing a junction site. Figure (a) recalls the effect of pumping in absence of a bias, i.e. for* $(\sigma_1, \sigma_2) = (0.5, 0.5)$. *(b) A bias introduces additional phases. (c) A strong bias.*

in terms of effective rates readily yields the two critical rates

$$\nu_1^* = \frac{1}{\sigma} \; < \; \frac{1}{\sigma_2} = \nu_2^* \tag{5.26}$$

where σ_1 and $\sigma_2 = 1 - \sigma_1$ are the probabilities of selecting the respective segments, and we take the first segment to be the favoured one ($\sigma_1 > \sigma_2$). This implies that we have to distinguish *three* different cases for the pumping rate. The corresponding sequences are

$$\begin{array}{lcccccccccc}
\nu<\nu_1^* & : & \text{LD:LD} & \rightarrow & \text{LD-HD:LD} & \rightarrow & \text{HD:LD} & \rightarrow & \text{HD:LD-HD} & \rightarrow & \text{HD:HD} \\
\nu_1^*<\nu<\nu_2^* & : & \text{LD:LD} & \rightarrow & \text{MC:LD} & \rightarrow & \text{HD:LD} & \rightarrow & \text{HD:LD-HD} & \rightarrow & \text{HD:HD} \\
\nu_2^*<\nu & : & \text{LD:LD} & \rightarrow & \text{MC:LD} & \rightarrow & & \text{MC:MC} & & \rightarrow & \text{HD:HD}
\end{array} \tag{5.27}$$

The ensemble of these results are represented graphically in Fig. 5.20, which also contains the information of the density ranges corresponding to each of those phases. From this diagram one can also deduce the sequence of phases which would be produced by the complementary approach, varying the pumping rate while maintaining the overall density ρ.

To summarise, the ensemble of these results shows that the statistics as well as the dynamics of the hopping process at the junctions crucially affects the transport properties. The local connectivity, a bias towards certain segments and a modified hopping rate out of the junction are examples for such effects, for which we have explored the scenarios in detail. The ensemble of these results underlines that acting at the junction constitutes a way not only to direct cargoes to a particular destination, but also to regulate the overall transport on the network.

5.3 Follow-up

A further publication [141] on TASEP-like transport processes on networks, only partially referred to above, extends our studies, and also aims to examine several questions concerning applications to biophysical problems. This comprises the ASEP, also known as PASEP (Partially Asymmetric Exclusion Process), a generalisation of TASEP where backward hops are also authorised, albeit with a smaller probability. This is a simple representation of the backstepping of molecular motors, which is indeed observed in experiments: for kinesin-I, they have been shown to account for 2-10% of the displacemements [116,173,194]. Most of the phenomenology remains valid and, most importantly, the effective rate approach and the network analysis in terms of effective rate plots remain applicable. Further details on the TASEP-LK process on the network are given, of which only some are reflected in the discussion above. In particular, estimations of the TASEP-LK parameters show that it might be possible to provoke a transition from the network-regime (dominated by LD and HD segments) to the segment-regime (dominated by LD-HD coexistence segments). One mechanism to do so would be to modify the exchange parameters $\Omega = \frac{\omega L}{\gamma}$, and one way of doing this is by changing the typical segment length L. This can be achieved by modifying the crosslinking, and indeed special proteins to do this are available [2]. It is thus tempting to speculate that this could indeed constitute a mechanism for regulating intra-cellular transport.

A very recent paper by Baek, Ha and Jeong [9] sheds further light onto the approximations we have made in our analysis by treating all segments essentially as independent mean-field segments, coupled only via the junctions. This study critically examines finite size effects for a regular network. It concludes that, even in the thermodynamic limit, the current-density relation still differs from the mean-field prediction: simulations yield a current for the coexistence plateau which is slightly above the mean-field value. An improved theory taking into account

cross-segment correlations at the junctions is proposed, which achieves better correspondence with the numerical data, in particular at the center of the current plateau. Furthermore an algebraically decreasing boundary zone is identified, which develops at the inlet of a HD segment or at the outlet of a HD segment. An analogy is established with the *slow bond problem* [117], for which such behaviour is known. The notion of a 'slow bond' refers to the fact that hopping through a junction is necessarily slower, since there are two outward links: note that this observation is analogous to what we have concluded by the study on junctions in the previous section.

Ezaki and Nishinari [65] have introduced the concept of *balance networks*, which consist of TASEP segments which couple to each other, or to a reservoir, via bi-directional links. They have shown that in this case one can establish a notion of detailed balance, which makes it possible to establish a statistical-mechanics approach, despite the fact that the constituents of the network are out-of-equilibrium. This does however not apply if unidirectional bonds are allowed, or if the network exchanges with multiple reservoirs.

Greulich and Santen [86] have undertaken mainly numerical work on networks constructed from intersecting segments in a plane, as one would in a criss-cross of filaments deposited on a glass surface. They consider both entirely regular (square) lattices and random structures, on which particles evolve according to TASEP-LK dynamics; the size distribution of particle queues is found to be unimodal in the first case but algebraic in the latter. They develop a phenomenological description of particle cluster formation, in which the intersections act as defects. The random length segments in the model are discussed as a feature of a network resulting from growing actin filaments.

Pesheva and Brankov [149] have revisited their earlier model of a double-chain section in the middle of a single filament, i.e. a bifurcation of two segments (in our notation a V(1:2) which then recombines via a V(2:1)). They have pointed out the possibility of a position-induced phase change for the case where the double section should be in a LD-HD coexistence phase: according to the position of the double-section within the single filament, the double section can be pushed either into a HD phase or into a LD phase. These are finite size effects, which would not occur in a thermodyamically large system, but it is speculated that they may nevertheless be interesting for regulation, since such a transition could for example significantly affect the travel time.

Further work by my local collaborators has explored the impact of the fact that, in contrast to what is assumed in TASEP-LK (and what is artificially imposed in many experiments), there is not actually an infinite reservoir of molecular motors in cells. Quite on the contrary, cells would be expected to keep the expenses of building and fuelling molecular motors to a minimum. This study [37] has envisaged two models. The first one acknowledges that the concentration in the (finite but homogeneous) bulk reservoir decreases as motors attach to the filament. The second model furthermore incorporates the fact that the bulk concentration cannot remain homogeneous: as motors are depleted from or restituted to the bulk, a diffusive transport process is required to make them available at another place. Albeit being much more difficult to treat mathematically, it turns out that many of the overall features of TASEP-LK remain valid. However, the phases requiring high particle numbers (LD and MC) progressively disappear from the phase diagram as the ressources become more and more scarce. In particular, it is observed that the position of the domain wall in coexisting phases now depends on the overall number of motors available. This prediction, if verified experimentally, would allow to appreciate the importance of the scarceness of motors, and the mechanism of supply-demand balance might then prove relevant to regulation of transport.

Chapter 6

Present work and outlook

Many aspects of the investigations presented above still generate further research activities today, and I am currently pursuing several of these. They leave many leads to be followed up, as well as several projects on a short to medium term time scale. They reflect biological elements which may require the models presented above to be refined, but they are also of interest in terms of fundamental physics. Finally, several lines of thought for more long-term projects will be sketched.

Ongoing projects: direct follow-up To start with the topic discussed last, non-equilibrium transport on quasi-1d structures, I think it is fair to say that our contributions have provided an angle to address the question of TASEP or TASEP-like transport on a network. At this general level, many interesting questions remain open. We may, for example, mention a detailed analysis of the link between flow and topology, on a local or on a global level. Little is known for instance on how the current through a given vertex correlates to its local connectivity. Even on a phenomenological level, such a description would be interesting and would allow to make contact with other processes on networks. We may also think about exploring other types of networks, such as fractal structures or small-world networks. Another aspect is the anisotropy of actual cytoskeletal networks: their structure differs, both geometrically and topologically, according to the location in the cell, its biological role, as well as the phase of the cell cycle.

Such questions have now become computationally feasible on large networks, due to the compromise of a mean-field approach, sustained by direct stochastic simulations, as advocated in the previous chapter. In principle the numerical method should also be applicable to other types of boundary-controlled flow, and the same holds for the analysis in terms of effective rate plots. This makes the approach potentially interesting to many applications (such as traffic control or queuing problems, to cite but these two).

On a more biologically oriented note it is obvious that the model presented, even in its most sophisticated formulation including the attachment and detachment of motors, is a rather dramatic simplification with respect to the actual transport processes on a cytoskeletal network. The PhD project of A. Raguin, only part of which has been reflected in this manuscript, has made one step towards taking into account additional features of how real motor proteins behave at junctions. Some such aspects have been included in the above discussions, others haven't and remain to be studied. One further line of thought is to acknowledge the structural complexity of the filaments, and in particular at the junctions. This has been partially explored, still in the context of A. Raguin's thesis, in terms of a model retaining several protofilaments on which the motors move. These individual 'lanes' then interconnect at the junction in a way which differentiates the protofilaments and attempts to resolve the spatial organisation of e.g.

a junction of two microtubules, at least in a schematic way. This is work well in progress, and it turns out that it leads to surprises as to what one would measure in experiments, given that it is not currently possible to spatially resolve transport on the individual protofilaments.

Other ongoing projects: role of fluctuating interactions Two further ongoing activities are concerned with the effect of fluctuating interactions in general, and shape fluctuations in particular, on the collective behaviour of stochastic systems subject to excluded volume interactions.

The first project aims at resolving the effect of fluctuating steric effects as molecular motors move along a filament. Within the simplified description of TASEP, no mention is made of the fact that there are typically *two* heads, which must step along consecutively. In reality, we are thus dealing with an internal state, requiring the stepping cycle to go through an intermediate step. For instance, in the hand-over-hand scenario, only *one* of the heads is attached during part of the cycle: this allows to alternate between having one head ahead to having the second head ahead. The two associated reaction rates are not necessarily equal. A related model for this hand-over-hand motion has been studied by Klumpp et al. [113]. However, a closer look suggests that a further feature should be taken into account, which is the fact that the steric interactions must be different in the intermediate phase of the stepping cycle.

This would thus correspond to a modified TASEP model, in which particles successively occupy one or two lattice sites, according to the phase of their stepping process. Alternatively, a 'reptating' motion has been proposed, in which the same motor always remains the leading one, stepping ahead an additional site during its hydrolysis cycle. Here we would thus be looking at a sequence of states occupying successively two and three lattice sites. Whereas TASEP has been generalised to extended objects [50, 122, 177], fluctuating sizes have not been studied, and it is a priori unclear whether such size fluctuations give rise to interesting correlations. With L. Ciandrini, we are currently exploring the question as to how such fluctuations in the steric exclusions modify the collective transport. First results indicate that a simple mean-field approach is no longer sufficient for this problem.

The second project may in some sense be considered to be similar in spirit, but also revives questions close to my postdoc activity, and in particular the topic of protein crystallisation. We are thus undertaking (PhD project of P. Nadal, with D. Coslovich and V. Lorman) to explore the effect of configurational changes, within simple fluid models. Competing structures in proteins are common, and can involve significant changes in the structure, usually by motion of entire sub-domains [187]. Typically one of the structures is favoured in the environment of the cell (the 'native' conformation), but being able to switch to alternative conformations can be important, for example for regulation or for catalytic activity. The idea is to model particles having an internal state which corresponds to several (say, two) competing conformations. The switching event being considered to be quick, the questions of interest within the protein context are twofold.

First: how does the stochastic switching between these states, which would be a 'native' and a 'non-native' protein conformation, alter the phase behaviour? To which extent do these fluctuations make the crystal less stable, or to which extent do they help the nucleation process? Indeed, evidence based on database analysis has been given that forming a regular crystal structure becomes very difficult in the presence of considerable conformational disorder [145]. The same study points out that an excess of flexible domains may have the same effect.

Second: which is the conformation which will be (predominantly) present once the crystal has formed? This too is relevant to proteins, since one issue is whether the structural analysis based on diffraction from crystals is representative of the 'native' protein structure. We are currently working towards these investigations, representing conformational transitions as simple changes in size, shape or interaction potential.

More long-term thoughts Being exposed to biological problems, even without penetrating Biology to any significant depth so far, has made me wonder about many questions, as it is bound to do with any physicist.

The first point one realises is the sheer complexity of even the simplest organism, cell or, for that matter, even the tiniest sub-system involved. The number of biochemical protagonists is usually huge, and not always is it obvious which ones are the important ones. Biologists, now seconded by powerful databases, somehow manage to develop an intuition allowing them to navigate through this complexity. A physicist's mind, however, just doesn't work this way (or in any case mine certainly doesn't).

A second difficulty arises from the fact that whenever a living organism is involved, we are almost always dealing with situations involving *regulation*: the effect of varying a parameter can trigger biochemical feedback, through regulation networks (such as gene expression networks), sensitive to the concentration of the biochemical agents to be produced. This is a sizeable complication when exploring the role of a parameter which one is interested in: the impact may be more dramatic than expected (if there is positive feedback) or much weaker (if a negative feedback mechanism compensates the response). A response may also be entirely absent, whenever an independent regulation mechanism is present which ensures a certain function otherwise (as is indeed often the case for vital functions). As a consequence, it is very difficult to identify well-defined control parameters, and to impose a variation of a single parameter, a strategy which is of course a key element in the success of Physics. Also, certain parameters simply do not allow for any significant variation, at the risk of simply killing the organism to be studied...

Finally, one has to be very wary to use any kind of minimisation principle, another cornerstone of Physics. This is partly related to the previous point, since regulation can often provide an escape mechanism. But it is also related to another seducing type of argument, such as optimal performance, minimum energy consumption, etc. Yes, at the level of an organism, all biochemical mechanisms at work have ultimately been selected by evolution. But there is no certainty as to whether any particular process has indeed evolved to its optimum, or whether evolution has simply gotten stuck in a local extremum.

It thus clearly appears delicate to claim that there will one day be a theory explaining biological reality in a particular mechanism from physics-based fundamental first principles. However, Physics does have its role to play. For one part, it is becoming increasingly possible to strip down important parts of cells and organisms to minimalist systems, or even to reconstruct these artificially. Such *in vitro* systems are much more suitable for a systematic physics-based approach. This is what is being done for many important problems, such as the phospholipid cell membrane, the backbone of a cytoskeleton, etc. *In vivo* systems are much more delicate, both experimentally and conceptually. But even here, it seems to me, a physics-based approach has many contributions to make. Elucidating specific microscopic processes is one such contribution. Exploring the resulting collective effects on a mesoscopic level is another one. An effective description on a macroscopic level is a further useful point of view. Often physics-based models can be helpful for exploring competing scenarios, and pinpoint measur-

able quantities which will ultimately allow to disciminate between them in an experiment. At other times, the study of even an over-simplified system can serve to establish fundamental limitations, and possibly to decide whether a certain biologically plausible mechanism can indeed respect the fundamental constraints on the time, length and energy scales involved.

The following paragraphs sketch a few ideas for such thoughts, which could become part of research projects in time.

Dynamical details of excluded volume interactions between cargos One project where I think simple models can contribute understanding in a bottom-up way concerns the role of cargos on collective effects in motor protein drive transport. Indeed, the model based on TASEP is formulated in terms of strict excluded volume interactions between motors. But for any physiological process there will be cargos attached to the motors, which are often vesicles or organelles, and thus of significant size. A simplistic model would describe the motor as a simple docking point which stochastically steps along a filament, pulling on an elastic spring (a short polymer-like chain domain in the motor) which attaches a hard sphere-like object (the cargo vesicle). Typical dimensions are about a hundred nanometres for the spring-like chain and about a hundred to a thousand nanometres for the diameter of the cargo. The first level of analysis concerns the roles of the viscous drag and the thermal motion of the cargo, and how they affect the effective behaviour of the motor.

This has indeed been explored recently by Erickson et al. [63], using a computational implementation of such a model, based on a Langevin equation. They have shown that the viscous drag reduces both the speed of the motor and the distance it covers before detaching. On the other hand, being bound to the slowly moving cargo helps a detached motor to re-attach to the filament before diffusing away, thus increasing its overall on-rate. Further simulations [62] have shown that the details of this process provide insight into how the switching process between two nearby microtubules operates.

To my knowledge, however, there is so far no study on the excluded volume effect between the cargos. Two limiting cases would appear simple: a very high motor stepping rate (for which all cargos should essentially be aligned in the wake of their motor) and a very slow stepping rate (such that the cargo can explore all configurations before stepping ahead). One question is to which extent one can establish a description in terms of an 'effective' interaction between motor molecules. Whenever this is possible, one would be dealing with an effective repulsion between motors, presumably quite soft but extending over distances much larger than that of the step size of an individual motor. The goal would be to include this repulsion on top of the regular TASEP exclusion at the filament level, and assess its impact on the transport process.

For intermediate stepping rates, however, one may expect a more complex picture. In any case, the time scale set by the viscous process is an entirely new factor: it must be expected to imply a velocity-dependent current-density relation, which is an intriguing new feature. As one application, it would be interesting to consider cargos being pulled along separate protofilaments of a microtubule: here, the diffusion of the cargo may make it possible for nearby cargos to overtake, and the probability for this to happen will again be velocity-dependent. The questions of finite processivity, as well as the fact that cargos can be bound by multiple motors, provide further aspects to be explored.

Intracellular delivery: targetting and traffic shared between multiple species This is another line of thought of obvious importance but daunting complexity. Beyond any

doubts and reservations as to the details of how active transport along the filamentary structure of the cytoskeleton should be modelled: yes, active transport provides a transport mechanism which is efficient over length scales where diffusion is no longer viable, it allows to transport material against existing gradients, and thus also to maintain gradients within the cell against the levelling effect of diffusion. But that is not all that is required: just how does a cell manage to deliver its cargos, at the right time to the right place, for a specific biological process to operate?

Again, the complexity of the overall intracellular traffic is mindblowing, and there is no way a simple physical model can even attempt to explain it. Regulation clearly is one important issue, targetting and sorting cargos via biological markers is another one. Many questions relating to such issues will be specific, and any attempt at modelling will require intense exchanges with specialists on the corresponding biology. Nevertheless, there may be more generic features which one could address.

One such question is the fact that many different types of biochemical cargos share the same physical cytoskeleton as a transport network, and they thus compete for transport capacity. Stated another way, the network must accomodate several types of 'payloads', and the fact that the excluded volume constraint applies also between different types means that their transport must be coupled. In terms of a simple TASEP model, one could think of various types of cargos, which are supplied to the network locally, at rates specific to each type, and received (or actively extracted) at other places. A basic model could be formulated on a single segment, a more sophisticated variant would require generalising the network descriptions established above to open networks with local sources and sinks. Such a model should allow to establish the main mechanisms accounting for the mutual hinderance between payloads. One of the reasons why the problem is non-trivial resides in the non-monotonuous current-density relation: having transport of an additional species interfere will always induce a slow-down but, depending on the overall saturation of the network, it may be marginal. It is tempting to speculate that this might lead to principles of how such shared transport should be organised in order to be efficient for all actors involved. Or, on the contrary, how it would be designed to tolerate a slow-volume traffic of other cargos to be carried while remaining selectively efficient for one particular actor.

There are other aspects to this line of thought. For example, what can one say about delivery times? We should remember that the same current can be achieved at two different densities (corresponding to LD and HD phases), but the travel times are very different for these two cases. If certain biological cargoes come with a (molecular) 'expiration date', then this puts additional constraints on how the transport must be organised.

Tissues Biological tissues are a fascinating example of naturally ocurring cellular structures, which are in many ways reminiscent of foams. Indeed, such analogies have been exploited repeatedly, and have reproduced interesting processes, such as *cell sorting*, where the cells in a structure reorganise according to their affinity [79]. The similarity between tissues and foams is visually striking, and particularly so in a 2-d scenario (tissues grown on a flat substrate). At second thoughts though, the analogy is in no way obvious: the cell membrane carries a curvature energy (absent in foams); there is no homogeneous interfacial tension (but rather a protein-mediated affinity for putting cell walls in contact); the cytoskeleton confers an entirely new set of elastic properties to each cell, and may even actively promote changes of the cell shape. On the other hand, volume constraints are present in both systems, threefold vertices dominate in 2-d cellular tissues too, and topological changes (such as the T1 process discussed above) do arise. And it indeed turns out that the language and phenomenology of foam physics

is useful for addressing certain aspects of cellular tissues [82,84]. Even minimum energy models, using and extending those of foams, have been shown to yield useful results, for example on the way different cell types organise in small cellular aggregates [91].

At this stage no particular project is outlined, but the study of tissues as a cellular 'liquid' is certainly a topic which I would be curious to explore. It would furthermore allow me to put to profit many of the things I have learned working on the heretofore somewhat complementary main topics summarised in this manuscript.

Bibliography

[1] A. Kabla ad G. Debregeas. Local stress relaxation and shear banding in a dry foam under shear. *Phys. Rev. Lett.*, 90:258303, 2003.

[2] B. Alberts, A. Johnson, J. Lewis, M. Raff, K. Roberts, and P. Walter. *Molecular Biology of the Cell.* Garland Science, Taylor & Francis, 2007.

[3] B. J. Alder and T. E. Wainwright. Phase transition for a hard sphere system. *J. Chem. Phys.*, 27:1208, 1957.

[4] J. R. Alford, B. S. Kendrick, J. F. Carpenter, and T. W. Randolph. Measurement of the second osmotic virial coefficient for protein solutions exhibiting monomer-dimer equilibrium. *Anal Biochem.*, 377(2):128–133, 2008.

[5] C. Appert-Rolland, J. Cividini, and H. J. Hilhorst. Intersection of two tasep traffic lanes with frozen shuffle update. *J. Stat. Mech.*, 2011:P10014, 2011.

[6] A.Saint-Jalmes and D. J. Durian. Vanishing elasticity for wet foams: Equivalence with emulsions and role of polydispersity. *J. Rheol.*, 43:1411, 1999.

[7] S. Asakura and F. Oosawa. Interaction between particles suspended in solutions of macromolecules. *J. of Polym. Sci.*, 33:183–192, 1958.

[8] J.-C. Bacri, V. Cabuil, A. Cebers, C. Menager, and R. Perzynski. Flattening of ferrovesicle undulations under a magnetic field. *Europhys. Lett.*, 33(3):235–240, 1996.

[9] Y. Baek, M. Ha, and H. Jeong. Effects of junctional correlations on the tasep on random regular networks. *Phys. Rev. E*, 90:062111, 2014.

[10] S. Bàlint, I. V. Vilanova, A. S. Álvarez, and M. Lakadamyali. Correlative live-cell and superresolution microscopy reveals cargo transport dynamics at microtubule intersections. *Proc. Natl Acad. Sci. USA*, 110:3375–80, 2013.

[11] B. Barboy. On a representation of the equation of state of fluids in terms of the adhesive hard-spheres model. *J. Chem. Phys.*, 61:3194, 1974.

[12] A. Barrat, M. Barthélemy, and A. Vespignani. *Dynamical Processes on Complex Networks.* Cambridge Universiy Press, New York, 2008.

[13] J.-L. Barrat and J.-P. Hansen. *Basic Concepts for Simple and Complex Fluids.* Cambridge University Press, 2003.

[14] J. D. Barry, D. Weaire, and S. Hutzler. Shear localisation with 2d viscous froth and its relation to the continuum model. *Rheologica Acta*, 49:687–698, 2010.

[15] S. Bartnicki-García, F. Hergert, and G. Gierz. Computer simulation of fungal morphogenesis and the mathematical basis for hyphal (tip) growth. *Protoplasma*, 153:46–57, 1989.

[16] R. J. Baxter. Percus–Yevick equation for hard spheres with surface adhesion. *J. Chem. Phys.*, 49:2770–2774, 1968.

[17] K. Ben-Harush, T. Maimon, I. Patla, E. Villa, and O. Medalia. Visualizing cellular processes at the molecular level by cryo-electron tomography. *J. Cell Sci.*, 123:7–12, 2010.

[18] J. Bergenholtz and M. Fuchs. Nonergodicity transitions in colloidal suspensions with attractive interactions. *Phys. Rev. E*, 59:5706–15, 1999.

[19] E. Bianchi, J. Largo, P. Tartaglia, E. Zaccarelli, and F. Sciortino. Phase diagram of patchy colloids: Towards empty liquids. *Phys. Rev. Lett.*, 97:168301, 2006.

[20] S. Biffi, R. Cerbino, E. M. Paraboschi, R. Asselta, F. Sciortino, and T. Bellini. Phase behavior and critical activated dynamics of limited-valence DNA nanostars. *PNAS*, 110(39):15633–15637, 2013.

[21] R. A. Blythe and M. R.Evans. Nonequilibrium steady states of matrix-product form: a solver's guide. *J. Phys. A.: Math. Theor.*, 40:R333–R441, 2007.

[22] G. Boedec, M. Jaeger, and M. Leonetti. Settling of a vesicle in the limit of quasispherical shapes. *Journal of Fluid Mechanics*, 690(227-261), 2012.

[23] G. Boedec, M. Leonetti, and M. Jaeger. 3d vesicle dynamics simulations with a linearly triangulated surface. *Journal of Computational Physics*, 230(4):1020–1034, 2011.

[24] F. Bolton and D. Weaire. Rigidity loss transition in a disordered 2d froth. *Phys. Rev. Lett.*, 65:3449, 1990.

[25] I. Bonnet, P. Marcq, F. Bosveld, L. Fetler, Y. Bellaïche, and F. Graner. Mechanical state, material properties and continuous description of an epithelial tissue. *J. R. Soc. Interface*, 9:2614–2623, 2012.

[26] K. Brakke. The surface evolver. *Exp. Math.*, 1:141, 1992.

[27] J. Brankov, N. Pesheva, and N. Bunzarova. Totally asymmetric exclusion process on chains with a double-chain section in the middle: Computer simulations and a simple theory. *Phys. Rev. E*, 69:066128, 2004.

[28] Paul C. Bressloff and Jay M. Newby. Stochastic models of intracellular transport. *Rev. Mod. Phys.*, 85:135, 2013.

[29] F. P. Bretherton. The motion of long bubbles in tubes. *J. Fluid Mech.*, 10:166, 1961.

[30] I. Cantat. Gibbs elasticity effect in foam shear flows: a non quasi-static 2d numerical simulation. *Soft Matter*, 7:448, 2011.

[31] I. Cantat, N. Kern, and R. Delannay. Dissipation in foam flowing through narrow channels. *Europhys. Lett*, 65:726–732, 2004.

[32] N. F. Carnahan and K. E. Starling. Equation of state for nonattracting rigid spheres. *J. Chem. Phys.*, 51:635, 1969.

[33] Y. C. Chiew and E. D.Glandt. Percolation behaviour of permeable and of adhesive spheres. *J. Phys. A*, 16:2599, 1983.

[34] T. Chou, K. Mallick, and R. K. P. Zia. Non-equilibrium statistical mechanics: from a paradigmatic model to biological. *Rep. Prog. Phys.*, 74:116601, 2011.

[35] D. Chowdhury. Collective effects in intra-cellular molecular motor transport: Coordination, cooperation and competition. *Physica A*, 372:84–95, 2006.

[36] D. Chowdhury, L. Santen, and A. Schadschneider. Statistical physics of vehicular traffic and some related systems. *Phys. Rep.*, 329:199–329, 2000.

[37] L. Ciandrini, I. Neri, J. C. Walter, O. Dauloudet, and A. Parmeggiani. Motor protein traffic regulation by supply–demand balance of resources. *Phys. Biol.*, 2014:056006, 2014.

[38] S. Cox. A viscous froth model for dry foams in the surface evolver. *Colloids and Surfaces A: Physicochemical and Engineering Aspects*, 263(1-3):81–89, 2005.

[39] N. Crampé and A. Trombettoni. Quantum spins on star graphs and the kondo model. *Nucl. Phys. B*, 871:526, 2013.

[40] A. Daanoun, C. F. Tejero, and M. Baus M. van der waals theory for solids. *Phys. Rev. E*, 50:2913, 1994.

[41] G. E. Dale, C. Oefner, and A. Darcy. The protein as a variable in protein crystallization. *J. Struct. Biol.*, 142:88, 2003.

[42] K. A. Dawson. The glass paradigm for colloidal glasses, gels, and other arrested states driven by attractive interactions. *Current Opinion in Colloid & Interface Science*, 7:218–227, 2002.

[43] J. de Gier and F. H. L. Essler. Bethe ansatz solution of the asymmetric exclusion process with open boundaries. *Phys. Rev. Lett.*, 95(240601), 2005.

[44] J. de Gier and F. H. L. Essler. Large deviation function for the current in the open asymmetric simple exclusion process. *Phys. Rev. Lett.*, 107:010602, 2011.

[45] G. Debrégeas, H. Tabuteau, and J.-M di Meglio. Deformation and flow of a two-dimensional foam under continuous shear. *Phys. Rev. Lett.*, 87:178305, 2001.

[46] B. Derrida, E. Domany, and D. Mukamel. An exact solution of a one dimensional asymmetric exclusion model with open boundaries. *J. Stat. Phys.*, 69:667, 1992.

[47] B. Derrida, M. R. Evans, V. Hakim, and V. Pasquier. Exact solution of a 1d asymmetric exclusion model using a matrix formulation. *J. Phys.*, A26:1493–1517, 1993.

[48] B. Derrida, S. A. Janowsky, J. L. Lebowitz, and J. E. R. Speer. Exact solution of the totally asymmetric simple exclusion process: Shock profiles. *Stat. Phys.*, 73:813, 1993.

[49] B. Dollet and I. Cantat. Deformation of soap films pushed through tubes at high velocity. *J. Fluid Mech.*, 652:529–539, 2010.

[50] J. J. Dong, B. Schmittmann, and R. K. P. Zia. Inhomogeneous exclusion processes with extended objects: The effect of defect locations. *Phys. Rev. E*, 76:051113, 2007.

[51] W. Drenckhan, S. J. Cox, G. Delaney, H. Holste, D. Weaire, and N. Kern. Rheology of ordered foams - on the way to discrete microfluidics. *Colloids and Surfaces A: Physicochem. Eng. Aspects*, 263:52–64, 2005.

[52] R. Dreyfus, M. E. Leunissen, R. Sha, A. Tkachenko, N. C. Seeman, D. J. Pine, and P. M. Chaikin. Aggregation-disaggregation transition of DNA-coated colloids: Experiments and theory. *Phys. Rev. E*, 81:041404, 2010.

[53] M. Durand and G. Martinotyand D. Langevin. Liquid flow through aqueous foams: from the Plateau border-dominated regime to the node-dominated regime. *D. Phys. Rev. E*, 60:R6307, 1999.

[54] D. J. Durian. Foam mechanics at the bubble scale. *Phys. Rev. Lett.*, 75:4780, 1995.

[55] D. J. Durian. Bubble-scale model of foam mechanics: Melting, nonlinear behavior, and avalanches. *Phys. Rev. E*, 55(2):1739, 1997.

[56] D. J. Earl and M. W. Deem. Parallel tempering: Theory, applications, and new perspectives. *Phys. Chem. Chem. Phys*, 7:3910–3916, 2005.

[57] F. Elias, E. Janiaud, J.-C. Bacri, and B. Andreotti. Elasticity of a soap film junction. *Phys. Fluids*, 26:037101, 2014.

[58] B. Embley and P. Grassia. Effects of volume conservation on Plateau border sag in foams. *Philosophical Magazine*, 87(36):5697–5718, 2007.

[59] B. Embley and P. Grassia. A simple sagging Plateau border. *Colloids and Surfaces A: Physicochemical and Engineering Aspects*, 309(1-3):20–29, 2007.

[60] B. Embley, A. Parmeggiani, and N. Kern. Hex-tasep: dynamics of pinned domains for tasep transport on a periodic lattice of hexagonal topology. *J. Phys.: Condens. Matter*, 20:295213, 2008.

[61] B. Embley, A. Parmeggiani, and N. Kern. Understanding Totally Asymmetric Simple Exclusion Process transport on networks: Generic analysis via effective rates and explicit vertices. *Phys. Rev. E*, 80:041128, 2009.

[62] R. P. Erickson, S. P. Gross, and C. C. Yu. Filament-filament switching can be regulated by separation between filaments together with cargo motor number. *PLoS One*, 8(2):e54298, 2013.

[63] R. P. Erickson, Z. Jia, S. P. Gross, and C. C. Yu. How molecular motors are arranged on a cargo is important for vesicular transpor. *PLoS Comput Biol*, 7(5):e1002032, 2011.

[64] D. Johannand C. Erlenkämper and K. Kruse. Length regulation of active biopolymers by molecular motors. *Phys. Rev. Lett 108*, 108:258103, 2012.

[65] T. Ezaki and K. Nishinari. Balance network of asymmetric simple exclusion process. *J. Stat. Mech Theory and Exp.*, 2012:P11002, 2012.

[66] F. Fleischer, R. Ananthakrischnan, S. Eckel, H. Schmidt, J. Käs, T. Svitkina, V. Schmidt, and M. Beil. Actin network architecture and elasticity in lamellipodia of melanoma cells. *New J. Phys.*, 9:420, 2007.

[67] G. Foffi, E. Zaccarelli, P. Tartaglia, F. Sciortino, and K. A. Dawson. Are particle gels "glasses"? *Progr. Colloid Polym. Sci.*, 118:221–225, 2001.

[68] M. A. Fortes and P. I. C. Teixeira. Triple-line decoration and line tension in simple three-dimensional foam clusters. *Phys. Rev. E*, 71:051404, 2005.

[69] D. Frenkel and B. Smit. *Understanding Molecular Simulation. From Algorithms to Applications.* Academic, Boston, 1996.

[70] E. Frey, A. Parmeggiani A, and T. Franosch. Collective phenomena in intracellular processes. *Genome Inform.*, 15(1):46–55, 2004.

[71] D. Fusco, T. J. Barnum, A. E. Bruno, J. R. Luft, E. H. Snell, S. Mukherjee, and P. Charbonneau. Statistical analysis of crystallization database links protein physico-chemical features with crystallisation mechanisms. *PLOS*, 9(7):e101123, 2014.

[72] D. Fusco, J. J. Headd, A. De Simone, J. Wang, and P. Charbonneau. Characterizing protein crystal contacts and their role in crystallization: rubredoxin as a case study. *Soft Matter*, 10:290, 2014.

[73] E. Domany G. Schütz. Phase transitions in an exactly soluble one-dimensional exclusion process. *Journal of Statistical Physics*, 72(1-2):277–296, 1993.

[74] A. P. Gast, C. K. Hall, and W. B. Russel. Polymer-induced phase separations in non-aqueous colloidal suspensions. *J. Colloid Interface Sci.*, 96:251, 1983.

[75] A. George and W. Wilson. Predicting protein crystallization from a dilute solution property. *Acta Crystallogr. D*, 50:361, 1994.

[76] C.J. Geyer and A. A. Thomson. Annealing Markov chain Monte Carlo with applications to ancestral inference. *J. Am. Stat. Assoc.*, 90:909, 1995.

[77] D. Ghonasgi and W. G. Chapman. Theory and simulation for associating fluids with four bonding sites. *Mol. Phys. 79*, 79(2):291, 1993.

[78] G. Gierz and S. Bartnicki-García. A three-dimensional model of fungal morphogenesis based on the vesicle supply center concept. *J. Theor. Biol.*, 208:151–164, 2001.

[79] J. A. Glazier and F. Graner. Simulation of the differential adhesion driven rearrangement of biological cells. *Phys. Rev. E*, 47:2128–2154, 1993.

[80] C. Gögelein, F. Romano, F. Sciortino, and A. Giacometti. Fluid-fluid and fluid-solid transitions in the Kern-Frenkel model from Barker-Henderson thermodynamic perturbation theory. *J. Chem. Phys.*, 136:094512, 2012.

[81] O. Golinelli and K. Mallick. The asymmetric simple exclusion process: an integrable model for non-equilibrium statistical mechanics. *J. Phys. A: Math. Gen.*, 39:12679, 2006.

[82] F. Graner. Can surface adhesion drive cell rearrangement? Part I: biological cell-sorting. *J. theor. Biol.*, 164:455–476, 1993.

[83] F. Graner and J. A. Glazier. Simulation of biological cell-sorting using a two-dimensional extended potts model. *Phys. Rev. Lett.*, 69:2013–2016, 1992.

[84] F. Graner and Y. Sawada. Can surface adhesion drive cell rearrangement? Part II: a geometrical model. *J. theor. Biol.*, 164:477–506, 1993.

[85] T. E. Green, A. Bramley, L. Lue, and P. Grassia. Viscous froth lens. *Phys. Rev. E*, 74:051403, 2006.

[86] P. Greulich and L. Santen. Active transport and cluster formation on 2d networks. *Eur. Phys. J. E*, 32(2):191–208, 2010.

[87] J.-C. Géminard, A. Zywocinski, F. Caillier, and P. Oswald. Observation of negative line tension from Plateau borders regions in dry soap films. *Phil. Mag. Lett.*, 84:199–204, 2004.

[88] M. H. J. Hagen and D. Frenkel. Determination of phase diagrams for the hard-core attractive Yukawa system. *J. Chem. Phys.*, 101(5):4093–4097, 1994.

[89] T. C. Hales. The honeycomb conjecture. *Discrete and Computational Geometry*, 25:1–22, 2001.

[90] J.-P. Hansen and I. R. MacDonald. *Theory of Simple Liquids.* Academic Press, 1990.

[91] T. Hayashi and R. W. Carthew. Surface mechanics mediate pattern formation in the developing retina. *Nature*, 431:647–652, 2004.

[92] W. Helfrich. Elastic properties of lipid bilayers: Theory and possible experiments. *Zeitschrift für Naturforschung c*, Heft 11/12:693–703, 1973.

[93] M. Henkel and G. Schütz. Boundary-induced phase transitions in equilibrium and non-equilibrium systems. *Physica A: Statistical Mechanics and its Applications*, 206(1-2):187–195, 1994.

[94] G. Hirasaki and J. B. Lawson. Mechanisms of foam flow in porous media: apparent viscosity in smooth capillaries. *Soc. Petrol. Engng. J.*, April Issue:176, 1985.

[95] J. Howard. *Mechanics of Motor Proteins and the Cytoskeleton.* Sinauer Associates, 2001.

[96] Z. H. Huang, M. Abkarian, and A. Viallat. Sedimentation of vesicles: from pear-like shapes to microtether extrusion. *New Journal of Physics*, 13:035026, 2011.

[97] A. Huerre, V. Miralles, and M.-C. Jullien. Bubbles and foams in microfluidics. *Soft Matter*, 10:6888, 2014.

[98] M. Hutchings, F. Morgan, M. Ritoré, and A. Ros. Proof of the double bubble conjecture. *Annals of Mathematics*, 155(2):459–489, 2002.

[99] S. Hutzler, D. Weaire, and R. Crawford. Convective instability in foam drainage. *Europhys. Lett.*, 41(4):461–465, 1998.

[100] S. M. Ilett, A. Orrock, W. C. K. Poon, and P. N. Pusey. Phase behavior of a model colloid-polymer mixture. *Phys. Rev. E*, 51:1344, 1995.

[101] Y. Ishimoto and Y. Morishita. Bubbly vertex dynamics: a dynamical and geometrical model for epithelial tissues with curved shapes. *Phys. Rev. E*, 90:052711, 2014.

[102] Y. Jiang, P. J. Swart, A. Saxena, M. Asipauskas, and J. A. Glazier. Hysteresis and avalanches in two-dimensional foam rheology simulations. *Phys. Rev. E*, 59(5):5819, 1999.

[103] A. Kabla and G. Debregeas. Quasistatic rheology of foams: I. Response to small deformations. *J. Fluid Mech.*, 587:23–44, 2007.

[104] A. Kabla, J. Scheibert, and G. Debregeas. Quasi-static rheology of foams. part 2. continuous shear flow. *J. Fluid Mech.*, 587:45–72, 2007.

[105] T. Kähärä, T. Tallinen, and J. Timonen. Numerical model for the shear rheology of two-dimensional wet foams with deformable bubbles. *Phys. Rev. E*, 90:032307, 2014.

[106] T. Kaneko. Percolation in fluid mixtures containing adhesive charged hard spheres. *Phys. Rev. E*, 53:6134, 1996.

[107] S Katz, JL Lebowitz, and H Spohn. Phase transitions in stationary nonequilibrium states of model lattice systems. *Physical Review B 28*, 3:1655, 1983.

[108] N. Kern, D.Weaire, A. Martin, S. Hutzler, and S. J. Cox. Two-dimensional viscous froth model for foam dynamics. *Phys. Rev. E*, 70:041411, 2004.

[109] N. Kern and B. Fourcade. Vesicles decorated with magnetic particles. *Europhys. Lett.,*, 38(5):395–400, 1996.

[110] N. Kern and B. Fourcade. Vesicles in linearly forced motion. *Europhys. Lett.,*, 46(2):262–267, 1999.

[111] N. Kern and D. Frenkel. Fluid-fluid coexistence in colloidal systems with short-ranged strongly directional attraction. *J. Chem. Phys.*, 118:9882, 2003.

[112] N. Kern and D. Weaire. Approaching the dry limit in foam. *Phil. Mag.*, 83(26):2973–2987, 2003.

[113] S. Klumpp, Y. Chai, and R. Lipowsky. Effects of the chemomechanical stepping cycle on the traffic of molecular motors. *Phys. Rev. E*, 28:041909, 2008.

[114] S. A. Koehler, S. Hilgenfeldt, and H. A. Stone. A generalized view of foam drainage: Experiment and theory. *Langmuir*, 16:6327–6341, 2000.

[115] S. A. Koehler, H. A. Stone, M. P. Brenner, and J. Eggers. Dynamics of foam drainage. *Phys. Rev. E*, 58(2):2097–2106, 1998.

[116] H. Kojima, E. Muto, H. Higuchi, and T. Yanagida. Mechanics of single kinesin molecules measured by optical trapping nanometry. *Biophys. J.*, 73:2012–2022, 1997.

[117] A. B. Kolomeisky. Asymmetric simple exclusion model with local inhomogeneity. *J. Phys. A: Math. Gen.*, 31:1153, 1998.

[118] A. B. Kolomeisky, G. M. Schütz, E. B. Kolomeisky, and J. P. Straley. Phase diagram of one-dimensional driven lattice gases with open boundaries. *J. Phys. A*, 31:6911, 1998.

[119] M. Kraus, W. Wintz, U. Seifert, and R. Lipowsky. Fluid vesicles in shear flow. *Phys. Rev. Lett.*, 77:3685, 1996.

[120] J. Krug. Boundary-induced phase transitions in driven diffusive systems. *Phys. Rev. Lett.*, 67(14):1882–1885, 1991.

[121] A. Kuijk, A. van Blaaderen, and A. Imhof. Synthesis of monodisperse, rodlike silica colloids with tunable aspect ratio. *J. Am. Chem. Soc.*, 133:2346, 2011.

[122] G. Lakatos and T. Chou. Totally asymmetric exclusion processes with particles of arbitrary size. *Journal of Physics A: Mathematical and General*, 36:2027–2041, 2003.

[123] I. Langmuir. The adsorption of gases on plane surfaces of glass, mica and platinum. *J. Am. Chem. Soc.*, 40(9):1361–1403, 1918.

[124] S. Lecommandoux, O. Sandre, F. Checot, and R. Perzynski. Smart hybrid magnetic self-assembled micelles and hollow capsules. *Progress in Solid State Chemistry*, 34(2-4):171–179, 2006.

[125] S. Lecommandoux, O. Sandre, F. Chécot, J. Rodriguez-Hernandez, and R. Perzynski. Self-assemblies of magnetic nanoparticles and di-block copolymers: Magnetic micelles and vesicles. *Journal of magnetism and magnetic materials*, 300(1):71–74, 2006.

[126] S. B. Lecommandoux, O. Sandre, F. Checot, J. Rodriguez-Hernandez, and R. Perzynski. Magnetic nanocomposite micelles and vesicles. *Advanced Materials*, 17(6):712, 2005.

[127] C. Leduc, K. Padberg-Gehlec, V. Vargaa, Dirk Helbing, S. Dieza, and J. Howard. Molecular crowding creates traffic jams of kinesin motors on microtubules. *Proc. Natl. Acad. Sci.*, 109:6100–6105, 2012.

[128] H. N. W. Lekkerkerker, W. C. K. Poon, P. N. Pusey, A. Stroobants, and P. B. Warren. Phase behaviour of colloid+ polymer mixtures. *Europhys. Lett.*, 20:559, 1992.

[129] M. Loewenberg and E. J. Hinch. Numerical simulation of a concentrated emulsion in shear flow. *J. Fluid Mech.*, 321:395–419, 1996.

[130] C. T. MacDonald, J. H. Gibbs, and A. C. Pipkin. Kinetics of biopolymerization on nucleic acid templates. *Biopolymers*, 6(1):1–25, 1968.

[131] M. Á. G. Maestre, R. Fantoni, A. Giacometti, and A. Santos. Janus fluid with fixed patch orientations: Theory and simulations. *Journal Chem. Phys.*, 138(9):094904, 2013.

[132] K. Mallick. Some recent developments in non-equilibrium statistical physics. *Pramana J. Phys.*, 73(3):417–451, 2009.

[133] K. Mallick. Some exact results for the exclusion process. *J. Stat. Mech.*, 2011:P01024, 2011.

[134] T. G. Mason, J. Bibette, and D. A. Weitz. Elasticity of compressed emulsions. *Phys. Rev. Lett.*, 75(1995):2051, 1995.

[135] O. Medalia, I. Weber, A. S. Frangakis, D. Nicastro, G. Gerisch, and W. Baumeister. Macromolecular architecture in eukaryotic cells visualized by cryoelectron tomography. *Science*, 298:1209–13, 2002.

[136] A. Melbinger, L. Reese, and E. Frey. Microtubule length regulation by molecular motors. *Phys. Rev. Lett*, 108:258104, 2012.

[137] D. Monroe. Focus: How cells regulate the length of filaments. *Physics*, 5:69, 2012.

[138] D. Monroe. http://physics.aps.org/articles/large_image/f1/10.1103/physics.5.69, 2012.

[139] W. W. Mullins. Two-dimensional motion of idealized grain boundaries. *Journal of Applied Physics*, 27:900, 1956.

[140] I. Neri, N. Kern, and A. Parmeggiani. Totally asymmetric simple exclusion process on networks. *Phys. Rev. Lett.*, 107:068702, 2011.

[141] I. Neri, N. Kern, and A. Parmeggiani. Exclusion processes on networks as models for cytoskeletal transport. *New J. Phys.*, 15:085005, 2013.

[142] I. Neri, N. Kern, and A. Parmeggiani. Modeling cytoskeletal traffic: An interplay between passive diffusion and active transport. *Phys. Rev. Lett.*, 110:098102, 2013.

[143] M. G. Noro, N. Kern, and D. Frenkel. The role of long-range forces in the phase behavior of colloids and proteins. *Europhys. Lett.*, 48:332, 1999.

[144] T. Okuzono and K. Kawasaki. Rheological properties of foams: Computer simulation of vertex model for two-dimensional random cellular structures. *Phys. Rev. E*, 51:1246, 1995.

[145] J. N. Onuchic and P. G. Wolynes. Theory of protein folding. *Current Opinion in Structural Biology*, 14:70–75, 2004.

[146] A. Parmeggiani, T. Franosch, and E. Frey. Phase coexistence in driven one-dimensional transport. *Phys. Rev. Lett.*, 90:086601, 2003.

[147] A. Parmeggiani, T. Franosch, and E. Frey. Totally asymmetric simple exclusion process with Langmuir kinetics. *Phys. Rev. E*, 70:046101, 2003.

[148] A. Parmeggiani, I. Neri, and N. Kern. *Modelling Collective Cytoskeletal Transport and Intracellular Traffic.* Springer, 2014.

[149] N. C. Pesheva and J. G. Brankov. Position-induced phase change in a tasep with a double-chain section (a model of biological transport). *Biomath*, 1(1211211):1–7, 2012.

[150] K. N. Pham, S. U. Engelhaaf, P. N. Pusey, and W. C. K. Poon. Glasses in hard spheres with short-range attractions. *Phys. Rev. E*, 69:011503, 2004.

[151] V. Popkov and G. M. Schütz. Steady-state selection in driven diffusive systems with open boundaries. *Europhys. lett.*, 48(3):257, 1999.

[152] D. Portran, J. Gaillard, M. Vantard, and M. Thery. Quantification of map and molecular motor activities on geometrically controlled microtubule networks. *Cytoskeleton*, 70:12–23, 2013.

[153] C. Pozrikidis. *Boundary Integral and Singularity Methods for Linearized Viscous Flow.* Cambridge Texts, Cambridge, 1991.

[154] H. M. Princen. Rheology of foams and highly concentrated emulsions. I. Elastic properties and yield stress of a cylindrical model system. *J. Colloid Interface Sci.*, 91:160–175, 1983.

[155] H. M. Princen. Osmotic pressure of foams and highly concentrated emulsions. I. Theoretical considerations. *Langmuir*, 2(4):519–524, 1986.

[156] H. M. Princen and A. D. Kiss. Rheology of foams and highly concentrated emulsions: III. Static shear modulus. *J. Colloid Interface Sci.*, 112:427, 1986.

[157] H. M. Princen and A. D. Kiss. Osmotic pressure of foams and highly concentrated emulsions. II. Determination from the variation in volume fraction with height in an equilibrated column. *Langmuir*, 3:36, 1987.

[158] E. Pronina and A. B. Kolomeisky. Theoretical investigation of totally asymmetric exclusion processes with on lattices with junctions. *J. Stat. Mech.: Theory Exp.*, 16:P07010, 2005.

[159] A. Raguin. *Trafic régulé par les jonctions: un modele stochastique motivé par le transport cytosquelettique.* PhD thesis, Universite Montpellier II, 2013.

[160] A. Raguin, A. Parmeggiani, and N. Kern. Role of network junctions for the totally asymmetric simple exclusion process. *Phys. Rev. E*, 88:042104, 2013.

[161] L. Reese, A. Melbinger, and E. Frey. Crowding of molecular motors determine microtubule depolymerization. *Biophys. J.*, 101:2190–2200, 2011.

[162] C. Regnaut and J. C. Ravey. Application of the adhesive sphere model to the structure of colloidal suspensions. *J. Chem. Phys.*, 9(1):1211, 1989.

[163] C. Regnaut and J. C. Ravey. Erratum: Application of the adhesive sphere model to the structure of colloidal suspensions. *J. Chem. Phys.*, 9(2):3250, 1990.

[164] T. Reichenbach, E. Frey, and T. Franosch. Traffic jams induced by rare switching events in two-lane transport. *New J. Phys.*, 9:159, 2007.

[165] A. Reymann, J.-L. Martiel, T. Cambier, L. Blanchoin, R. Boujemaa-Paterski, and M. Théry. Nucleation geometry governs ordered actin network structures. *Nature Mater.*, 9:827–32, 2010.

[166] F. Romano, E. Sanz, and F. Sciortino. Crystallization of tetrahedral patchy particles in silico. *J. Chem. Phys.*, 134:174502, 2011.

[167] D. Rosenbaum, P. C. Zamora, and C. F. Zukoski. Phase behavior of small attractive colloidal particles. *Phys. Rev. Lett.*, 76:150, 1996.

[168] R. E. Rosensweig. *Ferrohydrodynamics.* Dover Publications, 1985.

[169] R. E. Rosensweig. Magnetic fluids. *Ann. Rev. Fluid Mech*, 19:437–63, 1987.

[170] J. L. Ross, H. Shuman, E. L. Holzbaur, and Y. E. Goldman. Kinesin and dynein-dynactin at intersecting microtubules: motor density affects dynein function. *Biophys. J.*, 94:3115–3125, 2008.

[171] B. Ruzicka, E. Zaccarelli, L. Zulian, R. Angelini, M. Sztucki, A. Moussaïd, T. Narayanan, and F. Sciortino. Observation of empty liquids and equilibrium gels in a colloidal clay. *Nature Materials Letters*, 10:56, 2011.

[172] H. Salman, A. Abu-Arish, S. Oliel, A. Loyter, J. Klafter, R. Granek, and M. Elbaum. Nuclear localization signal peptides induce molecular delivery along microtubules. *Biophys J.*, 89(3):2134–45, 2005.

[173] M. J. Schnitzer and S. M. Block. Kinesin hydrolyses one atp per 8-nm step. *Nature*, 388:386–90, 1997.

[174] Harvard Medical School. http://hms.harvard.edu/news/molecular-motor-struts-drunken-sailor-1-8-12, 1999.

[175] F. Sciortino, S. V. Buldyrev, C. de Michele, G. Foffi, N. Ghofraniha, E. La Nave, A. Moreno, S. Mossa, I. Saika-Voivod, O. Tartagli, and E. Zaccarelli. Routes to colloidal gel formation. *Computer Physics Communications*, 169:166–171, 2005.

[176] F. Sciortino, A. Giacometti, and G. Pastore. Phase diagram of janus particles. *Phys. Rev. Lett.*, 103:237801, 2009.

[177] L. B. Shaw, R. K. P. Zia, and K. H. Lee. Totally asymmetric exclusion process with extended objects: A model for protein synthesis. *Phys. Rev. E*, 68:021910, 2003.

[178] A. De Simone, C. Kitchen, A. H. Kwan, M. Sunde, C. M. Dobson, and D. Frenkel. Intrinsic disorder modulates protein self-assembly and aggregation. *PNAS*, 109:6951–6956, 2012.

[179] B. Smit, P. d. Smedt, and D. Frenkel. Computer simulations in the gibbs ensemble. *Mol. Phys.*, 68:931, 1989.

[180] B. Smit and D. Frenkel. Calculation of the chemical potential in the gibbs ensemble. *Mol. Phys.*, 68:951, 1989.

[181] C. Smits, J. S. van Duijneveldt J. K. G. Dhont, H. N. W. Lekkerkerker, and W. J. Briels. Effect of the stabilizing coating and the presence of free polymer on the rate of crystallization of colloidal systems. *Phase Trans.*, 21:157–170, 1990.

[182] S. Srinivasa and M. Haenggi. The TASEP: A Statistical Mechanics Tool to Study the Performance of Wireless Line Networks. In *2010 International Conference on Computer Communication Networks (ICCCN'10)*, Zurich, Switzerland, August 2010.

[183] D. Stamenovic. A model of foam elasticity based upon the laws of Plateau. *J. Colloid Interface Sci.*, 145:255, 1991.

[184] M.-A. Suarez, N. Kern, E. Pitard, and W. Kob. Dynamics of a fractal model gel. *Journal Chem. Phys.*, 130(19):194904, 2009.

[185] J. M. Sullivan. The geometry of bubbles and foams. In J. F. Sadoc and N. Rivier, editors, *Foams and Emulsions*, volume 354 of *NATO ASI Series*, pages 379–402. Springer Netherlands, 1999.

[186] A. Surenjav, C. Priest, S. Herminghaus, and R. Seemann. Manipulation of gel emulsions by variable microchannel geometry. *Lab Chip*, 9:325, 2009.

[187] F. Tama and Y.-H. Sanejouand. Conformational change of proteins arising from normal mode calculations. *Protein Engineering*, 14(1):1 – 6, 2001.

[188] J. M. Tavares, P. I. C. Teixeira, and M. M. Telo da Gama. How patchy can one get and still condense? The role of dissimilar patches in the interactions of colloidal particles. *Mol. Phys.*, 107(453-466), 2009.

[189] P. R. ten Wolde and D. Frenkel. Enhancement of protein crystal nucleation by critical density fluctuations. *Science*, 277(5334):1975–8, 1997.

[190] W. Thomson. On the division of space with minimum partitional area. *Philosophical Magazine*, 24:503, 1887.

[191] S. H. Tindemans, N. Kern, and B. M. Mulder. The diffusive vesicle supply center model for tip growth in fungal hyphae. *J. Theor. Biol.*, 238:937–948, 2006.

[192] C. Vega and P. A. Monson. Solid-fluid equilibrium in a molecular model with short range directional forces. *J. Chem. Phys.*, 109:9938, 1998.

[193] G. Verbist and D. Weaire. A soluble model for foam drainage. *Europhys. Lett.*, 26(8):631, 1994.

[194] K. Visscher, M. J. Schnitzer, and S. M. Block. Single kinesin molecules studied with a molecular force clamp. *Nature*, 400:184–9, 1999.

[195] G. A. Vliegenthart and H. N. W. Lekkerkerker. Predicting the gas–liquid critical point from the second virial coefficient. *J. Chem. Phys.*, 112:5364, 2000.

[196] J. von Neumann. *Metal Interfaces (American Society of Metals, Cleveland)*, page 108, 1952.

[197] A. Vrij. Polymers at interfaces and the interactions in colloidal dispersions. *Pure Appl. Chem.*, 48:471, 1976.

[198] D. Weaire. The equilibrium structure of soap froths: inversion and decoration. *Phil. Mag. Lett.*, 79:491–495, 1999.

[199] D. Weaire and S. Hutzler. *The physics of foams*. Oxford University Press, 2001.

[200] D. Weaire, N. Kern, and G. Verbist. Loaded foam structures. *Phil. Mag. Lett.*, 84(2):117–125, 2004.

[201] D. Weaire, N. Pittet, S. Hutzler, and D. Pardal. Steady-state drainage of an aqueous foam. *Phys. Rev. Lett.*, 71:2670, 1993.

[202] S. Weaire and S. McMurry. Some fundamentals of grain growth. *Solid State Phys.*, 50:1–36, 1997.

[203] W. W. Wood and J. D. Jacobson. Preliminary results from a recalculation of the Monte Carlo equation of state of hard spheres. *J. Chem. Phys.*, 27:1207–1208, 1957.

[204] A. Yethiraj and A. van Blaaderen. A colloidal model system with an interaction tunable from hard sphere to soft and dipolar. *Letters to Nature*, 421:513–517, 2003.

[205] G.-R. Yi, D. Pine, and S. Sacanna. Recent progress on patchy colloids and their self-assembly. *J. Phys. Condens. Matter*, 25:193101, 2013.

[206] E. Zaccarelli, S. V. Buldyrev, E. La Nave, A. J. Moreno, I. Saika-Voivod, F. Sciortino, and P. Tartaglia. Model for reversible colloidal gelation. *Phys. Rev. lett.*, 94:218301, 2005.

[207] G. Zhang, D. Y. Wang, and H. Möhwald. Decoration of microspheres with gold nanodots-giving colloidal spheres valences. *Angew. Chem. Int. Ed. Engl.*, 44:7767, 2005.